An Introduction to the EFTofLSS

Oliver H. E. Philcox[1, 2, *]

[1]*Center for Theoretical Physics, Department of Physics,*
Columbia University, New York, NY 10027, USA
[2]*Simons Society of Fellows, Simons Foundation, New York, NY 10010, USA*

We provide a general reader-friendly introduction to the Effective Field Theory of Large Scale Structure and its application to modern cosmological data. Topics covered include the standard perturbation theory and the associated need for an effective theory, renormalization, Lagrangian formulations, infrared resummation, galaxy bias, redshift-space distortions, and the output correlators.

CONTENTS

1. INTRODUCTION

By measuring the three-dimensional positions of galaxies, we create a map of the late-time Universe, encoding both its initial conditions and later evolution. To date, spectroscopic surveys have observed some 10^6 galaxy positions [1]; in the next decade, this number will grow by at least an order of magnitude [e.g., 2, 3], and with it, the volume and depth of the known cosmological landscape.

Analyzing such a dataset presents a serious challenge, both theoretically and computationally. To aid this effort, it is common to compress the set of galaxy positions (or shapes) into 'summary statistics' encoding the distribution in a lower-dimensional form [e.g., 4]. Examples of these include descriptors specifying the pairwise separations of galaxies (the power spectrum and two-point correlation function), their generalization to triplets of galaxies (the bispectrum and three-point correlation function), quadruplets (the trispectrum and four-point correlation function), and many other extensions, including one-point functions, marked spectra, density-split statistics, cluster-weighted correlators, voids, peaks, to name but a few. This is not the only way in which to proceed; an alternative approach is to avoid

---

* ohep2@cantab.ac.uk

compression and predict the entire distribution of galaxies using simulations. Since the galaxy distribution is at heart stochastic, this is a complex procedure and is still nascent, but may prove to be of great use in the future.

a. *Theoretical Models* At the heart of all cosmological analyses, whether using summary statistics or the full distribution (so-called 'field-level' approaches), is a model capable of predicted the observed statistic, given assumptions about the Universe's composition and evolution. In general, these come in three flavors:

- **Analytic**: These are derived from physical equations approximating the Universe on some set of relevant scales. The equations are often solved perturbatively, and implemented via some numerical integrals. Usually, the models will depend on some free parameters intrinsic to the theory [e.g., 5–7].

- **Numerical**: In this case, one predicts the late-time Universe by evolving forwards from known initial conditions using an N-body or hydrodynamic simulation, obeying a number of physical laws. The summary statistics (or galaxy density field) are computed then from the final snapshot, often via emulators [e.g., 8–11].

- **Semi-Analytic**: This combines the two approaches, often with a heuristic picture of structure formation. An example would be halo models, in which lowest order perturbation theory is combined with a phenomenological description of small-scale matter clustering [e.g., 12–20], or 'halofit' [21, 22], supplementing analytic theory with simulations in the latter regime.

In this work, we will focus on the first class of models, in particular those derived from perturbation theory. This has several advantages over numerical approaches: (a) assuming the theory to be well-posed, the predictions can be made arbitrarily accurate by including more terms in the equations, (b) the summary statistics are usually quick to compute and do not require running a large number of simulations for each new cosmological model, (c) the theory carries with it an estimation of the theoretical error. Furthermore, the theories do not depend on (or have knowledge of) small-scale physics, and are thus unbiased by the large-scale manifestations of effects such as baryonic feedback. That said, perturbative approaches are fundamentally limited to the regimes in which the underlying equations are accurate, *i.e.* large scales. Furthermore, perturbative approaches make few assumptions about the Universe's evolution (by design), which leads to them being naturally conservative. If one wishes to extract cosmological information from smaller scales in the Universe, numerical or semi-analytic approaches are required.

b. *Perturbation Theories* Analytic descriptions of the Universe come in many shapes and sizes. Here, we discuss perturbative approaches, all of which aim to describe the dynamics and evolution of the cosmos by treating it is as a (possibly imperfect) fluid, and solving the relevant equations order-by-order in some parameter. The original approach, known as 'standard perturbation theory' (hereafter SPT) was first developed in the 1990s (see [5] for a review), and, as we will discuss below, yields inaccurate predictions for the clustering of matter and galaxies, since a number of physical assumptions are violated. This has led to the development of a number of alternative approaches which aim to avoid these issues via some epicyclic additions to the theory; examples include 'resummed perturbation theory' [23, 24], 'renormalized perturbation theory' [25], 'regularized perturbation theory' [26], the 'TNS' model [27], 'Galilean-invariant resummed perturbation theory' [28] and beyond.

In this review, we present a detailed discussion of the 'effective field theory of large scale structure' (hereafter EFTofLSS, first discussed in [6, 7]). As we will discuss below, the fundamental difference of EFTofLSS to SPT (and its various extensions) is that the theory solves different equations. In particular, the Universe is treated as a *non-ideal* fluid, with contributions from viscosity, sound speeds, and stress tensors, just as for terrestrial fluids. An important ramification is that the Universe contains *feedback* between physics on small and large scales; this can be simply parametrized by symmetry principles (involving 'counterterms'), following other effective field theories in physics (see [29, 30] for cosmological examples). Though the EFTofLSS has a reputation for complexity, its physical motivation is straightforward: it is a **self-consistent perturbative solution** of the **non-ideal fluid equations**, describing the **large-scale** Universe. Our hope is that this review will help to demystify this field.

In the below, we present a pedagogical overview of the EFTofLSS, aimed towards who wish to understand the basic concepts of the model without diving into its finer details. We focus first on SPT and its theoretical issues, before presenting the underlying basis of the EFTofLSS, paying special attention to the issue of feedback and the accompanying renormalization. After presenting the theory in its simplest case (matter in real-space), we will discuss the extension of the theory to more physical scenarios including biased tracers and redshift-space distortions, and finally, comment on its practical usage. Our aim here is not theoretical rigor, but conceptual understanding; as such, we will avoid any lengthy derivations and focus on the physics itself. A detailed and self-consistent discussion of each topic presented below can be found in the rest of the work. More technical topics not essential to the main discussion are marked with asterisks.

2. CONVENTIONS

We work in comoving coordinates, specified by comoving position $\mathbf{x}$ and conformal time τ. Given a field $X(\mathbf{x}, \tau)$, its forward and reverse Fourier-transforms are defined as

$$X(\mathbf{k}, \tau) = \int d\mathbf{x} \, e^{-i\mathbf{k}\cdot\mathbf{x}} X(\mathbf{x}, \tau) \qquad \Leftrightarrow \qquad X(\mathbf{x}, \tau) = \int_{\mathbf{k}} e^{i\mathbf{k}\cdot\mathbf{x}} X(\mathbf{k}, \tau), \tag{2.1}$$

where $\int_{\mathbf{k}} \equiv (2\pi)^{-3} \int d\mathbf{k}$.

If X is a random field, we can describe its behavior in terms of correlators, starting from the power spectrum, P_X:

$$\langle X(\mathbf{k}, \tau) X(\mathbf{k}', \tau') \rangle = P_X(\mathbf{k}, \tau, \tau')(2\pi)^3 \delta_{\mathrm{D}}(\mathbf{k} + \mathbf{k}') \qquad \Rightarrow \langle X(\mathbf{k}, \tau) X(\mathbf{k}', \tau') \rangle' = P_X(\mathbf{k}, \tau, \tau'), \tag{2.2}$$

where we have assumed homogeneity and (if the power spectrum depends only on k) isotropy. In general, we drop the Dirac function for clarity, indicated by the primed expectation $\langle ... \rangle'$, and usually work with equal-time correlators, *i.e.* $\tau = \tau'$. Beyond the power spectrum, we can define an (equal-time) bispectrum as

$$\langle X(\mathbf{k}_1, \tau) X(\mathbf{k}_2, \tau) X(\mathbf{k}_3, \tau) \rangle' = B_X(\mathbf{k}_1, \mathbf{k}_2, \mathbf{k}_3, \tau); \tag{2.3}$$

homogeneity requires $\mathbf{k}_1 + \mathbf{k}_2 + \mathbf{k}_3 = \mathbf{0}$, and isotropy implies $B_X \equiv B_X(k_1, k_2, k_3, \tau)$. Higher-order correlators can be defined similarly, as can their configuration-space equivalents.

By default we will assume a ΛCDM universe, with all plots computed using a cosmology close to *Planck*. We will generally ignore the effects of baryons and neutrinos in this discussion, though they can be self-consistently included (cf. §10). The EFTofLSS approach can straightforwardly account for a range of new post-ΛCDM physics; if this affects only the linear power spectrum, P_{L}, it is automatically included. Other phenomena can be included with small modifications to the theory, such as non-Gaussianity in the initial conditions, and dark matter phenomena that modify the fluid equations.

3. STANDARD PERTURBATION THEORY AND ITS PROBLEMS

To motivate why we need an effective field theory, it is instructive to first consider the non-effecive theory, SPT (see [5] for an extensive review). Before doing so however, let us begin by laying out our criteria for what makes a good theoretical model. We consider three key requirements:

1. **Convergence**: In essence, all perturbation theories are Taylor expansions in some parameter. For the theory to be accurate, this parameter must be small in the regimes of interest.

2. **Accuracy**: The theory must give accurate predictions of the statistics of interest, such as the power spectrum, bispectrum, or density field. Ideally, the theory would be *arbitrarily* accurate in some range of scales, such that any required level of accuracy can be achieved by the addition of enough higher-order corrections.

3. **Generality**: The theory should work regardless of the Universe's initial conditions, as long as the underlying equations remain valid. For example, if the spectral slope n_s took a different value, the theory should still be accurate and convergent.

As we will see below, SPT fails in all three cases, but the EFTofLSS (§4) does not.

a. Fluid Equations   To describe the Universe we will use the following variables:

$\delta(\mathbf{x}, \tau)$: Fractional overdensity of matter, related to the true density $\rho(\mathbf{x}, \tau)$ by $\delta(\mathbf{x}, \tau) = \rho(\mathbf{x}, \tau)/\bar{\rho}(\tau) - 1$

$\mathbf{v}(\mathbf{x}, \tau)$: Fluid velocity, which can be defined in terms of the momentum $\mathbf{p}(\mathbf{x}, \tau)$

$\phi(\mathbf{x}, \tau)$: Peculiar gravitational potential (corrected for the background expansion)

$\tau(\mathbf{x}, \tau)$: Viscous stress tensor

where we work in comoving coordinates, $\mathbf{x}$. The basic assumption of SPT is that the Universe can be described as a perfect fluid. As such, its distribution must satisfy the **collisionless Boltzmann** (or Vlasov) equation. In terms of

the above variables, this implies

$$\dot{\delta}(\mathbf{x}, \tau) + \nabla \cdot [(1 + \delta(\mathbf{x}, \tau))\mathbf{v}(\mathbf{x}, \tau)] = 0 \qquad \qquad \text{Continuity} \qquad (3.1)$$

$$\dot{\mathbf{v}}(\mathbf{x}, \tau) + [\mathbf{v}(\mathbf{x}, \tau) \cdot \nabla]\mathbf{v}(\mathbf{x}, \tau) = -\mathcal{H}(\tau)\mathbf{v}(\mathbf{x}, \tau) - \nabla\phi(\mathbf{x}, \tau) \qquad \qquad \text{Euler}$$

$$\nabla^2 \phi(\mathbf{x}, \tau) = 4\pi G a^2(\tau)\bar{\rho}(\tau)\delta(\mathbf{x}, \tau) = \frac{3}{2}\mathcal{H}^2(\tau)\Omega_m(\tau)\delta(\mathbf{x}, \tau) \qquad \qquad \text{Poisson,}$$

where dots indicate derivatives with respect to conformal time, $\mathcal{H}$ is the reduced Hubble parameter, a is the scale factor, Ω_m is the matter fraction and G is the gravitational constant. The assumption of a perfect fluid fixes the stress tensor to zero; $\tau = 0$. Note that the above equations additionally assume the Newtonian limit, *i.e.* the scales of interest are significantly smaller than $\mathcal{H}^{-1}$.

    b.   *Linear Order Solution*   At leading order, we can solve (3.1) by linearizing the fluid equations, *i.e.* dropping any terms of second or higher order in $\{\delta, \mathbf{v}, \phi\}$. This yields the following equations for the first-order fields, $\delta_1, \mathbf{v}_1$:

$$\dot{\delta}_1(\mathbf{x}, \tau) + \nabla \cdot \mathbf{v}_1(\mathbf{x}, \tau) = 0, \qquad \dot{\mathbf{v}}_1(\mathbf{x}, \tau) = -\mathcal{H}(\tau)\mathbf{v}_1(\mathbf{x}, \tau) - \frac{3}{2}\mathcal{H}^2(\tau)\Omega_m(\tau)\nabla\left[\nabla^{-2}\delta_1(\mathbf{x}, \tau)\right], \qquad (3.2)$$

eliminating the peculiar potential. Introducing the velocity potential $\theta(\mathbf{x}, \tau) \equiv \nabla \cdot \mathbf{v}(\mathbf{x}, \tau)$, we find

$$\theta_1(\mathbf{x}, \tau) = -\dot{\delta}_1(\mathbf{x}, \tau), \qquad \ddot{\delta}_1(\mathbf{x}, \tau) + \mathcal{H}(\tau)\dot{\delta}_1(\mathbf{x}, \tau) - \frac{3}{2}\mathcal{H}^2(\tau)\Omega_m(\tau)\delta_1(\mathbf{x}, \tau) = 0. \qquad (3.3)$$

These are easily solved by asserting a separable solution, such that

$$\delta_1(\mathbf{x}, \tau) = D(\tau)\delta_{\mathrm{L}}(\mathbf{x}), \qquad \theta_1(\mathbf{x}, \tau) = -\mathcal{H}(\tau)f(\tau)D(\tau)\delta_{\mathrm{L}}(\mathbf{x}), \qquad (3.4)$$

where $\delta_{\mathrm{L}}(\mathbf{x})$ is the *linear* density field set by inflation. This drops a decaying mode and defines the *growth factor* via

$$D(\tau) = D_0 \mathcal{H}(\tau) \int_0^{a(\tau)} \frac{da'}{\mathcal{H}^3(a')}, \qquad (3.5)$$

where D_0 ensures the normalization condition $D(a = 1) = 1$ today. For the velocity, we introduce the *velocity* growth rate $f(\tau) \equiv d \log D(\tau)/d \log a$ by convention. For an Einstein-de Sitter Universe (with $\Omega_m = 1$), $D(\tau)$ is simply the scale factor $a(\tau)$. As such, densities evolve according to $D(\tau)$ and velocities enhanced by a factor of $\mathcal{H}(\tau)f(\tau)$.

    Switching to Fourier-space, we obtain similar relations to before:

$$\delta_1(\mathbf{k}, \tau) = D(\tau)\delta_{\mathrm{L}}(\mathbf{k}), \qquad \theta_1(\mathbf{k}, \tau) = -\mathcal{H}(\tau)f(\tau)D(\tau)\delta_{\mathrm{L}}(\mathbf{k}), \qquad (3.6)$$

additionally with $\mathbf{v}(\mathbf{k}, \tau) = i(\mathbf{k}/k^2)\theta(\mathbf{k}, \tau)$. It follows that the linear-order matter power spectrum is given by

$$P_{\mathrm{linear}}^{\mathrm{SPT}}(\mathbf{k}, \tau) \equiv \langle \delta_1(\mathbf{k}, \tau)\delta_1(-\mathbf{k}, \tau') \rangle' = D^2(\tau)P_{\mathrm{L}}(k), \qquad (3.7)$$

where $P_{\mathrm{L}}(k)$ is the power spectrum of the initial conditions, and we have dropped a momentum-conserving Dirac delta function.

    c.   *General Solution*   Beyond linear order, the ideal fluid equations can be solved by rewriting them as convolutions in Fourier-space

$$\dot{\delta}(\mathbf{k}, \tau) + \theta(\mathbf{k}, \tau) = \int_{\mathbf{p}_1 \mathbf{p}_2} \alpha(\mathbf{p}_1, \mathbf{p}_2)\theta(\mathbf{p}_1, \tau)\delta(\mathbf{p}_2, \tau)(2\pi)^3\delta_{\mathrm{D}}\left(\mathbf{p}_1 + \mathbf{p}_2 - \mathbf{k}\right) \qquad (3.8)$$

$$\dot{\theta}(\mathbf{k}, \tau) + \mathcal{H}(\tau)\theta(\mathbf{k}, \tau) + \frac{3}{2}\mathcal{H}^2(\tau)\Omega_m(\tau)\delta(\mathbf{k}, \tau) = -\int_{\mathbf{p}_1 \mathbf{p}_2} \beta(\mathbf{p}_1, \mathbf{p}_2)\theta(\mathbf{p}_1, \tau)\theta(\mathbf{p}_2, \tau)(2\pi)^3\delta_{\mathrm{D}}\left(\mathbf{p}_1 + \mathbf{p}_2 - \mathbf{k}\right),$$

where the convolution kernels can be written

$$\alpha(\mathbf{p}_1, \mathbf{p}_2) = \frac{\mathbf{p}_1 \cdot \mathbf{k}}{p_1^2}, \qquad \beta(\mathbf{p}_1, \mathbf{p}_2) = \frac{k^2}{2}\frac{\mathbf{p}_1 \cdot \mathbf{p}_2}{p_1^2 p_2^2} \qquad (3.9)$$

for $\mathbf{k} \equiv \mathbf{p}_1 + \mathbf{p}_2$. Within SPT, one then proceeds via a perturbative stance, expanding the equations order-by-order in the (assumed small) parameters δ and θ. Explicitly, we begin with the series solutions

$$\delta(\mathbf{k}, \tau) = \sum_{n=1}^{\infty} D^n(\tau)\delta^{(n)}(\mathbf{k}), \qquad \theta(\mathbf{k}, \tau) = -\mathcal{H}(\tau)f(\tau)\sum_{n=1}^{\infty} D^n(\tau)\theta^{(n)}(\mathbf{k}), \qquad (3.10)$$

where the n-th order solution contains n copies of the linear solution, $\delta^{(1)}(\mathbf{k}) \equiv \delta_{\mathrm{L}}(\mathbf{k})$. Here, we have assumed separability in time and space: this is an excellent approximation in practice (and exact for Einstein de-Sitter universes), though deviations can occur at high order. Starting from the linear solution given in (3.6), the second order piece is found by inserting $\delta^{(1)}, \theta^{(1)}$ into (3.8) and solving for $\delta^{(2)}, \theta^{(2)}$, which can then be used to solve for $\delta^{(3)}, \theta^{(3)}$, *et cetera*. The n-th order contribution takes the form:

$$\delta^{(n)}(\mathbf{k}) = \int_{\mathbf{p}_1 \cdots \mathbf{p}_n} F_n(\mathbf{p}_1, \cdots, \mathbf{p}_n) \left\{ \delta_{\mathrm{L}}(\mathbf{p}_1) \cdots \delta_{\mathrm{L}}(\mathbf{p}_n) \right\} (2\pi)^3 \delta_{\mathrm{D}}(\mathbf{p}_1 + \cdots + \mathbf{p}_n - \mathbf{k}) \quad (3.11)$$

$$\theta^{(n)}(\mathbf{k}) = \int_{\mathbf{p}_1 \cdots \mathbf{p}_n} G_n(\mathbf{p}_1, \cdots, \mathbf{p}_n) \left\{ \delta_{\mathrm{L}}(\mathbf{p}_1) \cdots \delta_{\mathrm{L}}(\mathbf{p}_n) \right\} (2\pi)^3 \delta_{\mathrm{D}}(\mathbf{p}_1 + \cdots + \mathbf{p}_n - \mathbf{k}).$$

This is simply the convolution of n linear density fields with a kernel, F_n or G_n. The kernels can be computed recursively in terms of (3.9) and are given explicitly to higher order in [5]. As an example, the kernels up to second order are given by:

$$F_1(\mathbf{p}) = G_1(\mathbf{p}) = 1, \qquad F_2(\mathbf{p}_1, \mathbf{p}_2) = \frac{5}{7}\alpha(\mathbf{p}_1, \mathbf{p}_2) + \frac{2}{7}\beta(\mathbf{p}_1, \mathbf{p}_2), \qquad G_2(\mathbf{p}_1, \mathbf{p}_2) = \frac{3}{7}\alpha(\mathbf{p}_1, \mathbf{p}_2) + \frac{4}{7}\beta(\mathbf{p}_1, \mathbf{p}_2), \ (3.12)$$

with the third-order piece described in Appendix A.

The above equations provide all the necessary mathematics to compute density field statistics at arbitrary order. For example, the equal-time power spectrum, $P(k, \tau) \equiv \langle \delta(\mathbf{k}, \tau) \delta(-\mathbf{k}, \tau) \rangle'$ can be written in terms of $\delta^{(n)}$ correlators:

$$P^{\mathrm{SPT}}(k, \tau) = D^2(\tau) P^{(11)}(k) + D^4(\tau) \left[2P^{(13)}(k) + P^{(22)}(k) \right] + D^6(\tau) \left[2P^{(15)}(k) + 2P^{(24)}(k) + P^{33}(k) \right] + \cdots (3.13)$$

where $P^{(ij)}(k) \equiv \langle \delta^{(i)}(\mathbf{k}) \delta^{(j)}(-\mathbf{k}) \rangle'$, and we have assumed Gaussian initial conditions, such that any correlators involving an odd number of linear density fields vanish. Note that there are three groups of terms in the above expression: these involve 0, 1, and 2 $\mathbf{p}$-integrals respectively, and are therefore said to be 0-, 1-, and 2-loop contributions. Each power spectrum can be written in terms of the linear power spectrum P_{L} and the F_n kernels defined above: for example, the contributions up to one-loop are given explicitly by

$$P^{(22)}(k) = 2 \int_{\mathbf{p}} |F_2(\mathbf{p}, \mathbf{k} - \mathbf{p})|^2 P_{\mathrm{L}}(\mathbf{p}) P_{\mathrm{L}}(\mathbf{k} - \mathbf{p}), \qquad P^{(13)}(k) = 3 P_{\mathrm{L}}(k) \int_{\mathbf{p}} F_3(\mathbf{p}, -\mathbf{p}, \mathbf{k}) P_{\mathrm{L}}(\mathbf{p}). \quad (3.14)$$

Similar methods may be used to compute higher-order spectra or correlators involving velocity fields. An example of this is three-point functions, or bispectra: at lowest order this is given by

$$B(\mathbf{k}_1, \mathbf{k}_2, \mathbf{k}_3, \tau) \equiv \langle \delta(\mathbf{k}_1, \tau) \delta(\mathbf{k}_2, \tau) \delta(\mathbf{k}_3, \tau) \rangle' = D^4(\tau) B^{(211)}(\mathbf{k}_1, \mathbf{k}_2, \mathbf{k}_3) + \cdots \quad (3.15)$$

$$B^{(211)}(\mathbf{k}_1, \mathbf{k}_2, \mathbf{k}_3) = 2F_2(\mathbf{k}_1, \mathbf{k}_2) P_{\mathrm{L}}(k_1) P_{\mathrm{L}}(k_2) + 2 \text{ perms.},$$

with higher-order contributions containing loop integrals over the linear power spectrum.

d. Numerical Results Let us now consider the performance of SPT, by comparing its predictions for the matter power spectrum with those obtained from N-body simulations assuming a ΛCDM cosmology [31], and evolving the Universe down to $z = 0$. This is shown in Fig. 1, showing both the linear theory prediction for the power spectrum $(D^2 P^{(11)})$ and the one-loop correction (adding $D^4[2P^{(13)} + P^{(22)}]$). At low-$k$, we generally find good agreement between simulations and data; these correspond to large-scales, on which the Universe is close to a perfect fluid and traces the initial conditions to high accuracy. On smaller scales, linear theory starts to break down, due to the impact of gravitational evolution on large-scale structure. In principle, this deviation between simulations and theory should be captured by the addition of one-loop SPT contributions, at least on relatively large scales. However, this is not what we see in the figure! Adding one-loop SPT corrections does not appear to improve the fit to data; similarly, the addition of two-loop terms does not solve the problem, with the theory now underestimating the spectrum. From this simple test, we conclude that SPT does not satisfy condition (2) of a good theoretical model, as outlined in the beginning of the section, since it does not yield accurate predictions.

e. Perturbativity and Convergence As we will now see, accuracy is not the only problem intrinsic to SPT. Firstly, there are hidden subtleties in our treatment of the fluid equations. In particular, when solving (3.1) perturbatively, we have implicitly assumed that the density field and velocity divergence are small, *i.e.* that the variance $\sigma_\delta^2 \ll 1$. This is needed for a perturbative solution (or Taylor series) to exist, since if, for example, the second order solution is larger than the first order piece, the series does not converge. If we average over sufficiently large scales, we would
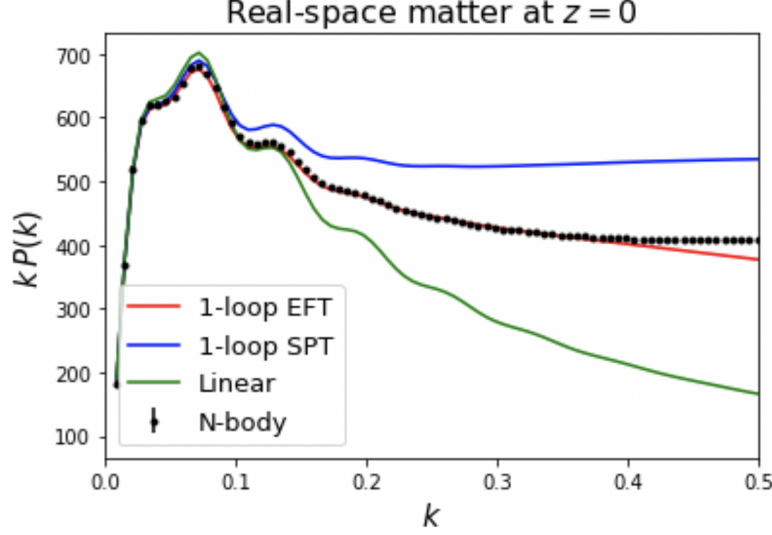
FIG. 1. Comparison of matter power spectra obtained from simulations (black points), linear theory (green), one-loop SPT (blue) and one-loop EFTofLSS (red). The numerical results are obtained from the QUIJOTE simulations at redshift zero [31], whilst theory spectra are computed with CLASS-PT [32]. For the EFTofLSS spectra, we fit the (necessary) counterterm to the simulated spectra up to $k_{\mathrm{max}} = 0.2h\,\mathrm{Mpc}^{-1}$. All quantities are given in $h\,\mathrm{Mpc}^{-1}$ units.

expect the overdensity to be small; however, such a smoothing is not built into the underlying SPT equations. As such, we necessarily obtain contributions from regimes where $|\delta|$ is large (*i.e.* small scales), which breaks the perturbative hierarchy, and thus condition (1) for a well-posed theory. Working only with smoothed quantities is a key part of the EFTofLSS, and requires a description based on the non-ideal fluid equation [cf. 6, 7].

A related problem can be seen by considering the loop corrections in detail. Let us look at the one-loop term $P^{(13)}$, which has the explicit form:

$$P^{(13)}(k) = 3P_{\mathrm{L}}(k) \int_0^\infty \frac{p^2 dp}{2\pi^2} P_{\mathrm{L}}(p) \int \frac{d\hat{\mathbf{p}}}{4\pi} F_3(\mathbf{p}, -\mathbf{p}, \mathbf{k}). \tag{3.16}$$

Noting that F_3 behaves as k^2/p^2 for hard internal momenta (*i.e.* large p), we see that the term involves an integral of $P_{\mathrm{L}}(p)$ up to infinitely large p. This itself is a problem. Perturbation theory theory is only valid on large scales, yet we are here summing over all scales down to those of individual galaxies, planets, and review articles. It is thus little surprise that the theory breaks down.

Finally, we note that, for some choices of initial condition, the SPT predictions themselves diverge. This can be seen by considering the one-loop SPT power spectra in the limit of small and large internal momentum p:

$$P^{\mathrm{UV}}_{1-\mathrm{loop}}(k) \ \sim \ k^2 P_{\mathrm{L}}(k) \int_{p \gg k} p^2 dp \, \frac{P_{\mathrm{L}}(p)}{p^2} \tag{3.17}$$

$$P^{\mathrm{IR}}_{1-\mathrm{loop}}(k) \ \sim \ P_{\mathrm{L}}(k) \int_{p \ll k} p^2 dp \, P_{\mathrm{L}}(p).$$

Assuming a power-law linear power spectrum with $P_{\mathrm{L}}(p) \propto p^n$, the high-$p$ (ultraviolet; UV) limits diverge for $n \geq -1$ and the low-p (infrared; IR) limits are divergent for $n \leq -3$. If the second is violated, however, the fluid equations themselves break down (and thus the above discussion is moot), but the first is an important limitation. For our Universe, $n \approx -3/2$ (at the non-linear scale), thus the integrals are convergent in both limits. However, this is a peculiarity of our Universe and not guaranteed in general, thus the theory violates condition (3) posed above.

In summary, the failure of SPT to predict the matter power spectrum (and other statistics) can be traced back to three problems with the theory:

1. **Convergence**: The expansion parameter, δ, is not guaranteed to be small.

2. **Accuracy**: The theory integrates over regimes where perturbative treatments are not valid, and does not yield accurate predictions for correlation functions.

3. **Generality**: The predictions can diverge for certain choices of initial conditions.

In the next section, we consider how the EFTofLSS avoids all three of these problems.

4.   FORMULATING THE EFFECTIVE FIELD THEORY

The primary goal of the EFTofLSS program is straightforward: to develop a convergent perturbation theory for the Universe which is convergent, accurate, and can be applied in the presence of arbitrary initial conditions. The underlying formalism is described in depth in [6, 7] and subsequent works (including [33–43]), and we review it below.

To understand the theory, our starting point is the notion of *smoothing*, *i.e.* the replacement of the standard fluid variables with those smoothed on some scale Λ^{-1}:

$$\delta(\mathbf{x}, \tau) \to \delta_\Lambda(\mathbf{x}, \tau), \quad \mathbf{v} \to \mathbf{v}_\Lambda(\mathbf{x}, \tau), \quad \phi(\mathbf{x}, \tau) \to \phi_\Lambda(\mathbf{x}, \tau). \tag{4.1}$$

Here the smoothing is defined by $X_\Lambda(\mathbf{k}, \tau) = W_\Lambda(k)X(\mathbf{k}, \tau)$ in Fourier-space, where $W_\Lambda(k)$ is some window excising scales with $k \gtrsim \Lambda$.[1] By working with smoothed fields, we are explicitly restricting our theory model to scales $k \lesssim \Lambda$; if Λ is below the non-linear scale $k_{\rm NL}$ (whence perturbation theory breaks down), we avoid explicit contributions from scales that cannot be modeled within the framework. Furthermore, if the smoothing scale is sufficiently large, the smoothed overdensity field, δ_Λ, is guaranteed to be small, with characteristic size

$$\sigma_\delta^2(\Lambda) \equiv \int_0^\Lambda \frac{p^2 dp}{2\pi^2} P_{\rm L}(p) \approx \frac{\Lambda^3 P_{\rm L}(\Lambda)}{2\pi^2}, \tag{4.2}$$

with $\sigma_\delta^2(\Lambda) < 1$ for $\Lambda < k_{\rm NL}$ (by definition). This lies in contrast with SPT (§3), where the unsmoothed field does *not* have to be small, and implies that condition (1) for a well-posed theory is valid. In essence, this is the main difference between SPT and the EFTofLSS: all the further complexities of non-ideal fluid equations and renormalization can be considered to be a consequence of this smoothing.

a.   The Non-Ideal Fluid Equations   Let us now consider the underlying equations for the smoothed density field. To achieve this we will start from the fluid equations given in (3.1) and apply the smoothing operator W_Λ, a procedure usually known as 'coarse graining'. For full generality, we will retain the stress-tensor τ in the Euler equation, though this vanishes for an ideal fluid.[2] We find the following equations:

$$\dot{\delta}_\Lambda(\mathbf{x}, \tau) + \nabla \cdot [(1 + \delta_\Lambda(\mathbf{x}, \tau))\mathbf{v}_\Lambda(\mathbf{x}, \tau)] = 0 \qquad \qquad \text{Continuity}$$

$$\tag{4.3}$$

$$\dot{\mathbf{v}}_\Lambda(\mathbf{x}, \tau) + [\mathbf{v}_\Lambda(\mathbf{x}, \tau) \cdot \nabla]\mathbf{v}_\Lambda(\mathbf{x}, \tau) = -\mathcal{H}(\tau)\mathbf{v}_\Lambda(\mathbf{x}, \tau) - \nabla\phi_\Lambda(\mathbf{x}, \tau) - \frac{1}{\rho_\Lambda(\mathbf{x}, \tau)}\left[\nabla\tau_\Lambda(\mathbf{x}, \tau) + \nabla\tau_\Lambda^{\rm UV}(\mathbf{x}, \tau)\right] \quad \text{Euler}$$

$$\nabla^2\phi_\Lambda(\mathbf{x}, \tau) = \frac{3}{2}\mathcal{H}^2(\tau)\Omega_m(\tau)\delta_\Lambda(\mathbf{x}, \tau) \qquad \qquad \text{Poisson.}$$

These are identical to the starting fluid equations (with the inclusion of the stress tensor τ) except for the appearance of a new term $\tau_\Lambda^{\rm UV}$ in the Euler equation. This arises from the coarsening operation, and takes the form

$$\nabla\tau_\Lambda^{\rm UV} = \left[[\rho\nabla\phi]_\Lambda - \rho_\Lambda\nabla\phi_\Lambda\right] + \left[[(\rho\mathbf{v} \cdot \nabla)\mathbf{v}]_\Lambda - (\rho_\Lambda\mathbf{v}_\Lambda \cdot \nabla)\mathbf{v}_\Lambda\right]. \tag{4.4}$$

This arises since multiplication and smoothing do not commute: the smoothed product of two fields (first and third terms) are not equal to the product of two smoothed fields (second and fourth terms). This difference occurs due to correlated small-scale fluctuations; separating a field X into long (X_l) and short (X_s) modes, the product of two smoothed fields contains only X_lY_l, but the smoothed product contains also $(X_sY_s)_\Lambda$, which acts similar to a noise term. Physically speaking, the intuition for the above stress tensor $\tau^{\rm UV}$ is that small scale modes appearing in the fluid equations non-linearly modify the dynamics of large scale modes.

---

[1] For velocity fields, we smooth the momentum density $\rho\mathbf{v}$ rather than $\mathbf{v}$ itself, such that $\mathbf{v}_\Lambda = [\rho\mathbf{v}]_\Lambda/\rho_\Lambda$.

[2] In the language of particle physics, we are effectively performing an on-shell Wilson renormalization around the SPT solution, where the free-field is described by the ideal fluid equations with (optionally) a non-vanishing stress tensor. See [44] for details.

Armed with this split into long and short modes, let us consider the form of $\tau_\Lambda^{\mathrm{UV}}$ more carefully. Following some calculation, this can be shown to equal

$$\tau_{ij,\Lambda}^{\mathrm{UV}} = \frac{1}{4\pi G}\left(\partial_i\phi_s\partial_j\phi_s - \frac{1}{2}\delta_{ij}^{\mathrm{K}}\partial_k\phi_s\partial^k\phi^s\right) + \rho v_{s,i}v_{s,j} \tag{4.5}$$

using the Poisson equation and switching to coordinate notation. Notably, this new term, sourced by small-scale physics at $k > \Lambda$, enters the smoothed fluid equations in the same manner as the usual stress tensor in the unsmoothed equations (as the derivative of a symmetric tensor). Furthermore, by expanding the short-scale fluctuations around their expectations (*i.e.* replacing $[X_s Y_s]_\Lambda$ with $\langle X_s Y_s\rangle_\Lambda$ and its perturbations and responses to long-wavelength modes), the stress tensor can be recast in terms of familiar non-ideal fluid variables (at lowest order in smoothed variables):

$$\tau_{ij,\Lambda}^{\mathrm{UV}} = \delta_{ij}^{\mathrm{K}}\left(p_\Lambda + \bar{\rho}c_{s,\Lambda}^2\delta_\Lambda - \bar{\rho}\frac{c_{v,b,\Lambda}^2}{\mathcal{H}}\partial^k v_{k,\Lambda}\right) - \frac{3}{4}\bar{\rho}\frac{c_{v,s,\Lambda}^2}{\mathcal{H}}\left[\partial_i v_{j,\Lambda} + \partial_j v_{i,\Lambda} - \frac{2}{3}\delta_{ij}^{\mathrm{K}}\partial^k v_{k,\Lambda}\right] + \Delta\tau_{ij,\Lambda} + \cdots, \tag{4.6}$$

where p_Λ is an (isotropic) pressure, $\tilde{c}_{s,\Lambda}^2$ is the sound-speed, $\tilde{c}_{v,b,\Lambda}^2$ and $\tilde{c}_{v,s,\Lambda}^2$ are bulk and shear viscosities, and $\Delta\tau_\Lambda$ is a stochastic term uncorrelated with the smoothed fields. We have used a subscript Λ to indicate that each term arises from small-scale behavior at $k > \Lambda$. The form of the stress tensor could be alternatively derived by symmetry prescriptions: (4.6) is the unique $\mathcal{O}(\delta_\Lambda, \mathbf{v}_\Lambda)$ solution consistent with the equivalence principle (requiring at least second derivatives of ϕ) and symmetries of the known Universe (such as isotropy and homogeneity). Each term in (4.6) is fixed by the small-scale behavior of the fluid, e.g., the expectations $\langle\delta_s v_s\rangle$, $\partial\langle\delta_s v_s\rangle/\partial\delta_\Lambda$, *et cetera*. Technically speaking, the various coefficients encapsulate the *backreaction* of 'ultraviolet (UV) physics' of the Universe, *i.e.* that operating on scales beyond our cut-off Λ; furthermore, they are fully degenerate with the pressures, viscosities, *et cetera*, entering the original stress tensor τ. We absorb the latter quantities into the former hereafter, though return to this issue when considering renormalization below.

Let us pause briefly and discuss the consequences of the above results. Starting from the non-ideal fluid equations and smoothing on a scale Λ^{-1}, we have derived equations for the smoothed variables δ_Λ, $\mathbf{v}_\Lambda$ and ϕ_Λ. After coarse graining, we have found that the smoothed variables are described by the same equations as before, but with an extra stress tensor, which can be written in a form involving the usual microphysical variables, such as pressure and sound-speed. This is an important observation: even if the unsmoothed Universe was described by the perfect fluid equations (with $\tau = 0$), the smoothed Universe requires the imperfect fluid equations (or equivalently, the collisional Boltzmann hierarchy). As such, the appearance of a stress tensor is generic, and, given that we must work with smoothed variables to ensure perturbativity, forces us to always describe the the description of the Universe as a *non-ideal fluid*.

A second consequence is that our fluid equations necessarily depend on microphysical parameters, such as $\tilde{c}_s^2$, which describe the backreaction of small-scale physics onto the large-scale Universe. These are sourced by UV physics at $k > \Lambda$ (such as dark matter halo formation and baryonic effects), and, as such, cannot be predicted within our theoretical framework. Instead, they must be fit from data or simulations. At first glance, the appearance of free parameters in the theory may seem alarming. In fact, this is a common phenomenon, as can be seen from the following analogy. Consider the flow of water in a pipe. Usually, this is described by fluid equations, which necessarily include viscous stresses. At its heart, viscosity is a microphysical phenomenon arising from the interactions between individual atoms, and cannot be predicted by fluid dynamics; instead it must be measured by experiment or predicted using advanced quantum mechanics (the UV completion). If one omits viscosity from the equations, our fluid descriptions of water would break down; the same is true if one omits the small-scale backreactions in cosmology. Finally, we note that the limitation imprinted by unknown microphysical parameters is also a selling point for the theory: all relevant UV physics is contained within a small set of numbers that are fit from data. As such, the EFTofLSS does not need to make assumptions on small-scale dynamics, unlike simulation-based approaches, which can be biased by the omission of UV physics, such as hydrodynamics.

b. Solving the Fluid Equations Given the non-ideal fluid equations of (4.3) and an understanding of the UV stress tensor, we may now proceed to solve the system perturbatively and obtain predictions for the density field and its correlators. At linear order, we recover the same solution as in §3, noting that the terms sourced by the stress tensor contribute only at third order (after applying the long-short split). As such:

$$P_{\mathrm{linear}}^{\mathrm{EFT}}(k,\tau) = D^2(\tau)P_{\mathrm{L}}(k), \qquad (k < \Lambda). \tag{4.7}$$

At higher order, we can apply the same perturbative approaches as for SPT, yielding the following system of equations:

$$\dot{\delta}_\Lambda(\mathbf{k},\tau) + \theta_\Lambda(\mathbf{k},\tau) = \int_{\mathbf{p}_1\mathbf{p}_2} \alpha(\mathbf{p}_1,\mathbf{p}_2)\theta_\Lambda(\mathbf{p}_1,\tau)\delta_\Lambda(\mathbf{p}_2,\tau)(2\pi)^3\delta_{\mathrm{D}}\left(\mathbf{p}_1+\mathbf{p}_2-\mathbf{k}\right) \tag{4.8}$$

$$\dot{\theta}_\Lambda(\mathbf{k},\tau) + \mathcal{H}(\tau)\theta_\Lambda(\mathbf{k},\tau) + \frac{3}{2}\mathcal{H}^2(\tau)\Omega_m(\tau)\delta_\Lambda(\mathbf{k},\tau) = -\int_{\mathbf{p}_1\mathbf{p}_2} \beta(\mathbf{p}_1,\mathbf{p}_2)\theta(\mathbf{p}_1,\tau)\theta(\mathbf{p}_2,\tau)(2\pi)^3\delta_{\mathrm{D}}\left(\mathbf{p}_1+\mathbf{p}_2-\mathbf{k}\right) - \tau_{\theta,\Lambda}(\mathbf{k},\tau)$$

ignoring velocity vorticity for simplicity (though this can be generated at third order). The only differences between this and (3.8) is the use of smoothed fields and the appearance of the stress operator τ_θ in the final line. This is defined in real-space as

$$\tau_{\theta,\Lambda}(\mathbf{x},\tau) = \partial^i \frac{1}{\rho_\Lambda(\mathbf{x},\tau)}\partial^j \tau_{ij,\Lambda}^{\mathrm{UV}}(\mathbf{x},\tau) = \tilde{c}_{s,\Lambda}^2 \nabla^2 \delta_\Lambda(\mathbf{x},\tau) - \frac{1}{\mathcal{H}}(\tilde{c}_{v,b,\Lambda}^2 + \tilde{c}_{v,s,\Lambda}^2)\nabla^2\theta_\Lambda(\mathbf{x},\tau) + \cdots \tag{4.9}$$

$$= \left[\tilde{c}_{s,\Lambda}^2 + f(\tilde{c}_{v,b,\Lambda}^2 + \tilde{c}_{v,s,\Lambda}^2)\right](\tau)\nabla^2\delta_\Lambda(\mathbf{x},\tau) + \cdots,$$

where we have expanded to lowest order in δ_Λ in the final line (noting that the microphysical parameters start at second order). At this order, therefore, the backreaction of UV physics enters as an effective sound-speed $c_{s,\Lambda}^2 \equiv \left[\tilde{c}_{s,\Lambda}^2 + f(\tilde{c}_{v,b,\Lambda}^2 + \tilde{c}_{v,s,\Lambda}^2)\right]$.[3] To self-consistently account for the small-scale physics, we need simply solve the equations as before, but with an extra source of the form $c_{s,\Lambda}^2(\tau)k^2\delta_\Lambda(\mathbf{k},\tau)$. At higher-orders, the stress tensor contains more terms; this is relevant for two-loop calculations and beyond.

Up to third-order, we thus find the EFT prediction for the matter density field and velocity field:

$$\delta^{\mathrm{EFT}}(\mathbf{k},\tau) = D(\tau)\delta^{(1)}(\mathbf{k},\tau) + D^2(\tau)\delta_\Lambda^{(2)}(\mathbf{k},\tau) + D^3(\tau)\delta_\Lambda^{(3)}(\mathbf{k},\tau) - c_{s,\Lambda}^2(\tau)k^2 D(\tau)\delta^{(1)}(\mathbf{k},\tau) + \cdots \tag{4.10}$$

$$-\frac{1}{f(\tau)\mathcal{H}(\tau)}\theta^{\mathrm{EFT}}(\mathbf{k},\tau) = D(\tau)\theta^{(1)}(\mathbf{k},\tau) + D^2(\tau)\theta_\Lambda^{(2)}(\mathbf{k},\tau) + D^3(\tau)\theta_\Lambda^{(3)}(\mathbf{k},\tau) - c_{s,\Lambda}^2(\tau)D(\tau)k^2\delta^{(1)}(\mathbf{k},\tau) + \cdots,$$

where the first three terms match those predicted by SPT (though are defined only for $k < \Lambda$). The matter power spectrum (up to one-loop order), follows straightforwardly:

$$P_\Lambda^{\mathrm{EFT}}(k,\tau) = D^2(\tau)P_{\mathrm{L}}(k) + D^4(\tau)\left[2P_\Lambda^{(13)}(k) + P_\Lambda^{(22)}(k)\right] - 2c_{s,\Lambda}^2(\tau)D^2(\tau)k^2 P_{\mathrm{L}}(k) \tag{4.11}$$

At this order, there are two key differences between the SPT and EFTofLSS predictions: (1) the loop integrals extend only to Λ, since we have smoothed the fields, (2) the appearance of the final term involving the sound-speed $c_{s,\Lambda}^2$. As we shall see, the union of the two ensures that the theory is self-consistent, and that it yields accurate results.

  c.   *Renormalization*   Intrinsic to the above procedure was the smoothing scale, Λ^{-1}. Assuming $\Lambda < k_{\mathrm{NL}}$, we argued that the non-ideal fluid equations could be solved perturbatively, yielding loop integrals truncated at Λ, alongside the introduction of microphysical parameters such as $c_{s,\Lambda}^2$, describing the fluctuations of the field at $k > \Lambda$. Importantly, both the truncated loop integrals and the microphysical parameters will depend on the value adopted for Λ. This may seem alarming, since the physical Universe does not contain a fixed smoothing scale; rather this is a tool that we have added to the equations in order to simplify calculations, and decouple the short- and large-scale regime. As such, observables such as the power spectrum should not depend on our choice of Λ. In fact, the EFTofLSS predictions do *not* depend on Λ: the procedure for understanding this is known as 'renormalization', by analogy with similar approaches in quantum field theory. Here, we will paint a heuristic picture of renormalization: the finer mathematical details can be found in subsequent sections and associated works [e.g., 6, 7, 33].

We begin by examining the truncated $P^{(13)}$ loop integral, which has the explicit form:

$$P_\Lambda^{(13)}(k) = 3P_{\mathrm{L}}(k)\int_{|\mathbf{p}|<\Lambda} F_3(\mathbf{p},-\mathbf{p},\mathbf{k})P_{\mathrm{L}}(\mathbf{p}). \tag{4.12}$$

To understand the effects of the cut-off, it is instructive to consider varying it slightly, from $\Lambda \to \Lambda'$, where Λ is large. Inserting the high-p limit of the F_3 kernel, we can find the change in the loop integral:

$$P_{\Lambda'}^{(13)}(k) = P_\Lambda^{(13)}(k) - \frac{61}{210}k^2 P_{\mathrm{L}}(k)\int_\Lambda^{\Lambda'}\frac{p^2 dp}{6\pi^2}\frac{P_{\mathrm{L}}(p)}{p^2} \equiv P_\Lambda^{(13)}(k) - k^2 P_{\mathrm{L}}(k)[f(\Lambda') - f(\Lambda)], \tag{4.13}$$

---

[3] In full, there is an additional term appearing at this order, arising due to the stochastic stress $\Delta\tau_\Lambda$. Due to mass and momentum conservation, this is suppressed by k^2, and thus (for our Universe) smaller than two-loop contributions.

for some function $f(\Lambda)$. This has an important implication: as we vary Λ, the loop integral changes by an amount proportional to $k^2 P_{\mathrm{L}}(k)$, which takes the same form as the speed-of-sound term in (4.11). Furthermore, the microphysical parameter $c_{s,\Lambda}^2$ will also change as we increase Λ, since we include fewer small-scale modes, and, moreover, do so in such a way as to *exactly* cancel the change in $P^{(13)}$. For this reason, the $c_{s,\Lambda}^2$ term is known usually as an *ultraviolet counterterm* (with the sound-speed being a Wilson coefficient). The essence of renormalization is that, although the individual loop integrals ($P_{\Lambda}^{(13)}$) and counterterms ($c_{s,\Lambda}^2$) vary as a function of Λ, their sum does not: therefore the overall theory is independent of the cut-off scale Λ. Mathematically, this implies that

$$D^2(\tau)P_{\Lambda}^{(13)}(k) - c_{s,\Lambda}^2(\tau)k^2 P_{\mathrm{L}}(k) = D^2(\tau)P_{\Lambda'}^{(13)}(k) - c_{s,\Lambda'}^2(\tau)k^2 P_{\mathrm{L}}(k), \tag{4.14}$$

for all $\Lambda, \Lambda' \gg k$ and at all times τ. Roughly speaking, as we vary Λ, modes at $p \sim \Lambda$ shift from the loop integrals (where they are classed as long modes) to the microphysical parameters (being short modes). This conservation implies that our theory does not depend on Λ.

So far, we have considered only the 13-part of the matter power spectrum. However, renormalization is a general phenomenon and can be applied to any loop integral and any statistic. The 22-loop integral can be similarly analyzed by examining the dependence on the smoothing scale and identifying it with a relevant counterterm: in this case we find

$$P_{\Lambda'}^{(22)}(k) = P_{\Lambda}^{(22)}(k) + \frac{9}{98}k^4 \int_{\Lambda}^{\Lambda'} \frac{p^2 dp}{2\pi^2} \frac{P_{\mathrm{L}}^2(p)}{p^4}, \tag{4.15}$$

i.e. a cut-off dependence of the form k^4. This is matches by the lowest-order term in the stochastic stress tensor $\Delta\tau_{\Lambda}$, which enters the density field as $\delta^{\mathrm{EFT}}(\mathbf{k}, \tau) \supset \delta_J(\mathbf{k}, \tau)$ with $\langle \delta_J \delta_J \rangle \sim k^4$. In practice, this is small, and can usually be neglected. Combining the 13- and 22-type results we obtain the following one-loop EFTofLSS matter power spectrum:

$$P^{\mathrm{EFT}}(k, \tau) = D^2(\tau)P_{\mathrm{L}}(k) + D^4(\tau)\left[2P^{(13)}(k) + P^{(22)}(k)\right] - 2c_{s,\infty}^2(\tau)D^2(\tau)k^2 P_{\mathrm{L}}(k), \tag{4.16}$$

where we have taken Λ (formally) to infinity, noting that the results do not depend on this choice. We see that the SPT result (the first three terms) is modified only by the last piece, which is the EFTofLSS correction. Similar results can be derived for any spectrum of interest, including one-point functions [45], bispectra [46? –49], trispectra [50, 51], marked correlators [52, 53], lognormal spectra [54], and beyond.

d. Numerical Results In Fig. 1 we show a numerical calculation of the EFTofLSS matter power spectrum, as obtained with the CLASS-PT code [32]. At redshift-zero, we find good agreement of theory and simulations up to $k \approx 0.2h\,\mathrm{Mpc}^{-1}$, using the model of (4.16) with the c_s^2 counterterm fit from the N-body simulations. As expected, the inclusion of one-loop terms in the EFTofLSS model greatly improves the fit relative to the linear prediction; extension to two-loops improves this further (up to $k \approx 0.3h\,\mathrm{Mpc}^{-1}$). The difference between the EFTofLSS and SPT prescriptions can be attributed to the counterterm, *i.e.* that we allow for the backreaction of small-scale modes via the counterterm. From this plot, it is clear that the EFTofLSS satisfies our second criterion for a good theory, as laid out at the start of §3 (see also [55]).

e. Counterterms and Divergences Before proceeding to the extensions of the EFTofLSS, let us spend a moment considering the counterterms (or microphysical parameters) in greater depth. As noted above, the counterterms are the sum of two contributions: one from the physical non-idealities in the underlying fluid (known as the finite part), and the second arising from the smoothing operation (the infinite part), which depends on Λ. The two are fully degenerate, *i.e.* since smoothing is a necessary part of the theory, we can never extract the physical part itself; rather, the value measured in experiments always depends on how we computed the loop integrals. Since the counterterms cannot be predicted by theory (without knowledge of the UV completion), this is not a problem in practice.

Up to this point, our intuition for the counterterms has come from their microphysical origin, *i.e.* the appearance of a stress tensor in the fluid equations. In most modern works, however, the counterterms are derived not from the fluid equations, but from the loop integrals themselves. For example, the dependence of $P_{\Lambda}^{(13)}(k)$ on Λ informs us that the power spectrum must contain a counterterm of the form $g(\Lambda)k^2 P_{\mathrm{L}}(k)$ such that the full expression is independent of Λ. Such an argument does not require knowledge of the stress tensor, and is fully equivalent to our previous approaches (given that physical and Λ-dependent parts of the counterterms are always degenerate). This is of particular use when considering higher loop calculations, since one does not need to compute the stress tensor at high order; instead, one just considers the high-p (UV) limits of the relevant integrals.

Finally, let us consider the generality of our results, *i.e.* their dependence on the initial conditions. In §3, we considered the behavior of the SPT loop integrals for large internal momentum ($p \gg k$) and found them to be divergent for certain choices of power law cosmologies. In the EFTofLSS, however, there are no such divergences. This occurs

since the domain of integration is bounded; since p is limited by Λ and the integrand is analytic, the loop integrals are guaranteed to be finite. If there are divergences lurking in the high-p regime, they are themselves absorbed within the counterterms. Thus our third criterion for a good physical theory is satisfied.

f. *Summary* We conclude by summarizing the basic reasoning behind the EFTofLSS prescription. In brief, our pathway towards the density field model is the following:

1. **Smoothing**: To apply perturbation theory, we must work with a small expansion parameter. The usual density field in SPT is not guaranteed to be small, thus we smooth it on some characteristic wavenumber $\Lambda < k_{\mathrm{NL}}$.

2. **Non-Ideal Fluids**: To derive equations for the smoothed variables, we must smooth the fluid equations via a coarsening procedure. This generates a stress tensor, even if none was present in the unsmoothed theory.

3. **Stress Tensor**: By expanding the fields into long $(k < \Lambda)$ and short $(k > \Lambda)$ components, we can write the stress tensor in terms of microphysical parameters including pressures and sound speeds. This can also be derived purely from symmetry arguments. We then solve the resulting equations perturbatively, finding corrections to the SPT results in the form of counterterms.

4. **Renormalization**: Both the limits of the loop integrals and the counterterm parameters depend on our choice of smoothing scale. Since the overall predictions should be independent of Λ, the counterterms must absorb the cut-off dependence of the integrals. The resulting forms yield accurate predictions of matter correlators and do not suffer from UV divergences. Furthermore, it is agnostic to the details of small-scale physics.

In the succeeding sections, we discuss the extension of these ideas to more general scenarios, and related subtleties.

5. THE LAGRANGIAN DESCRIPTION

In fluid dynamics, there are two ways in which to describe the system: (1) in the observer's frame, or (2) in the fluid's frame. Up to now, we have considered the first scenario, which leads to the *Eulerian* EFTofLSS. However, we may equivalently work in the fluid frame, resulting in *Lagrangian* perturbation theory (LPT) and the counterterm corrections thereof. In the below, we will briefly outline this approach, working first in the pure LPT framework, before introducing the EFTofLSS corrections [e.g., 56–62].

a. **From Eulerian to Lagrangian Space* In the Eulerian picture we describe the cosmic fluid via its density and momentum variables. In contrast, the Lagrangian description considers the displacement of individual fluid elements from their initial positions, $\mathbf{q}$, to their late-time positions, $\mathbf{x}(\mathbf{q}, \tau)$ via the displacement vector $\boldsymbol{\Psi}$ (see [5] for a review):

$$\mathbf{x}(\mathbf{q}, \tau) = \mathbf{q} + \boldsymbol{\Psi}(\mathbf{q}, \tau). \tag{5.1}$$

We also note the following continuity relation:

$$d\mathbf{q} = [1 + \delta(\mathbf{x}, \tau)]d\mathbf{x}, \tag{5.2}$$

which follows from conservation of mass in the Eulerian (left) and Lagrangian (right) frame. Taking the Fourier transform of this, coupled with (5.1), we can write:

$$\int d\mathbf{q}\, e^{i\mathbf{k} \cdot (\mathbf{q} + \boldsymbol{\Psi}(\mathbf{q}, \tau))} = \int d\mathbf{x}\, e^{i\mathbf{k} \cdot \mathbf{x}}[1 + \delta(\mathbf{x}, \tau)] = (2\pi)^3 \delta_{\mathrm{D}}(\mathbf{k}) + \delta(\mathbf{k}, \tau); \tag{5.3}$$

this (exactly) defines the density field δ in terms of the displacement $\boldsymbol{\Psi}$. For example, in the limit of small $\boldsymbol{\Psi}$, we can expand the exponential, finding $\delta(\mathbf{k}, \tau) = i\mathbf{k} \cdot \boldsymbol{\Psi}(\mathbf{k}, \tau) + \cdots$.

b. **Solving for $\boldsymbol{\Psi}$* To proceed, we require the equations of motion for $\boldsymbol{\Psi}$. These can be derived from the Newtonian geodesic equations of motion for $\mathbf{x}$, combined with (5.1):

$$\ddot{\boldsymbol{\Psi}}(\mathbf{q}, \tau) + \mathcal{H}(\tau)\dot{\boldsymbol{\Psi}}(\mathbf{q}, \tau) = -\nabla_{\mathbf{x}}\phi(\mathbf{q} + \boldsymbol{\Psi}(\mathbf{q}, \tau), \tau), \tag{5.4}$$

noting that the derivative is with respect to the Eulerian coordinate $\mathbf{x}$. At linear order, the equation simplifies

$$\nabla \cdot \ddot{\boldsymbol{\Psi}}_1(\mathbf{q}, \tau) + \mathcal{H}(\tau)\nabla \cdot \dot{\boldsymbol{\Psi}}_1(\mathbf{q}, \tau) = -\frac{3}{2}\mathcal{H}^2(\tau)\Omega_m(\tau)\delta_1(\mathbf{q}, \tau), \tag{5.5}$$

taking the dot product and utilizing the Poisson equation. As in SPT, this is solved by asserting a separable solution, yielding

$$\boldsymbol{\Psi}_1(\mathbf{k}, \tau) = D(\tau)\frac{i\mathbf{k}}{k^2}\delta_{\mathrm{L}}(\mathbf{k}), \tag{5.6}$$

where $D(\tau)$ is the growth function used previously.

Beyond linear order, we may solve the LPT equation (5.4) by first rewriting it in Fourier-space:

$$\ddot{\boldsymbol{\Psi}}(\mathbf{k}, \tau) + \mathcal{H}(\tau)\dot{\boldsymbol{\Psi}}(\mathbf{k}, \tau) = \frac{3}{2}\mathcal{H}^2(\tau)\Omega_m(\tau)\int_{\mathbf{p}} \frac{i\mathbf{p}}{p^2}\delta(\mathbf{p}, \tau)\int d\mathbf{q}\, e^{-i\mathbf{k}\cdot\mathbf{q}}e^{i\mathbf{p}\cdot[\mathbf{q}+\boldsymbol{\Psi}(\mathbf{q}, \tau)]}, \tag{5.7}$$

where we have inserted the Poisson equation. The expression is then solved via perturbative expansion, defining the general solution:

$$\boldsymbol{\Psi}(\mathbf{q}, \tau) = \sum_{n=0}^{\infty} D^n(\tau)\boldsymbol{\Psi}^{(n)}(\mathbf{q}), \tag{5.8}$$

assuming approximate time-space separation (which becomes exact in the Einstein de-Sitter limit). As in the Eulerian case, the n-th order solution can be written as a convolution over n copies of the linear density field δ_{L}:

$$\boldsymbol{\Psi}^{(n)}(\mathbf{k}, \tau) = \frac{i}{n!}\int_{\mathbf{p}_1\cdots\mathbf{p}_n} \mathbf{L}_n(\mathbf{p}_1, \cdots, \mathbf{p}_n)\Big\{\delta_{\mathrm{L}}(\mathbf{p}_1)\cdots\delta_{\mathrm{L}}(\mathbf{p}_n)\Big\}(2\pi)^3\delta_{\mathrm{D}}\left(\mathbf{p}_1 + \cdots + \mathbf{p}_n - \mathbf{k}\right), \tag{5.9}$$

where $\mathbf{L}_n$ are the LPT kernels.[4] These kernels can be obtained from (5.7), and the first two take the form [cf. 23, 63]:

$$\mathbf{L}_1(\mathbf{k}) = \frac{\mathbf{k}}{k^2}, \qquad \mathbf{L}_2(\mathbf{p}_1, \mathbf{p}_2) = \frac{3}{7}\frac{\mathbf{k}}{k^2}\left[1 - \frac{(\mathbf{p}_1 \cdot \mathbf{p}_2)^2}{p_1^2 p_2^2}\right], \tag{5.10}$$

with $\mathbf{k} \equiv \mathbf{p}_1 + \mathbf{p}_2$.

c. *Correlators* Armed with the perturbative expansion for $\boldsymbol{\Psi}$, we can compute correlators of the matter density field. Using the relation between δ and $\boldsymbol{\Psi}$ (5.3), the power spectrum can be written at arbitrary order

$$
\begin{aligned}
P^{\mathrm{LPT}}(k, \tau) &= \int d\mathbf{q}\, d\mathbf{q}'\, e^{i\mathbf{k}\cdot(\mathbf{q}-\mathbf{q}')}\left\langle\left[e^{i\mathbf{k}\cdot\boldsymbol{\Psi}(\mathbf{q}, \tau)}-1\right]\left[e^{-i\mathbf{k}\cdot\boldsymbol{\Psi}(\mathbf{q}', \tau)}-1\right]\right\rangle \\
&= \int d\mathbf{q}\, e^{i\mathbf{k}\cdot\mathbf{q}}\left\langle\left[e^{i\mathbf{k}\cdot\Delta\boldsymbol{\Psi}(\mathbf{q}, \tau)}-1\right]\right\rangle,
\end{aligned} \tag{5.11}
$$

switching to relative variables in the second line and defining $\Delta\boldsymbol{\Psi}(\mathbf{q}, \tau) = \boldsymbol{\Psi}(\mathbf{q}, \tau) - \boldsymbol{\Psi}(\mathbf{0}, \tau)$. Whilst one could evaluate this by Taylor expanding the exponential, this is valid only if $\boldsymbol{\Psi}$ is small. Instead, we can proceed via the cumulant theorem, which states that $\left\langle e^{iX}\right\rangle = e^{-\left\langle X^2\right\rangle/2}$ for a mean-zero Gaussian random field X. For the first-order solution, this implies

$$P^{\mathrm{Zel}}(k, \tau) = \int d\mathbf{q}\, e^{i\mathbf{k}\cdot\mathbf{q}}\left[e^{-\frac{1}{2}\left\langle|\mathbf{k}\cdot\Delta\boldsymbol{\Psi}_1(\mathbf{q}, \tau)|^2\right\rangle}-1\right] = \int d\mathbf{q}\, e^{i\mathbf{k}\cdot\mathbf{q}}\left[\exp\left(D^2(\tau)k_i k_j\int_{\mathbf{p}} \frac{p^i p^j}{p^4}P_{\mathrm{L}}(p)\left(e^{i\mathbf{q}\cdot\mathbf{p}}-1\right)\right)-1\right] \tag{5.12}$$

which is usually known as the *Zel'dovich* solution [e.g., 61]. In the second equality, we have evaluated the expectation in terms of the $\boldsymbol{\Psi}^{(1)}$ functions and simplified. The remaining integral can be simplified further, yielding

$$P^{\mathrm{Zel}}(k, \tau) = \int d\mathbf{q}\, e^{i\mathbf{k}\cdot\mathbf{q}}\exp\left(-D^2(\tau)k^2\int \frac{p^2 dp}{2\pi^2}\frac{P_{\mathrm{L}}(p)}{p^2}\left[\frac{1}{3}\left(1 - j_0(pq) - j_2(pq)\right) + (\hat{\mathbf{k}}\cdot\hat{\mathbf{q}})^2 j_2(pq)\right]\right), \tag{5.13}$$

dropping a term contributing only to $\mathbf{k} = \mathbf{0}$.

Beyond leading order, the LPT power spectra can be evaluated by Taylor expansions of the form:

$$e^{i\mathbf{k}\cdot\Delta\boldsymbol{\Psi}(\mathbf{q}, \tau)} = e^{iD(\tau)\mathbf{k}\cdot\Delta\boldsymbol{\Psi}^{(1)}(\mathbf{q}, \tau)}\left[1 - iD^2(\tau)\mathbf{k}\cdot\Delta\boldsymbol{\Psi}^{(2)}(\mathbf{q}, \tau) - iD^3(\tau)\mathbf{k}\cdot\Delta\boldsymbol{\Psi}^{(3)}(\mathbf{q}, \tau) + \cdots\right], \tag{5.14}$$

---

[4] Note that, by convention, this expression contains an extra factor of $i/n!$ compared to the SPT equivalent.

where we expand higher order terms (assuming them to be small), but leave the Gaussian piece ($\mathbf{\Psi}^{(1)}$) exponentiated. The resulting expressions can be evaluated in terms of the linear power spectrum using cumulant theorems of the form

$$\left\langle (iX)^n e^{iX} \right\rangle \equiv \left(\frac{\partial}{\partial t} \right)^n \left[e^{-\frac{t^2}{2} \langle X^2 \rangle} \right] \Big|_{t=1}, \tag{5.15}$$

where X is some linear function of δ_{L}. Such results have been used to obtain the LPT power spectra and bispectra to high loop order [62]; we will not quote the results here for the sake of brevity, but note that their form generically involves loop integrals over copies of the linear power spectrum.

Before continuing, let us briefly remark on the differences between SPT and LPT. Both approaches employ solve their defining equations as perturbative expansions in the first-order solution, be it $\delta^{(1)} \equiv \delta_{\mathrm{L}}$ or $\Psi^{(1)}$. Since the underlying equations are equivalent, one might expect LPT and SPT to produce the same correlators. In fact, this is not the case, as can be seen from comparing the first-order solutions: P_{L} (SPT) and the Zel'dovich power spectrum (5.13). The main difference arises since we left the first-order displacement exponentiated in the LPT derivation; as such, the solution contains exponentials in P_{L}. In the limit of small power spectra, we can expand this term finding

$$P^{\mathrm{Zel}}(k, \tau) = D^2(\tau) P_{\mathrm{L}}(k) + \cdots, \tag{5.16}$$

dropping terms at second order in $P_{\mathrm{L}}(k)$. Thus, the first-order LPT and SPT solutions agree to $\mathcal{O}(P_{\mathrm{L}})$. This is a general result: it can be shown that, at any given order, the LPT solution is equivalent to that of SPT, with differences arising only from terms of higher order.

d. *Small-Scale Contributions* Having outlined the standard formulation of LPT, we now turn to its modifications within the EFTofLSS [e.g., 57–60]. The overall picture is similar to that of §4; the conventional procedure does not correctly account for non-perturbative matter fluctuations on small-scales, which leads to inaccurate predictions for cosmological correlators.

Analogous to the Eulerian case, we begin by reformulating the theory in terms of smoothed variables, here the displacement field and peculiar potential:

$$\mathbf{\Psi}(\mathbf{q}, \tau) \to \mathbf{\Psi}_\Lambda(\mathbf{q}, \tau), \quad \phi(\mathbf{x}, \tau) \to \phi_\Lambda(\mathbf{x}, \tau). \tag{5.17}$$

The equation of motion (5.4) is transformed as

$$\begin{aligned} \ddot{\mathbf{\Psi}}_\Lambda(\mathbf{q}, \tau) + \mathcal{H}(\tau) \dot{\mathbf{\Psi}}_\Lambda(\mathbf{q}, \tau) &= -\left[\nabla_{\mathbf{x}} \phi(\mathbf{q} + \mathbf{\Psi}(\mathbf{q}, \tau), \tau) \right]_\Lambda \\ &= -\nabla_{\mathbf{x}} \phi_\Lambda(\mathbf{q} + \mathbf{\Psi}_\Lambda(\mathbf{q}, \tau), \tau) + \mathbf{a}_\Lambda(\mathbf{q}, \mathbf{\Psi}_\Lambda(\mathbf{q}, \tau), \tau) \end{aligned} \tag{5.18}$$

,

where, in the second line we separate out the usual gradient term (in ters of smoothed variables) and a new acceleration piece. The latter arises from small-scale fluctuations at $k > \Lambda$, which are present due to the non-linear structure of $\nabla_{\mathbf{x}} \phi(\mathbf{q} + \mathbf{\Psi}(\mathbf{q}, \tau), \tau)$.

As before, the precise source term $\mathbf{a}_\Lambda$ cannot be predicted within our smoothed theory; it is set by the dynamics of the short-wavelength fields. Rather than consider this explicitly (see [57] for details), we here derive its physical form by symmetry arguments, importantly including its dependence on the smoothed (long-wavelength) variables in our theory. Given that $\mathbf{a}$ must transform as a vector and obey the equivalence principle, as well as isotropy and homogeneity, the simplest dependence of $\mathbf{a}$ on δ_Λ must be a term involving $\nabla\delta$. At leading order in δ_Λ, we therefore find:

$$\mathbf{a}_\Lambda(\mathbf{q}, \mathbf{\Psi}_\Lambda(\mathbf{q}, \tau), \tau) = \mathbf{a}_{0,\Lambda}(\tau) + a_{1,\Lambda}(\tau) \nabla_{\mathbf{x}} \delta_\Lambda(\mathbf{q} + \mathbf{\Psi}(\mathbf{q}, \tau), \tau) + \cdots, \tag{5.19}$$

where $\mathbf{a}_{0,\Lambda}$ is a piece uncorrelated with the large-scale modes, and $a_{1,\Lambda}$ is a (Wilson) coefficient whose value cannot be predicted by theory. Here, the free coefficients $\mathbf{a}_{0,\Lambda}$ and $a_{1,\Lambda}$ act analogously to the pressures and sound-speeds entering the Eulerian description (which could also be obtained from symmetry arguments).

To obtain the EFTofLSS prediction for the LPT power spectra, we must thus solve the equations of motion in the presence of the counterterms involving $\mathbf{a}_\Lambda$. This yields a simple modification to the previous results:

$$\mathbf{\Psi}_\Lambda^{\mathrm{EFT}}(\mathbf{k}, \tau) = D(\tau) \mathbf{\Psi}^{(1)}(\mathbf{k}, \tau) + D^2(\tau) \mathbf{\Psi}_\Lambda^{(2)}(\mathbf{k}, \tau) + D^3(\tau) \mathbf{\Psi}_\Lambda^{(3)}(\mathbf{k}, \tau) + \boldsymbol{\alpha}_{0,\Lambda}(\tau) + \alpha_{1,\Lambda}(\tau) D(\tau) (i\mathbf{k}) \delta_\Lambda^{(1)}(\mathbf{k}, \tau) + \cdots \tag{5.20}$$

where $\alpha_{i,\Lambda}$ encode the small-scale physics. As in SPT, the presence of smoothing also instructs us to truncate any loop integrals at momentum Λ. Given these results, we can compute arbitrary correlators, though caution that these are
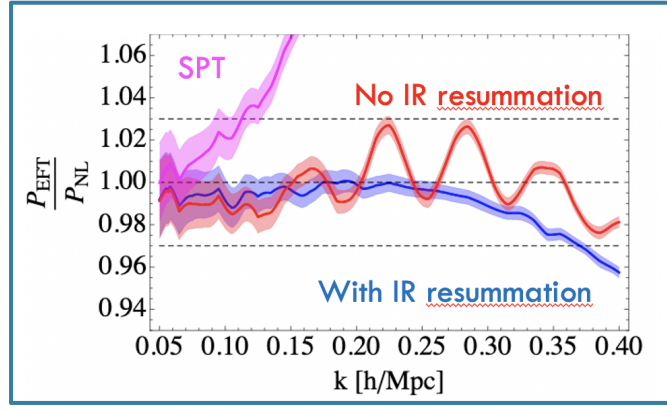
FIG. 2. The impact of infra-red resummation on the matter power spectrum. We plot the ratio of perturbative predictions for the matter power spectrum to that obtained from simulations for three models: two-loop SPT (pink); the EFTofLSS without IR resummation (red); the EFTofLSS including IR resummation (blue). The pre-resummed spectra exhibit additional wiggles in the fit, due to mistreatment of non-perturbative displacements. IR resummation recitifies this, resulting in a much improved fit to data. Figure adapted from [64].

usually more involved than their SPT equivalents. Whilst we do not give the full forms here, let us consider briefly the effects of the counterterms on the one-loop power spectrum (working to leading order in P_{L}):

$$P^{\mathrm{LPT-EFT}}(k,\tau) = P_{\Lambda}^{\mathrm{LPT}}(k,\tau)\left[1 - \tilde{\alpha}_{\Lambda}(\tau)k^2 + \cdots\right]. \tag{5.21}$$

As before, the counterterm gives a correction of the form $k^2 P_{\mathrm{L}}(k)$ accompanied by an unknown coefficient $\tilde{\alpha}_{\Lambda}(\tau)$. As in §4, this has two contributions: (a) a piece absorbing the cut-off dependence of the theory, ensuring that the final correlator is independent of Λ and thus renormalized; (b) a term encapsulating small-scale physics that cannot be modelled by the smoothed theory. With its inclusion, we can obtain good fits of theory to data, whose accuracy increases as we include higher loops (and thus more counterterms) in the theory.

6. INFRARED RESUMMATION

We now turn to one of the more mysterious facets of the EFTofLSS: infrared (IR) resummation. As before, our emphasis is on physical intuition rather than mathematical completeness, so the discussion herein will be somewhat heuristic (though we note that all results have been proved precisely elsewhere [e.g. 48, 64–70]).

In short, infrared resummation is a procedure induced to fix a shortcoming in the Eulerian formulation of the EFTofLSS, which causes the resulting power spectra to be overly wiggly (first described in [64]). This is shown in Fig. 2; we note that the ratio of EFTofLSS to simulated spectra (red) exhibits percent-level oscillations around the baryon acoustic oscillation (BAO) frequency. Although the model correctly predicts the overall shape of the spectrum (known as the broadband), it fails to fully capture the oscillations. Physically, the reason behind this is as follows. In the initial conditions, the BAO feature is a sharp oscillation induced by the preferred clustering of matter on distances of $r \sim 100 h^{-1}\mathrm{Mpc}$. As the Universe evolves, galaxies shift relative to their initial positions due to large-wavelength bulk flows, thus any formerly sharp phenomenon gets blurred out on the scale of displacement scale. For correlators such as the matter power spectrum, such features manifest themselves as bumps or wiggles, whose amplitudes must decay with time. This is damping is not captured by pure Eulerian theories.

a. Long-Wavelength Displacements in the EFTofLSS Why do Eulerian theories fail to model the blurring of primordial features? To understand this, we must look to the Lagrangian picture. In particular, we recall the relation between the density field δ and the displacement $\boldsymbol{\Psi}$ given in (5.3):

$$\delta(\mathbf{k},\tau) = \int d\mathbf{q}\, e^{i\mathbf{k}\cdot\mathbf{q}}\left(e^{i\mathbf{k}\cdot\boldsymbol{\Psi}(\mathbf{q},\tau)} - 1\right) \stackrel{?}{=} \int d\mathbf{q}\, e^{i\mathbf{k}\cdot\mathbf{q}}\left(i\mathbf{k}\cdot\boldsymbol{\Psi}(\mathbf{q},\tau) - \frac{1}{2}(\mathbf{k}\cdot\boldsymbol{\Psi}(\mathbf{q},\tau))^2 + \cdots\right). \tag{6.1}$$

Under-the-hood, any Eulerian perturbation theory proceeds by Taylor expanding the exponential term (as in the right-hand equation), and assuming the displacements to be small. However, this assumption may be invalid! Working

in the Zel'dovich limit (where $\mathbf{\Psi}(\mathbf{k}, \tau) = (i\mathbf{k}/k^2)D(\tau)\delta_{\mathrm{L}}(\mathbf{k})$), we can estimate the mean square displacement:

$$\sigma_\Psi^2(\tau) \equiv \frac{1}{3} \left\langle \mathbf{\Psi}_{\mathrm{Zel}}(\mathbf{q}, \tau) \cdot \mathbf{\Psi}_{\mathrm{Zel}}^*(\mathbf{q}, \tau) \right\rangle = D^2(\tau) \int \frac{k^2 dk}{6\pi^2} \frac{P_{\mathrm{L}}(k)}{k^2}; \tag{6.2}$$

for our Universe the integral yields $\approx 20h^{-1}\mathrm{Mpc}$. Importantly, this scale is large, which indicates (a) that considerable smoothing of the BAO feature has occurred, and (b) that we should not have Taylor expanded the displacement term. A formal statement of this problem is that Eulerian perturbation theories incorrectly treat long-wavelength displacements (on scales σ_Ψ) by assuming them to be perturbative.

One may ask why this effect only impacts features in the power spectrum, *i.e.* why the broadband shape is unaffected. This can be simply demonstrated by symmetry arguments: bulk flows must conserve both mass and momentum, which implies that their corrections to the broadband power spectrum must enter only at k^4 (since integrated mass scales as k^0 and momentum as k^2). These corrections are highly subdominant to standard one- and two-loop corrections. We further note that this problem is generic: semi-analytic models based on linear theory (such as halofit [21, 22]), also exhibit spurious enhancements of the BAO wiggles at low redshift. Furthermore, it applies similarly to any other sharp primordial features [e.g., 71], if present.

b. Solution: Heuristic Picture The above discussion gives hints as to how this effect can be ameliorated. Whilst leaving the entire displacement exponentiated would solve the problem (and is the approach of conventional Lagrangian treatments, cf. §5), the resulting integrals are difficult to compute, and, working in an Eulerian framework is often desirable. A more practical method is to instead leave only part of the displacement term exponentiated, *i.e.* that corresponding to long-wavelength displacements [e.g., 48, 69, 70]. We briefly outline this below in the context of the matter power spectrum.

To separate out the impact of bulk flows on the broadband and features, it is useful to decompose the primordial matter power spectrum into two pieces, denoted 'non-wiggly' and 'wiggly':

$$P_{\mathrm{L}}(k) = P_{\mathrm{L,nw}}(k) + P_{\mathrm{L,w}}(k), \tag{6.3}$$

where oscillations appear only in the latter component. This can be done via discrete sine transforms, and is usually implemented such that wiggly spectra do not contribute to displacement terms (*i.e.* $\sigma_\Psi^2 = 0$ if one replaces P_{L} with $P_{\mathrm{L,w}}$ in 6.2). Next, we take the defining equation for LPT power spectra (5.11), which can be written [e.g., 61]

$$(2\pi)^3\delta_{\mathrm{D}}(\mathbf{k}) + P(k, \tau) \equiv \int d\mathbf{q}\, e^{i\mathbf{k}\cdot\mathbf{q}} \exp\left(-\frac{1}{2} k_i k_j A^{ij}(\mathbf{q}, \tau) + \cdots\right), \tag{6.4}$$

where $A^{ij}(\mathbf{q}, \tau) = \left\langle \Delta\Psi^i(\mathbf{q}, \tau)\Delta\Psi^j(\mathbf{q}, \tau) \right\rangle$ and the ellipsis represents higher-order cumulants. At leading order, the variance takes the form

$$A^{ij}(\mathbf{q}, \tau) = 2D^2(\tau) \int_{\mathbf{p}} \frac{p^i p^j}{p^4} P_{\mathrm{L}}(p) \left(1 - e^{i\mathbf{p}\cdot\mathbf{q}}\right) + \cdots \equiv A_{\mathrm{lin}}^{ij}(\mathbf{q}, \tau) + \cdots \tag{6.5}$$

(cf. 5.12). Utilizing the above wiggly-smooth decomposition, this can be written as the sum of two pieces: $A_{\mathrm{nw}}^{ij} + A_{\mathrm{w}}^{ij}$, where the first takes the form of (6.5) but using only the broadband power spectrum $P_{\mathrm{L,nw}}$, and the second is the remainder. Schematically, this gives the following power spectrum (dropping a term contributing only to $\mathbf{k} = \mathbf{0}$)

$$P(k, \tau) = \int d\mathbf{q}\, e^{i\mathbf{k}\cdot\mathbf{q}} \exp\left(-\frac{1}{2} k_i k_j \left[A_{\mathrm{nw}}^{ij}(\mathbf{q}, \tau) + A_{\mathrm{w}}^{ij}(\mathbf{q}, \tau)\right] + \text{higher-order}\right). \tag{6.6}$$

Up to this point, we have made no approximations, with (6.6) being simply a rearrangement of the previous LPT power spectrum. The trick of IR resummation is to perform a *partial* Taylor expansion of this expression, expanding lower order terms whilst keeping the first-order part of A_{nw}^{ij} exponentiated. This works since the non-perturbative displacements are confined to the no-wiggle variance A_{nw}^{ij} (by definition of P_{w}), and are primarily sourced at linear order, *i.e.* by $A_{\mathrm{lin,nw}}^{ij}$. Again working schematically, we find the following IR-resummed expression (derived in [69]):

$$P^{\mathrm{IR-res}}(k, \tau) = \int d\mathbf{q}\, e^{i\mathbf{k}\cdot\mathbf{q}} e^{-\frac{1}{2} k_i k_j A_{\mathrm{lin,nw}}^{ij}(\mathbf{q}, \tau)} \left(1 + \text{higher-order no-wiggle}\right) \tag{6.7}$$

$$+ \int d\mathbf{q}\, e^{i\mathbf{k}\cdot\mathbf{q}} e^{-\frac{1}{2} k_i k_j A_{\mathrm{lin,nw}}^{ij}(\mathbf{q}, \tau)} \left(-\frac{1}{2} k_i k_j A_{\mathrm{lin,w}}^{ij}(\mathbf{q}, \tau) + \text{higher-order wiggly}\right),$$

which can be extended to arbitrary order. Noting that long-wavelength displacements do not affect the broadband, the first term is just the usual power spectrum (evaluated using SPT, or the EFTofLSS), except with the linear power

spectrum replaced by its dewiggled equivalent, which we will write as $P_{\mathrm{nw}}(k,\tau)$ to all orders. Following some a little algebra (analogous to that done for the Zel'dovich spectrum in §5), the second can be written

$$P^{\mathrm{IR-res}}(k,\tau) - P_{\mathrm{nw}}(k,\tau) = e^{-k^2\Sigma^2(\tau)}\left(D^2(\tau)P_{\mathrm{L,w}}(k) + \text{higher-order wiggly}\right). \qquad (6.8)$$

Thus, the wiggly part is damped by a scale Σ, given by

$$\Sigma^2(\tau) \approx D^2(\tau)\int_0^{0.2h\,\mathrm{Mpc}^{-1}}\frac{p^2dp}{6\pi^2}\frac{P_{\mathrm{L,nw}}(p)}{p^2}\left[1 - j_0(pq_{\mathrm{BAO}}) + j_2(pq_{\mathrm{BAO}})\right]; \qquad (6.9)$$

this gives the characteristic amplitude of bulk flows at the BAO wavenumber, $q_{\mathrm{BAO}} \approx 2\pi/100h\,\mathrm{Mpc}^{-1}$.

Collecting results, the leading-order IR-resummed power spectrum is given by

$$P^{\mathrm{IR-res}}_{\mathrm{lin}}(k,\tau) = D^2(\tau)\left[P_{\mathrm{L,nw}}(k) + e^{-k^2\Sigma^2(\tau)}P_{\mathrm{L,w}}(k)\right], \qquad (6.10)$$

since $P_{\mathrm{nw}}(k,\tau) = D^2(\tau)P_{\mathrm{L,nw}}(k)$ at leading order. Here, we see that IR resummation has achieved the desired result: it has suppressed the BAO wiggles by an appropriate factor, whilst leaving the broadband unchanged (at least up to two-loop terms). A similar calculation can be used to compute the one-loop EFTofLSS power spectrum, including IR resummation. In this case, we find [70]

$$\begin{aligned} P^{\mathrm{IR-res}}_{1-\mathrm{loop}} &= D^2(\tau)\left[P_{\mathrm{L,nw}}(k) + e^{-k^2\Sigma^2(\tau)}(1 + k^2\Sigma^2(\tau))P_{\mathrm{L,w}}(k)\right] \\ &\quad + D^4(\tau)\left[P_{1-\mathrm{loop,nw}}(k) + e^{-k^2\Sigma^2(\tau)}P_{1-\mathrm{loop,w}}(k)\right]. \end{aligned} \qquad (6.11)$$

This involves two one-loop terms: the no-wiggle term is given by the usual EFTofLSS (or SPT) formulae with P_{L} replaced by $P_{\mathrm{L,nw}}$, and the second is the difference, *i.e.* $P_{1-\mathrm{loop}} - P_{1-\mathrm{loop,nw}}$. As before, the action of IR resummation is to suppress the wiggly contributions; here, we note that the linear piece contains an extra factor $(1 + k^2\Sigma^2)$ to avoid double-counting of long-wavelength displacements, since this factor has already been expanded from the exponential in the one-loop terms. The resulting power spectrum (at two-loop order) is shown in Fig. 2, and, as expected, finds a much improved fit to the data, without the spurious wiggles (though applicable to the same range of scales, since we have not modified the broadband).

Though our derivation here has been heuristic, the above ideas can be formalized precisely. This has been achieved both with reference to Lagrangian perturbation theory and via the mechanics of 'time-sliced perturbation theory'; the interested reader can consult [67, 68] for further details. We finally note that the above procedure extends similarly to higher-order statistics; we once again find that the non-wiggly parts of the spectrum are unaffected, whilst the wiggly components are suppressed by factors akin to $e^{-k^2\Sigma^2}$.

c. *Solution: Exact Picture* The above IR resummation procedure (based on wiggly-smooth decompositions) is accurate and has been successfully applied to data on a number of occasions, with any approximations incurring errors that are always loop-suppressed. For completeness however, we note an alternative procedure that does not require such decompositions, based on [64–66]. This is the original manner in which IR resummation was conceived.

This procedure starts by identifying two parameters intrinsic to perturbative solutions of the matter power spectrum [cf. 64]:

$$\epsilon_\delta(k,\tau) = D^2(\tau)\int_0^k\frac{p^2dp}{2\pi^2}P_{\mathrm{L}}(p), \qquad \epsilon_\Psi(k,\tau) = k^2D^2(\tau)\int_0^k\frac{p^2dp}{6\pi^2}\frac{P_{\mathrm{L}}(p)}{p^2}, \qquad (6.12)$$

which control the amplitude of density perturbations (equal to the variance of the smoothed field Λ) and long-wavelength displacements respectively (analogus to σ_Ψ^2 in 6.2). In the conventional perturbative solution of the fluid equations, we implicitly perform a Taylor expansion in both variables; in practice, the latter parameter is not small, sourcing the underdamped wiggles. In the approach of [64], one recasts the solutions as Taylor series only in ϵ_δ (which are valid on perturbative scales), avoiding the requirement of small ϵ_Ψ.

In practice, this is done by working with the Lagrangian kernel

$$K(\mathbf{k},\mathbf{q},\tau) = \left\langle e^{i\mathbf{k}\cdot\Delta\mathbf{\Psi}(\mathbf{q},\tau)}\right\rangle = \exp\left(-\frac{1}{2}k_ik_jA^{ij}(\mathbf{q},\tau) + \cdots\right), \qquad (6.13)$$

as in (6.4), dropping higher-order cumulants. This can be Taylor expanded up to N-th order in two ways: (a) as a double power series in ϵ_δ and ϵ_Ψ, denoted $K|_N$; (b) as a power series only in ϵ_δ (leaving other terms in the exponential),

denoted $K|_N$. Denoting the lowest-order (Zel'dovich) solution as K_0, the N-th order term can be written:

$$K(\mathbf{k}, \mathbf{q}, \tau)\big|_N \approx K_0(\mathbf{k}, \mathbf{q}, \tau) \cdot \frac{K(\mathbf{k}, \mathbf{q}, \tau)}{K_0(\mathbf{k}, \mathbf{q}, \tau)}\bigg\|_N \tag{6.14}$$

$$= \sum_{j=0}^{N} \left(K_0(\mathbf{k}, \mathbf{q}, \tau) \cdot K_0^{-1}(\mathbf{k}, \mathbf{q}, \tau)\big\|_{N-j} \right) \cdot K_j(\mathbf{k}, \mathbf{q}, \tau).$$

In the first line, we have multiplied and divided by the Gaussian solution, and noted that we can replace the exact ratio ($[K/K_0]|_N$) with that truncated at N-th order also in ϵ_Ψ ($[K/K_0]|_N$), since long-wavelength displacements mostly cancel in the ratio. In the second line, we have rewritten the ratio as a product of two terms (valid to N-th order in ϵ_δ), where $K_j(\mathbf{q}, \mathbf{k}, \tau)$ represents the j-th order term (in both expansion parameters). Whilst this may seem only to be a gimmick, it is relatively fundamental, since we have expressed the full kernel (including long wavelength modes) in terms of expressions with the long-wavelengths mdes expanded (*i.e.* a Taylor series in ϵ_Ψ), which can be evaluated with the usual EFTofLSS (or SPT) formulae.

To proceed, we can insert (6.14) into the relevant correlators, such as the matter power spectrum. At N-th order in ϵ_δ, *i.e.* $(N-2)/2$ loops

$$P^{\mathrm{IR-res}}(k, \tau)\big|_N = \int d\mathbf{q}\, e^{i\mathbf{k}\cdot\mathbf{q}} \sum_{j=0}^{N} F_{||_{N-j}}(\mathbf{k}, \mathbf{q}, \tau) \cdot K_j(\mathbf{k}, \mathbf{q}, \tau), \tag{6.15}$$

defining

$$F_{||_{N-j}}(\mathbf{k}, \mathbf{q}, \tau) = K_0(\mathbf{k}, \mathbf{q}, \tau) \cdot K_0^{-1}(\mathbf{k}, \mathbf{q}, \tau)\big\|_{N-j}. \tag{6.16}$$

Here, the relevant power spectrum kernel is the usual form K_j, Taylor expanded as per usual perturbative prescriptions, and a new kernel $F_{||N-j}$, which corrects for the effects of this expansion. Following a little manipulation, the final result can be easily expressed in real-space, through the correlation function $\xi(\mathbf{r})$ at $(N-2)/2$-loop order:

$$\xi^{\mathrm{IR-res}}(r, \tau)\big|_N = \sum_{j=0}^{N} \int_0^\infty q^2 dq\, P_{\mathrm{int}||_{N-j}}(r, q, \tau)\xi_j(q, \tau). \tag{6.17}$$

This is a summation of conventional EFTofLSS (or SPT) correlators, $\xi_j(q, \tau)$, multiplied by the probability a fluid element at $\mathbf{q}$ moves a distance $\mathbf{r}$:

$$P_{\mathrm{int}||_{N-j}}(r, q, \tau) = \int_{\mathbf{p}} e^{i\mathbf{p}\cdot(\mathbf{q}-\mathbf{r})} F_{||_{N-j}}(\mathbf{p}, \mathbf{q}, \tau). \tag{6.18}$$

In practice, these can be straightforwardly computed using Fast Fourier transforms, facilitating accurate comparison of theory and data. To close, we note that the above approaches can be extended to higher-order statistics such as bispectra, as well as the complexities of redshift-space and biased tracers, and permit a number of simplifications [e.g., 65, 66]. Finally, we note that the two approaches described above are equivalent at any given order in perturbation theory, and EFTofLSS implementations vary as to which is adopted.

d. Summary We finish this section with an recapitulation of the whys, hows, and wherefores of IR resummation:

1. **Bulk Flows**: Long-wavelength displacements move matter on scales $\sim 20h^{-1}\mathrm{Mpc}$ from the Universe's initial conditions to today, thus blurring out any sharp features in the primordial distribution such as baryon acoustic oscillations.

2. **Perturbativity**: The SPT and EFTofLSS formulations described in §3 and §4 implicitly assume these displacements to be small, and expand them from the exponential. This causes an underdamping of wiggly features in the spectra, but, by mass and momentum conservation, does not affect the broadband.

3. **Resummation**: IR resummation ameliorates this issue by keeping the long-wavelength displacement exponentiated, *i.e.* expanding only in perturbative small-wavelength corrections. This can be done either as a formal expansion series in the relevant kernels, or by splitting the spectra into smooth and wiggly components, and damping the latter appropriately.

4. **Results**: Comparing standard and IR-resummed EFTofLSS power spectra, we find much improved results in the latter case, without spurious oscillations.

In what follows, we will assume IR resummation is included whenever the EFTofLSS is discussed.

7. BIASED TRACERS

Up to this point, we have considered only the statistics of dark matter fluctuations in the Universe. In practice, most observational probes measure either the integrated mass distribution (weak lensing) or the galaxy distribution (photometric or spectroscopic surveys). For this reason, we now discuss biasing, and the associated calculation of galaxy power spectra and beyond. Detailed discussion of the EFTofLSS approach to biasing (and its precursors) can be found in [e.g., 72–92].

a. The Eulerian Bias Expansion   Biasing explores the relation of the dark matter density field with that of galaxies, dark matter halos, 21-cm emission, Lyman-alpha flux and beyond (see [78] for a comprehensive review). Given a general tracer with overdensity δ_g, we can compute correlation functions using the EFTofLSS if we understand the relation between δ_g and the matter field $\delta(\mathbf{k}, \tau)$. Various options exist for modeling this, including a number of semi-analytic approaches such as halo models, halo-occupation distributions and halo abundance matching. In general, these propose some scheme for associating galaxies or diffuse emission with dark matter halos identified in simulations (or stochastically, for the halo model), depending on the sources of interest. In perturbation theory, one does not have access to individual dark matter halos (though field-level approaches can predict these to high accuracy), nor to the UV physics that sets galaxy formation physics. As such, we seek an analytic relation between tracers and dark matter, that can be expressed as a perturbative expansion.

In the simplest approach, one writes the tracer field δ_g as a Taylor expansion in the Eulerian density field δ, such that, in real-space:

$$\delta_g(\mathbf{x}, \tau) = \sum_{n=1}^{\infty} \frac{b_n(\tau)}{n!} \left[\delta_\Lambda(\mathbf{x}, \tau)\right]^n, \tag{7.1}$$

where $\{b_n\}$ are bias parameters and δ_Λ is the matter density field smoothed on some wavenumber Λ. We will leave the smoothing implicit from now on, but return to its impact below. The bias coefficients are not known *a priori*, but can be estimated from simulations and observational data, just like the counterterm parameters. In the EFTofLSS solutions discussed in §4, the expansion parameter was given by $\sigma_\delta(k) \sim k/k_{\mathrm{NL}}$; here, the perturbative variable is kR_{halo}, for some characteristic halo scale R_{halo}. If $R_{\mathrm{halo}}^{-1} < k_{\mathrm{NL}}$, our theories will be limited by the non-linearities of halo formation; if the opposite holds, matter non-linearities are dominant. In this case, alternative approaches such as hybrid EFTofLSS scheme (combining bias expansions with simulations) may be of use [93, 94], though we caution that this requires Lagrangian bias $b_1^{\mathrm{L}} < 1$.

In practice, the bias expansion given in (7.1) is not the whole story, since the tracer field δ_g can depend on δ_R in other manners. For example, it can correlate with the tidal field, s_{ij}, defined as

$$s_{ij}(\mathbf{x}, \tau) = \left[\frac{\partial_i \partial_j}{\partial^2} - \frac{1}{3}\delta_{ij}^{\mathrm{K}}\right] \delta(\mathbf{x}, \tau), \tag{7.2}$$

or non-locally, via the gradient $\nabla^2\delta$. We refer to these functions as *bias operators*, *i.e.* combinations of the matter density field which the tracer field depends on. The EFTofLSS approach to galaxy biasing is the following [e.g., 72–74, 76, 77, 82, 83, 87, 90]:

1. At a given order N, write down all N-th order bias operators, $\{\mathcal{O}\}$, consistent with the symmetries.

2. Orthogonalize to remove degenerate operators.

3. Write the N-th order solution as a sum over all operators, each with a free bias coefficient, *i.e.*

$$\delta_g(\mathbf{x}, \tau) = \sum_{\mathcal{O}} b_{\mathcal{O}}(\tau)\mathcal{O}(\mathbf{x}, \tau). \tag{7.3}$$

This approach matches our discussion of the stress tensor in §4, where we expand τ_{ij} in terms of all combinations of the density and velocity fields allowed by symmetry at a given order. Aside from the symmetry assertions, this does not make assumptions about the physics of galaxy formation (or diffuse emission); instead, we remain agnostic to ultraviolet physics as per the EFTofLSS philosophy, and are maximally conservative. All small-scale information (beyond the maximum wavenumber of our theory) is encoded within a set of unknown coefficients, which now include the bias parameters.

To formulate this expansion, we must know the relevant symmetries. Three are usually relevant: (a) statistical isotropy, such that only fully contracted tensors without an expectation value can appear (e.g., δ_g cannot contain

terms in $a^i \partial_i \delta$ for constant vector a^i); (b) statistical homogeneity, such that there can be no dependence on absolute positions; (c) equivalence principle, such that all operators must be formed from the Newtonian potential and at least two derivatives. A fourth assumption, that δ_g is invariant under point reflections (*i.e.* parity transforms) can also be added, but is rarely needed in practice. From condition (c), all bias operators can be constructed from the following tensor (see [78, 84, 85]):

$$\Pi_{ij}^{[1]}(\mathbf{x}, \tau) = \frac{2}{3\Omega_m(\tau)\mathcal{H}^2(\tau)} \partial_i \partial_j \phi(\mathbf{x}, \tau), \tag{7.4}$$

with $\delta = \mathrm{Tr}\left[\Pi_{ij}^{[1]}\right]$ and peculiar potential ϕ. Higher-order equivalents can be constructed recursively from (7.4) via convective derivatives (along the fluid flow, denoted $D/D\tau$): these yield the symmetric forms

$$\Pi_{ij}^{[n]}(\mathbf{x}, \tau) = \frac{1}{(n-1)!}\left[\frac{1}{\mathcal{H}(\tau)f(\tau)}\frac{D}{D\tau}\Pi_{ij}^{[n-1]}(\mathbf{x}, \tau) - (n-1)\Pi_{ij}^{[n-1]}(\mathbf{x}, \tau)\right], \tag{7.5}$$

which starts at order n in perturbation theory. Finally, we can construct bias operators from all allowable combinations of these, finding the following at first, second, and third order (removing degenerate combinations):

$$\mathrm{Tr}\left[\Pi^{[1]}\right] \tag{7.6}$$
$$\mathrm{Tr}\left[(\Pi^{[1]})^2\right], (\mathrm{Tr}\left[\Pi^{[1]}\right])^2$$
$$\mathrm{Tr}\left[(\Pi^{[1]})^3\right], \mathrm{Tr}\left[(\Pi^{[1]})^2\right]\mathrm{Tr}\left[\Pi^{[1]}\right], (\mathrm{Tr}\left[\Pi^{[1]}\right])^3, \mathrm{Tr}\left[\Pi^{[1]}\Pi^{[2]}\right].$$

Whilst the above picture is formally complete, it is not necessarily the simplest description. As demonstrated in [82], an alternative, but equivalent, approach is to construct a basis from powers of the density field δ and *Galileon* operators [92, 95], where the first few are defined as

$$\mathcal{G}_2(\mathbf{x}, \tau) = [\partial_i \partial_j \Phi(\mathbf{x}, \tau)]^2 - [\partial^2 \Phi(\mathbf{x}, \tau)]^2 \tag{7.7}$$
$$\mathcal{G}_3(\mathbf{x}, \tau) = -\partial_i \partial_j \Phi(\mathbf{x}, \tau)\partial^j \partial_k \Phi(\mathbf{x}, \tau)\partial^k \partial^i \Phi(\mathbf{x}, \tau) - \frac{1}{2}[\partial^2 \Phi(\mathbf{x}, \tau)]^3 + \frac{3}{2}[\partial_i \partial_j \Phi(\mathbf{x}, \tau)]^2 \partial^2 \Phi(\mathbf{x}, \tau)$$
$$\Gamma_3(\mathbf{x}, \tau) = \mathcal{G}_2[\Phi](\mathbf{x}, \tau) - \mathcal{G}_2[\Phi_v](\mathbf{x}, \tau),$$

where $\Phi = \partial^{-2}\delta$, $\Phi_v = \partial^{-2}\theta$ are rescaled density and velocity potentials. These are functions of the Newtonian potential that are not degenerate with the δ^n operators. The $\mathcal{G}_2$ tensor can be related to the tidal field of (7.2) via $\mathcal{G}_2 = s_{ij}s^{ij} - (2/3)\delta^2$. These lead to the following bias expansion, up to third order [e.g., 82, 92]:

$$\delta_g(\mathbf{x}, \tau) = b_1(\tau)\delta(\mathbf{x}, \tau) \tag{7.8}$$
$$+ \frac{b_2(\tau)}{2}\delta^2(\mathbf{x}, \tau) + b_{\mathcal{G}_2}(\tau)\mathcal{G}_2(\mathbf{x}, \tau)$$
$$+ \frac{b_3(\tau)}{6}\delta^3(\mathbf{x}, \tau) + b_{\mathcal{G}_3}(\tau)\mathcal{G}_3(\mathbf{x}, \tau) + b_{\mathcal{G}_2\delta}(\tau)\mathcal{G}_2(\mathbf{x}, \tau)\delta(\mathbf{x}, \tau) + b_{\Gamma_3}(\tau)\Gamma_3(\mathbf{x}, \tau)$$

where each order is shown on a different line. In (7.8), we find two types of bias operators: (1) powers of δ, as in the Taylor series expansion of (7.1); (2) tidal biases, $\mathcal{G}_n$ and Γ_3. Further types, including derivative and stochastic operators also appear; these will be discussed below. Similar expansions can be found also at higher-order, though require a large number of operators.[5] In the below, we will use the bias expansion of (7.8) by default.

*b. *The Lagrangian Bias Expansion* The above section formulated the bias expansion in terms of the late-time density field δ_g. Alternatively, we may work in the Lagrangian picture, whereupon bias must be specified in the initial conditions, via some fractional density $F(\mathbf{q})$ (equal to unity without bias) [e.g., 78, 96, 97]. The presence of bias leads to a modified continuity equation between Lagrangian and Eulerian coordinates:

$$F(\mathbf{q})d\mathbf{q} = [1 + \delta_g(\mathbf{x}, \tau)]d\mathbf{x} \tag{7.9}$$

---

[5] One can also form the expansion in terms of the *linear* density field $D(\tau)\delta_L(\mathbf{x}, \tau)$, instead of the late-time field $\delta(\mathbf{x}, \tau)$. This approach was advocated for in [REF:] and dubbed 'monkey bias'. It yields identical correlation functions in practice.

cf. (5.2), where $\mathbf{x} = \mathbf{q} + \mathbf{\Psi}(\mathbf{q}, \tau)$, as before.

The Lagrangian basis must be constructed from functions appearing in the Lagrangian description; a natural choice is the distortion tensor, $M_{ij}(\mathbf{q}, \tau) = \partial s_j / \partial q^i$, which describes the coordinate transformation. At leading order $\text{Tr}[M] \propto \delta$, returning conventional linear bias. In terms of M_{ij}, the bias operators up to third order can be written analogously to (7.6) [cf. 78]

$$\text{Tr}\left[M^{(1)}\right] \tag{7.10}$$
$$\text{Tr}\left[(M^{(1)})^2\right], (\text{Tr}\left[M^{(1)}\right])^2$$
$$\text{Tr}\left[(M^{(1)})^3\right], \text{Tr}\left[(M^{(1)})^2\right]\text{Tr}\left[M^{(1)}\right], (\text{Tr}\left[M^{(1)}\right])^3, \text{Tr}\left[M^{(1)}M^{(2)}\right],$$

where $M^{(n)}$ is the n-th order contribution to M (noting that we do not require convective derivatives, since we work in the fluid frame). As before, we proceed by combining all of these operators with associated bias coefficients to compute $F(\mathbf{q})$, and thus any late-time correlators.

As in the Eulerian case, it is common place to use a simpler redefinition of the above, in terms of density and tidal operators defined in Lagrangian coordinates. This can be written at second order

$$F(\mathbf{q}, \tau) = 1 + b_1^L \delta(\mathbf{q}) + \frac{b_2^L}{2}\delta^2(\mathbf{q}) + b_{s^2}s^2(\mathbf{q}), \tag{7.11}$$

where $s^2 \equiv s_{ij}s^{ij}$, and we drop third-order terms, following standard conventions. These will be used to compute tracer power spectra (and beyond) in the (effective) Lagrangian picture. Note that the bias parameters do not depend on time, since we are working in the Lagrangian picture; however, they are specific to the choice of tracer population, which itself depends on τ. To implement this in practice, one commonly works in terms of the one-dimensional Fourier-transform of F, $F(\lambda)$ [96]:

$$F(\mathbf{q}, \tau) = \int_{-\infty}^{\infty} \frac{d\lambda}{2\pi} F(\lambda, \tau)e^{i\lambda\delta(\mathbf{q},\tau)}. \tag{7.12}$$

The ensuing relation of density and position is given by

$$(2\pi)^3 \delta_{\text{D}}(\mathbf{k}) + \delta_g(\mathbf{k}, \tau) = \int d\mathbf{q}\, e^{i\mathbf{k}\cdot\mathbf{q}} \left(\int_{-\infty}^{\infty} \frac{d\lambda}{2\pi} F(\lambda, \tau)e^{i\lambda\delta(\mathbf{q},\tau)}e^{i\mathbf{k}\cdot\mathbf{\Psi}(\mathbf{q},\tau)} - 1 \right) \tag{7.13}$$

(cf. 5.3). This can be used to compute power spectra analogously to §5, now depending on the kernel

$$\exp\left(-\frac{1}{2}\left[k_i k_j \left\langle \Delta\Psi^i(\mathbf{q})\Delta\Psi^j(\mathbf{0}) \right\rangle + (\lambda_1^2 + \lambda_2^2)\sigma_\Lambda^2 + 2\lambda_1\lambda_2 \left\langle \delta(\mathbf{q})\delta(\mathbf{0}) \right\rangle + 2(\lambda_1 + \lambda_2)k_i \left\langle \Delta\Psi^i(\mathbf{q},\tau)\delta(\mathbf{0},\tau) \right\rangle \right] \right), \quad (7.14)$$

which is integrated with respect to $F(\lambda_1)F(\lambda_2)e^{i\mathbf{k}\cdot\mathbf{q}}$. The Gaussian λ integrals can be performed leading to a tractable Zel'dovich solution. As before, higher-orders follow by expanding the exponential. Full details are presented in [58, 61, 96, 98].

*c. *Renormalization and Counterterms* The previous discussion of bias contains some subtleties relating to renormalization, and the ensuing cut-off dependence of bias parameters (discussed in detail in [82, 84, 90]). For an example of this, let us consider the quadratic (Eulerian) bias term; in expectation,

$$\frac{b_2(\tau)}{2}\left\langle \delta^2 \right\rangle = \frac{b_2(\tau)}{2}\sigma_\delta^2(\Lambda) \tag{7.15}$$

(at leading order). This sources two problems: (a) we find explicit dependence on the smoothing scale Λ; (b) the mean of $\delta_g(\mathbf{x}, \tau)$ should be zero. This can be ameliorated by redefining the bias operator as follows:[6]

$$\delta^2(\mathbf{x}, \tau) \rightarrow \delta^2(\mathbf{x}, \tau) - \sigma_\delta^2(\Lambda). \tag{7.16}$$

---

[6] Note that one can also account for these effects by absorbing the relevant bias coefficients into the stochastic part of the correlators, which will be discussed below.

At leading order, this is the only modification needed to ensure $\langle \delta_g \rangle = 0$.

Our problems, however, do not end there. Whilst δ_g contains no terms contributing to $\langle \delta_g \rangle$, it contains multiple terms scaling as δ_L. This can be seen by considering the expectation $\langle \delta_L \delta_g \rangle$, which should involve linear bias, *i.e.* only linear bias should contribute to the linear power spectrum! Let us consider the cubic term:

$$\langle \delta_L(-\mathbf{k})\delta^3(\mathbf{k}, \tau) \rangle' = 3D^3(\tau)P_L(k)\sigma_\delta^2(\Lambda) + \cdots, \tag{7.17}$$

at leading order. Thus the linear power spectrum contains the following:

$$\langle \delta_L(-\mathbf{k})\delta_g(\mathbf{k}, \tau) \rangle' = \left[b_1(\tau) + \frac{b_3(\tau)}{2}D^2(\tau)\sigma_\delta^2(\Lambda) \right] D(\tau)P_L(k) + \cdots \neq b_1(\tau)D(\tau)P_L(k) \tag{7.18}$$

This is clearly a problem since it destroys the perturbative hierarchy, and gives explicit dependence on Λ, requiring cutoff-dependent bias parameters, *i.e.* $b_1(\tau) = b_1(\tau, \Lambda)$. As before, we can solve by defining a new operator, removing this contribution:

$$\delta^3(\mathbf{x}, \tau) \rightarrow \delta^3(\mathbf{x}, \tau) - 3\sigma_\delta^2(\Lambda)\delta(\mathbf{x}, \tau). \tag{7.19}$$

In fact, the second piece acts as a counterterm, removing the cut-off dependence of δ^3. Such a term is needed since δ^3 is a *contact term*, *i.e.* one involving multiple fields at the same location. As in §4, this contains contributions from short-scale modes, which must be treated consistently.

The above arguments can be extended further, and lead to to redefinitions of all contact operators, to form *renormalized operators*, defined at any given order in perturbation theory. Denoting these by $[\mathcal{O}]$, the new bias expansion becomes

$$\delta_g(\mathbf{x}, \tau) = \sum_{\mathcal{O}} b_{\mathcal{O}}^R(\tau)[\mathcal{O}](\mathbf{x}, \tau), \tag{7.20}$$

where $b_{\mathcal{O}}^R$ are the redefined bias parameters. We stress that these coefficients do not depend on the cut-off, and further, they are physical, *i.e.* measuring $\langle \delta_g \delta \rangle / \langle \delta\delta \rangle$ in simulations would give b_1^R and not b_1. The derivation of all renormalized operators can be found in [82]; here, we simply state the forms entering the one-loop power spectrum:

$$[\delta](\mathbf{x}, \tau) = \delta(\mathbf{x}, \tau) \tag{7.21}$$
$$[\delta^2](\mathbf{x}, \tau) - \delta^2(\mathbf{x}, \tau) - \sigma_\delta^2(\Lambda)\left[1 + \frac{68}{21}\delta \right] + \cdots$$
$$[\mathcal{G}_2](\mathbf{x}, \tau) = \mathcal{G}_2(\mathbf{x}, \tau)$$
$$[\Gamma_3](\mathbf{x}, \tau) = \Gamma_3(\mathbf{x}, \tau).$$

We further note that Galilean operators are not contact operators and do not get corrections from renormalization at any order (unless products of them arise, such as $\mathcal{G}_2\delta$). We will assume renormalized operators by default in the below, and drop the explicit notation.

d. Derivatives & Stochasticity The bias expansion of (7.8) is a Taylor series in the gravitational potential Φ. However, the true large-scale relation between tracers and matter contains two additional contributions: (1) derivatives of the potential operators [e.g., 73, 76, 83, 92]; (2) random fields uncorrelated with the initial conditions [e.g., 78, 84, 86, 99]. Below, we consider each in turn.

Above, we have assumed a local-in-time dependence of the tracer distribution on the potential, *i.e.* that $\delta_g(\mathbf{x}, \tau)$ depends on ϕ at time τ. In practice, this is not the case, and we should strictly integrate over the entire lightcone history [e.g., 72, 73, 92]. For a bias operator $\mathcal{O}$, this implies

$$\delta_g(\mathbf{x}, \tau) \supset \int^\tau d\tau' \, b_{\mathcal{O}}(\tau', \tau)\mathcal{O}(\mathbf{x}(\tau'), \tau'), \tag{7.22}$$

where $\mathbf{x}(\tau')$ is the position of the fluid element at time $\tau' < \tau$, with $\mathbf{x} = \mathbf{x}(\tau)$. This may be simplified by perturbatively expanding the fluid trajectory in the small parameter $\Psi(\mathbf{x}, \tau) - \Psi(\mathbf{x}(\tau'), \tau')$, yielding

$$\delta_g(\mathbf{x}, \tau) \supset b_{\mathcal{O}}^{(0)}(\tau)\mathcal{O}(\mathbf{x}, \tau) + b_{\mathcal{O}}^{(2)}(\tau)\nabla_\mathbf{x}^2\mathcal{O}(\mathbf{x}, \tau) + \cdots. \tag{7.23}$$

Here, we have redefined bias parameters as integrals of $b_{\mathcal{O}}(\tau', \tau)$ and its derivatives, and employed integration by parts. Importantly, the non-locality in time can be recast as an expansion in derivatives; equivalently speaking, we are forced to include also the gradients of operators in the bias expansion.

At third order, non-locality in time leads to only one new operator in the bias expansion of (7.8):

$$\delta_g(\mathbf{x}, \tau) \supset b_{\nabla^2\delta}(\tau)\nabla^2_{\mathbf{x}}\delta(\mathbf{x}, \tau). \tag{7.24}$$

Due to the Laplacian, this term is suppressed by $(kR_{\mathrm{halo}})^2$ relative to linear theory, and thus the same order as loop corrections (assuming $k_{\mathrm{NL}} \sim R^{-1}_{\mathrm{halo}}$). At leading order, this term is precisely degenerate with the EFTofLSS counterterm (§4), which takes the form $-c_s^2(\tau)\delta_{\mathrm{L}}(\mathbf{x}, \tau)$, and thus often dropped in practice.

Finally, we must account for fluctuations uncorrelated with the linear density field, δ_{L} [e.g., 78, 99]. The canonical example of this is shot-noise; this is a quasi-Poissonian process present in any analysis of discrete tracers due to its finite density. This sources a contribution:

$$\delta_g(\mathbf{x}, \tau) \supset \epsilon(\mathbf{x}, \tau), \qquad \langle\epsilon(\mathbf{x}, \tau)\epsilon(\mathbf{x}', \tau)\rangle = P_\epsilon(\tau)\delta_{\mathrm{D}}(\mathbf{x} - \mathbf{x}'), \tag{7.25}$$

where $P_\epsilon(\tau) = 1/\bar{n}(\tau)$ for a purely Poissonian system of density $\bar{n}(\tau)$ (which is rarely a good approximation in practice). The stochastic field $\epsilon(\mathbf{x}, \tau)$ is uncorrelated with the matter density (such that $\langle\epsilon\delta\rangle = 0$), and does not need a bias coefficient, since its amplitude is set by its correlation $\langle\epsilon\epsilon\rangle \sim P_\epsilon$.

In practice, the stochastic nature of the field is slightly more complicated. The stochastic field ϵ may not obey Gaussian statistics, implying that correlators such as $av\epsilon^3$ could be non-zero. This will source shot-noise in the tracer bispectrum. Next, we can have products of stochastic and deterministic fields in the tracer expansion: at third order we find

$$\delta_g(\mathbf{x}, \tau) \supset \epsilon(\mathbf{x}, \tau) + \epsilon_\delta(\mathbf{x}, \tau)\delta(\mathbf{x}, \tau); \tag{7.26}$$

analogous contributions (e.g., the combination $\epsilon_{\mathcal{G}_2}\mathcal{G}_2$) enter at higher order. Here we have defined a new stochastic field ϵ_δ, again satisfying $\langle\epsilon_\delta\delta\rangle = 0$, but with non-trivial (and possibly non-Gaussian) correlators with itself and with ϵ. Finally, though temporal and spatial locality would require the correlators to be white, *i.e.* proportional to k^0, the above lightcone evolution arguments demand also an expansion in derivatives, such that

$$\langle\epsilon(\mathbf{k}, \tau)\epsilon(-\mathbf{k}, \tau)\rangle' = P^{(0)}_\epsilon(\tau) + k^2 P^{(2)}_\epsilon(\tau) + \cdots , \tag{7.27}$$

and similar for other correlators.[7] From scaling arguments, these coefficients are proportional to $\bar{n}^{-1}(\tau)R^n_{\mathrm{halo}}$. In full, we find the following stochastic tracer power spectrum at third-order:

$$P^{\mathrm{stoch}}(k, \tau) = P^{(0)}_\epsilon(\tau) + k^2 P^{(2)}_\epsilon(\tau) + \cdots , \tag{7.28}$$

with other terms (including $P_{\epsilon\delta}$) relevant for the bispectrum and beyond.

e. Correlators We have now assembled all necessary ingredients in the bias expansion: deterministic bias (which is a functional of ϕ), the derivative expansion (from non-locality-in-time), stochasticity, and the associated renormalization. Using this, we can now proceed to compute correlators, such as the tracer power spectrum and bispectrum. Before doing so, let us recapitulate the bias expansion, including all terms relevant to the calculation of the one-loop power spectrum [e.g., 82, 87, 88, 100]:

$$\delta_g(\mathbf{x}, \tau) = b_1(\tau)\delta(\mathbf{x}, \tau) + \frac{b_2(\tau)}{2}[\delta^2](\mathbf{x}, \tau) + b_{\mathcal{G}_2}(\tau)\mathcal{G}_2(\mathbf{x}, \tau) + b_{\Gamma_3}(\tau)\Gamma_3(\tau) + b_{\nabla^2\delta}(\tau)\nabla^2\delta(\mathbf{x}, \tau) + \epsilon(\mathbf{x}, \tau) + \cdots \tag{7.29}$$

noting explicitly that the δ^2 term is renormalized. We drop various third-order terms in $\delta_g(\mathbf{x}, \tau)$ (such as $\mathcal{G}_3$) since these do not contribute to the one-loop power spectrum (but appear, for example, in tree-level trispectra).

Before computing the power spectrum, it is useful to expand (7.29) in terms of the linear density field, δ_{L}, using the definitions of $[\delta^2]$, $\mathcal{G}_2$ and beyond. For δ^2, for example, we can write

$$\delta^2(\mathbf{x}, \tau) = D^2(\tau)\delta^{(1)}(\mathbf{x}, \tau)\delta^{(1)}(\mathbf{x}, \tau) + 2D^3(\tau)\delta^{(2)}(\mathbf{x}, \tau)\delta^{(1)}(\mathbf{x}, \tau) + \cdots , \tag{7.30}$$

up to third-order, where we expand δ in terms of its perturbative components, $\delta^{(n)}$, as in §3. Furthermore, we can expand $\delta^{(2)}$ as a convolution of two powers of δ_{L}, such that

$$\begin{aligned}\delta^2(\mathbf{k}, \tau) &= D^2(\tau)\int_{\mathbf{p}_1\mathbf{p}_2}(2\pi)^3\delta_{\mathrm{D}}(\mathbf{p}_1 + \mathbf{p}_2 - \mathbf{k})\,\delta_{\mathrm{L}}(\mathbf{p}_1)\delta_{\mathrm{L}}(\mathbf{p}_2) \\ &\quad + 2D^3(\tau)\int_{\mathbf{p}_1\mathbf{p}_2\mathbf{p}_3}(2\pi)^3\delta_{\mathrm{D}}(\mathbf{p}_1 + \mathbf{p}_2 + \mathbf{p}_3 - \mathbf{k})\,F_2(\mathbf{p}_1, \mathbf{p}_2)\delta_{\mathrm{L}}(\mathbf{p}_1)\delta_{\mathrm{L}}(\mathbf{p}_2)\delta_{\mathrm{L}}(\mathbf{p}_3) + \cdots .\end{aligned} \tag{7.31}$$

---

[7] Note that one can also get mixed derivatives, from terms of the form $(\partial_i\delta)\epsilon^i$, for stochastic vector field ϵ^i. These are important for the one-loop bispectrum and beyond.

The same can be done for all other deterministic terms. For clarity, it is useful to rewrite the deterministic part as a sum over lower-order contributions, in the form

$$\delta_{g,\text{det}}(\mathbf{k}, \tau) = \sum_{n=1}^{\infty} D^n(\tau) \delta_{g,\text{det}}^{(n)}(\mathbf{k}, \tau), \tag{7.32}$$

where, just as in matter SPT, we can write the n-th order contribution as a convolution of n linear density fields:

$$\delta_{g,\text{det}}^{(n)}(\mathbf{k}, \tau) = \int_{\mathbf{p}_1 \cdots \mathbf{p}_n} (2\pi)^3 \delta_{\text{D}} (\mathbf{p}_1 + \cdots \mathbf{p}_n - \mathbf{k}) K_n(\mathbf{p}_1, \cdots, \mathbf{p}_n, \tau) \delta_{\text{L}}(\mathbf{p}_1) \cdots \delta_{\text{L}}(\mathbf{p}_n), \tag{7.33}$$

defining kernels K_n. The first two are defined as

$$
\begin{aligned}
K_1(\mathbf{p}_1, \tau) &= b_1(\tau) \\
K_2(\mathbf{p}_1, \mathbf{p}_2, \tau) &= b_1(\tau) F_2(\mathbf{p}_1, \mathbf{p}_2) + \frac{b_2(\tau)}{2},
\end{aligned}
\tag{7.34}
$$

in terms of the bias parameters and matter kernels F_n. Higher-order kernels follow similarly, and the third-orde term is given explicitly in Appendix A. Just as for SPT, we can compute power spectra from these kernels:

$$P_g^{(22)}(k, \tau) = 2 \int_{\mathbf{p}} |K_2(\mathbf{p}, \mathbf{k} - \mathbf{p}, \tau)|^2 P_{\text{L}}(\mathbf{p}) P_{\text{L}}(\mathbf{k} - \mathbf{p}), \qquad P_g^{(13)}(k, \tau) = 3 P_{\text{L}}(k) \int_{\mathbf{p}} K_3(\mathbf{p}, -\mathbf{p}, \mathbf{k}, \tau) P_{\text{L}}(\mathbf{p}). \tag{7.35}$$

cf. (3.14), giving the following deterministic part of the power spectrum:

$$P_g^{\text{det}}(k, \tau) = D^2(\tau) b_1^2(\tau) P_{\text{L}}(k) + D^4(\tau) \left[2 P_g^{(13)}(k, \tau) + P_g^{(22)}(k, \tau) \right] \tag{7.36}$$

As in §6, we must additionally account for long-wavelength modes via IR resummation. This proceeds by the same logic as before; we first compute the above spectra using the 'dewiggled' linear power spectra as input, then add the residual, damped as in (6.11). We will assume this by default in the below.

In addition to the deterministic parts, we have contributions to the matter power spectrum from the derivatives and stochasticity: these impact the power spectrum as

$$P_g^{\text{deriv+stoch}}(k, \tau) = -2 D^2(\tau) b_{\Delta^2 \delta}(\tau) k^2 P_{\text{L}}(k) + P_\epsilon^{(0}(\tau) + k^2 P_\epsilon^{(2)}(\tau). \tag{7.37}$$

Furthermore, the spectra given in (7.35) have dependence on the smoothing scale Λ, *i.e.* the maximum wavenumber. This dependence is captured by the counterterms, via renormalization. Similar to before, we find the counterterm contribution:

$$P_g^{\text{ct}}(k, \tau) = -2 D^2(\tau) b_1^2(\tau) c_s^2(\tau) k^2 P_{\text{L}}(k), \tag{7.38}$$

where the sound-speed absorbs the cut-off dependence of the theory. Note that this is fully degenerate with the higher-derivative bias in (7.37). We further note that the large-p limits of (7.35) also source k^0 and k^2 components: these divergences are captured by the stochasticity parameters.

Finally, we note that the full tracer power spectrum is given by the sum of the above components:

$$P_g^{1-\text{loop}}(k, \tau) = P_g^{\text{det}}(k, \tau) + P_g^{\text{deriv+stoch}}(k, \tau) + P_g^{\text{ct}}(k, \tau). \tag{7.39}$$

We stress that this does not make assumptions about halo-scale physics, aside from the symmetry considerations.

8. REDSHIFT-SPACE DISTORTIONS

A number of cosmological observables, such as galaxy densities, are measured in redshift-space rather than real-space. This occurs since galaxy distances are measured through their redshifts, whose relation is confused by the presence of galaxy peculiar velocities. In this section, we discuss the extension of the EFTofLSS to redshift-space and the various subtleties arising therein (with detailed derivations found in [e.g., 23, 74, 75, 97–99, 101–105]).

a. Relating Real- and Redshift-Space Consider a galaxy at Eulerian position $\mathbf{x}$ and with peculiar velocity $\mathbf{v}$. The observed redshift-space position, $\mathbf{s}$, is given by [e.g., 5]

$$\mathbf{s}(\mathbf{x}, \tau) = \mathbf{x}(\tau) + \frac{[\mathbf{v}(\mathbf{x}, \tau) \cdot \hat{\mathbf{z}}]}{\mathcal{H}(\tau)}\hat{\mathbf{z}}, \tag{8.1}$$

where $\hat{\mathbf{z}}$ is the line-of-sight (usually the z-axis) and $\mathcal{H}(\tau)$ is the Hubble parameter. Analogous to converting from Lagrangian to Eulerian space, we can compute the redshift-space tracer field, $\delta_{g,s}(\mathbf{s}, \tau)$, by the continuity equation:

$$[1 + \delta_{g,s}(\mathbf{s}, \tau)]d\mathbf{s} = [1 + \delta_g(\mathbf{x}, \tau)]d\mathbf{x}, \tag{8.2}$$

which is just the number of objects in a differential volume. Converting to Fourier-space, and using (8.1), we find the Eulerian relation

$$\delta_{g,s}(\mathbf{k}, \tau) = \int d\mathbf{x}\, e^{i\mathbf{k}\cdot\mathbf{x}}\left\{[1 + \delta_g(\mathbf{x}, \tau)]e^{i(\mathbf{k}\cdot\hat{\mathbf{z}})(\mathbf{v}(\mathbf{x},\tau)\cdot\hat{\mathbf{z}})/\mathcal{H}(\tau)} - 1\right\}. \tag{8.3}$$

The implication of this is that the redshift-space galaxy density depends both on the real-space equivalent and the velocity density, projected along the line-of-sight.

b. Perturbative Solutions At linear order, one can evaluate the redshift-space density field by expanding the exponential in (8.3), assuming the peculiar velocity to be small. This yields

$$\delta_{g,s}(\mathbf{k}, \tau) = \delta_g(\mathbf{k}, \tau) + \frac{i}{\mathcal{H}(\tau)}k_\parallel v_\parallel(\mathbf{k}, \tau) + \cdots, \tag{8.4}$$

where we define $X_\parallel \equiv \mathbf{X} \cdot \hat{\mathbf{z}}$. We can also define the angle of $\mathbf{k}$ to the line-of-sight, $\mu \equiv k_\parallel/k$. Inserting the linear order solutions for density and velocity gives the classical Kaiser formula [106, 107]:

$$\delta_{g,s}(\mathbf{k}, \tau) = \left[b_1(\tau) + f(\tau)\mu^2\right] D(\tau)\delta_{\mathrm{L}}(\mathbf{k}), \tag{8.5}$$

where $f(\tau)$ is the growth rate, as in §3.

The same logic extends similarly to higher order. Expanding the exponential up to third order, we find

$$\begin{aligned}
\delta_{g,s}(\mathbf{k}, \tau) &= \delta_g(\mathbf{k}, \tau) + \frac{i}{\mathcal{H}(\tau)}k_\parallel v_\parallel(\mathbf{k}, \tau) + \frac{i}{\mathcal{H}(\tau)}k_\parallel[\delta_g * v_\parallel](\mathbf{k}, \tau) - \frac{1}{2\mathcal{H}^2(\tau)}k_\parallel^2[v_\parallel * v_\parallel](\mathbf{k}, \tau) \\
&\quad - \frac{1}{2\mathcal{H}^2(\tau)}k_\parallel^2[\delta_g * v_\parallel * v_\parallel](\mathbf{k}, \tau) - \frac{i}{6\mathcal{H}^3(\tau)}k_\parallel^3[v_\parallel * v_\parallel * v_\parallel](\mathbf{k}, \tau) + \cdots,
\end{aligned} \tag{8.6}$$

where $*$ indicates a convolution (or a real-space product). To compute the perturbative solution, one replaces the tracer and velocity fields with their expansion in terms of δ_{L}, just as for biased tracers. We are thus motivated to write the following expansion:

$$\delta_{g,s}(\mathbf{k}, \tau) = \sum_{n=1}^\infty D^n(\tau)\delta_{g,s}^{(n)}(\mathbf{k}, \tau), \tag{8.7}$$

with the n-th order solution

$$\delta^{(n)}(\mathbf{k}, \tau) = \int_{\mathbf{p}_1\cdots\mathbf{p}_n}(2\pi)^3\delta_{\mathrm{D}}(\mathbf{p}_1 + \cdots \mathbf{p}_n - \mathbf{k})\, Z_n(\mathbf{p}_1, \cdots, \mathbf{p}_n, \tau)\delta_{\mathrm{L}}(\mathbf{p}_1)\cdots\delta_{\mathrm{L}}(\mathbf{p}_n). \tag{8.8}$$

The new redshift-space kernels encapsulate both tracer bias and velocities, with the first two taking the form

$$Z_1(\mathbf{p}_1, \tau) = b_1(\tau) + f(\tau)\mu^2 \tag{8.9}$$

$$Z_2(\mathbf{p}_1, \mathbf{p}_2, \tau) = K_2(\mathbf{p}_1, \mathbf{p}_2, \tau) + f(\tau)\mu^2 G_2(\mathbf{p}_1, \mathbf{p}_2) + \frac{b_2(\tau)}{2} + \frac{f(\tau)b_1(\tau)}{2}(\mu k)\left(\frac{\mu_1}{p_1} + \frac{\mu_2}{p_2}\right) + \frac{f^2(\tau)}{2}(\mu k)^2\frac{\mu_1\mu_2}{p_1 p_2},$$

where $\mu_i = p_{1,\parallel}/p_1$, G_n are the velocity kernels and K_n are the real-space galaxy bias kernels. In the limit of $f \to 0$, this yields the real-space solutions, K_n, and, for $b_n \to 0$ ($n > 1$) and $b_1 = 1$, we find the matter solutions. The third order piece is given in Appendix A.

c. Renormalization Using the above perturbative expansions, we can construct power spectra, just as in the biased tracer case. By exact analogy with the real-space case, the deterministic piece gives

$$P_{g,s}(\mathbf{k},\tau) = D^2(\tau)[b(\tau) + f(\tau)\mu^2]^2 P_{\mathrm{L}}(k) + D^4(\tau)\left[2P_{g,s}^{(13)}(\mathbf{k},\tau) + P_{g,s}^{(22)}(\mathbf{k},\tau)\right] \tag{8.10}$$

with

$$P_{g,s}^{(22)}(\mathbf{k},\tau) = 2\int_{\mathbf{p}} |Z_2(\mathbf{p},\mathbf{k}-\mathbf{p},\tau)|^2 P_{\mathrm{L}}(\mathbf{p})P_{\mathrm{L}}(\mathbf{k}-\mathbf{p}), \qquad P_{g,s}^{(13)}(\mathbf{k},\tau) = 3P_{\mathrm{L}}(k)\int_{\mathbf{p}} Z_3(\mathbf{p},-\mathbf{p},\mathbf{k},\tau)P_{\mathrm{L}}(\mathbf{p}), \tag{8.11}$$

which now depend explicitly on the direction of $\mathbf{k}$.

As discussed in §4, the loop integrals in (8.11) should be cut-off at some scale Λ, which results from working with smoothed density and velocity fields (needed for a convergent theory). Such a truncation leads to the loop integrals having explicit dependence on the (non-physical) parameter Λ. The process of renormalization again saves us here, since it introduces new microphysical parameters (through the stress tensor) which absorb the cut-off dependence [e.g., 74, 101, 103, 104]. Unlike the previous section, renormalization will require counterterms with respect to the real-space matter theory, since there are new divergences emerging.[8] These are associated with symmetry breaking; due to the emergence of a preferred axis, $\hat{\mathbf{z}}$, our theory is now symmetric only around the line-of-sight.

In §4, we argued that the backreaction of small-scale physics onto large scale modes was sourced by contact terms, *i.e.* products of fields at the same physical location. From (8.6), it is evident that such terms arise, including $v_{\parallel}^2(\mathbf{x},\tau)$, $v_{\parallel}(\mathbf{x},\tau)\delta(\mathbf{x},\tau)$ and beyond. To understand the impact of this, let us consider the UV limit of a specific term in the power spectrum, generated by correlating $v_{\parallel}^2\delta_g$ with δ_g:

$$\begin{aligned} P_{g,s}(\mathbf{k},\tau) \supset -\frac{k_{\parallel}^2}{2\mathcal{H}^2(\tau)}\left\langle [v_{\parallel}^2\delta_g](\mathbf{k},\tau)\delta_g(-\mathbf{k},\tau)\right\rangle' &\to D^4(\tau)b_1^2(\tau)f^2(\tau)k_{\parallel}^2 P_{\mathrm{L}}(k)\int_{\mathbf{p}\gg\mathbf{k}} \frac{\mu_{\mathbf{p}}^2}{p^2}P_{\mathrm{L}}(p) \\ &= D^4(\tau)b_1^2(\tau)f^2(\tau)P_{\mathrm{L}}(k)(\mu k)^2\int_{p\gg k}^{\Lambda} \frac{p^2 dp}{2\pi^2}\frac{P_{\mathrm{L}}(p)}{p^2} \end{aligned} \tag{8.12}$$

where we have inserted the linear solution for $\mathbf{v}(\mathbf{x},\tau)$ and simplified. The UV limit scales as $(\mu k)^2 P_{\mathrm{L}}(k)$, implying the existence of an analogous counterterm to absorb the cut-off dependence. This is different to the previous forms, and arises due to the broken polar symmetry. Following similar arguments for the other terms, we find the following counterterms in the power spectrum at third-order:

$$P_{g,s}^{\mathrm{ct}}(\mathbf{k},\tau) = \left[c_0 + c_2 k^2 + c_4 k^2\mu^2\right] + \left[c_1 + c_3\mu^2 + c_5\mu^4\right] k^2 P_{\mathrm{L}}(k) + \cdots, \tag{8.13}$$

where each coefficient is time dependent and we absorb factors of $D(\tau)$ and $f(\tau)$. c_0, c_1 and c_2 arise also in the real-space case (though c_0 and c_2 are fully degenerate with stochasticity, and thus usually dropped), but the others are new. c_4 arises from 22-like diagrams correlating $v_{\parallel}^2$ and $b_2\delta^2$, and c_5, with its quartic dependence on μ, arises from the product of $v_{\parallel}^3$ and δ_g. With these definitions, the one-loop power spectrum becomes cut-off independent. Similar procedures apply to higher-order statistics.

d. Stochasticity & Fingers-of-God As discussed in §7, the bias expansion also contains contributions from derivative bias and stochasticity, which may take different forms in redshift-space. In the former case, there is no change to the bias expansion (which is defined in real-space), with the $\nabla^2\delta$ term now contributing to the one-loop power spectrum as follows [76]:

$$P_s^{\mathrm{deriv}}(\mathbf{k},\tau) = -2D^2(\tau)b_{\nabla^2\delta}(\tau)k^2\left[b_1(\tau) + f\mu^2\right]P_{\mathrm{L}}(k), \tag{8.14}$$

picking up a Kaiser factor, with the term scaling as $(kR_{\mathrm{halo}})^2 P_{\mathrm{L}}(k)$, as before. In practice, this is degenerate with the c_1 and c_3 counterterms in (8.13) and can be dropped.

More notable are the effects of stochasticity. Physically speaking, the redshift-space power spectrum contains stochastic contributions from both the bias expansion and the velocity fields. In galaxy survey contexts, the latter is known as the 'fingers-of-God' effect (hereafter FoG), and is sourced by the random motions of galaxies within a dark matter halo, which are uncorrelated with δ_{L} [108]. For certain galaxy populations, such as small galaxies in large dark

---

[8] Whilst there were new counterterms for biased tracers in real-space, these were fully degenerate with the stochasticity parameters.

matter halos, these effects can be significant, and lead to the theory quickly becoming non-perturbative. Detailed semi-analytic modeling of FoG is difficult, due to the phenomenon's dependence on local properties such as the halo mass; however, one can employ a perturbative treatment within the EFTofLSS. As long as we restrict to scales where the theory is valid, the stochastic velocities can be fully encapsulated. In practice, this requires small $k\sigma_{\mathrm{FoG}}$, where σ_{FoG} is the random velocity dispersion of the population [cf. 109, 110].

Within our perturbative framework, we treat stochastic velocities in an analogous manner to stochastic densities. From (8.6), the redshift-space tracer density depends on powers of the velocity field, v_i, contracted with the line-of-sight $\hat{z}^i$. To introduce stochasticity, we must add new fields $\epsilon_i, \epsilon_{ij}, \ldots$ to the bias expansion in the same manner:

$$\delta_{g,s}(\mathbf{k}, \tau) \supset k_{\parallel}\hat{z}^i \left(\epsilon_i(\mathbf{k}, \tau) + \epsilon_{\delta,i}[\delta\epsilon_i](\mathbf{k}, \tau) + \cdots\right) + k_{\parallel}^2\hat{z}^i\hat{z}^j \left(\epsilon_{ij}(\mathbf{k}, \tau) + [\epsilon_{\delta,ij}\delta](\mathbf{k}, \tau)\cdots\right) + \cdots . \tag{8.15}$$

Each of these new fields is uncorrelated with δ, but have non-trivial correlations with themselves, for example

$$\begin{aligned}
\langle\epsilon_i(\mathbf{x})\rangle &= 0 \\
\langle\epsilon_{\delta,ij}(\mathbf{x})\rangle &= \delta_{ij}^{\mathrm{K}} P_{\epsilon_{\delta,ij}}^{(0)}(\tau) + \cdots \\
\langle\epsilon_i(\mathbf{k}, \tau)\epsilon_j(-\mathbf{k}, \tau)\rangle' &= \hat{k}_i\hat{k}_j \left[P_{\epsilon_i}^{(0}(\tau) + k^2 P_{\epsilon_i}^{(2)}(\tau) + \cdots\right]
\end{aligned} \tag{8.16}$$

where we expand in derivatives as before. Note that the tensor indices are set by symmetry (with all anisotropy in the $\hat{\mathbf{z}}$ vectors) and we drop a k-independent term in the last line. The new contributions to the one-loop power spectrum can be written [e.g., 32]:

$$P_{g,s}^{\mathrm{stoch}}(\mathbf{k}, \tau) \supset a_2(\tau)k^2\mu^2 + \left[a_3(\tau) + a_5(\tau)\mu^2\right] k^2\mu^2 P_{\mathrm{L}}(k)+ \tag{8.17}$$

at leading order, writing the parameters as a_i for clarity, each of which scales as σ_{FoG}^2. Combining these parameters with the real-space stochastic contributions, we find five new parameters, which are fully degenerate with the c_n counterterms mentioned above. In practice, we therefore only need to consider one such set. Note that this is as expected; smoothing fields shifts modes from stochastic contributions to counterterms and vice versa. Finally, we note that a_0 and a_2 vanish for the matter field due to conservation of momentum (both isotropically and in the $\hat{\mathbf{z}}$-direction).

e.   **The Lagrangian Picture*   We now move to a discussion of the subtle aspects of the EFTofLSS in redshift-space. First, we discuss the Lagrangian picture of redshift-space distortions [23, 97, 98, 111–113], which will be motivate our modifications to the IR resummation procedure.

As in §5, LPT starts by considering the transformation between Lagrangian and Eulerian coordinates. With redshift-space distortions included, this takes the form

$$\mathbf{s}(\mathbf{q}, \tau) = \mathbf{q} + \mathbf{\Psi}(\mathbf{q}, \tau) + \frac{1}{\mathcal{H}(\tau)}\left[\hat{\mathbf{z}}\cdot\mathbf{v}(\mathbf{q} + \mathbf{\Psi}(\mathbf{q}, \tau), \tau)\right]\hat{\mathbf{z}} \tag{8.18}$$

Within the Einstein de-Sitter approximation, the velocity field can be written as

$$\mathbf{v}(\mathbf{q} + \mathbf{\Psi}(\mathbf{q}, \tau), \tau) = \sum_{n=1}^{\infty} nf(\tau)D^n(\tau)\mathbf{\Psi}^{(n)}(\mathbf{q}, \tau) \tag{8.19}$$

cf. (5.8). This motivates the definition of the n-th order redshift-space displacement field:

$$\Psi_{s,i}^{(n)}(\mathbf{q}, \tau) = [\delta_{ij}^{\mathrm{K}} + nf(\tau)\hat{\mathbf{z}}_i\hat{\mathbf{z}}_j]\mathbf{\Psi}^{(n),j}(\mathbf{q}, \tau) \equiv R_{ij}^{(n)}(\tau)\mathbf{\Psi}^{(n),j}(\mathbf{q}, \tau), \tag{8.20}$$

where $R_{ij}^{(n)}$ is a spatially-constant distortion matrix. After defining (8.20), the remainder of redshift-space LPT follows by inserting this into the pipeline of §5. Starting from the relation between Eulerian and Lagrangian densities (ignoring bias for now), we can write:

$$\delta_s(\mathbf{k}, \tau) = \int d\mathbf{q}\, e^{i\mathbf{k}\cdot\mathbf{q}}\left[e^{i\mathbf{k}\cdot\mathbf{\Psi}_s(\mathbf{q},\tau)} - 1\right] . \tag{8.21}$$

At leading order, this permits the Zel'dovich solution

$$\delta_{\mathrm{Zel},s}(\mathbf{k}, \tau) = \int d\mathbf{q}\, e^{i\mathbf{k}\cdot\mathbf{q}}\left[e^{iD(\tau)\mathbf{k}\cdot\mathsf{R}^{(1)}\cdot\mathbf{\Psi}^{(1)}(\mathbf{q},\tau)} - 1\right] . \tag{8.22}$$

Following some calculation (analogous to (5.13), since we have just redefined $\mathbf{k} \to \mathbf{k} \cdot \mathsf{R}^{(1)}$), we obtain the power spectrum [e.g., 61]

$$P_s^{\text{Zel}}(\mathbf{k}, \tau) = \int d\mathbf{q}\, e^{i\mathbf{k} \cdot \mathbf{q}} \exp\left(-D^2(\tau) k^i k^j R_{ik}^{(1)} R_{jl}^{(1)} \int \frac{p^2 dp}{2\pi^2} \frac{P_{\text{L}}(p)}{p^2} \left[\frac{\delta_{\text{K}}^{jl}}{3}\left(1 - j_0(pq) - j_2(pq)\right) + \hat{q}^j \hat{q}^l j_2(pq)\right]\right). \quad (8.23)$$

Higher-order corrections and modifications for biased tracers can be computed in the same manner as before, by expanding the higher-order displacements $\boldsymbol{\Psi}^{(n>1)}$ from the exponential.

*f.   *IR Resummation*   As discussed in §6, we incur a significant error by treating bulk flows as perturbative, which manifests in underdamped BAO wiggles. By formulating the initial theory in Lagrangian space and keeping the long-wavelength displacements exponentiated we were able to resum these features, and thus obtain an accurate analytic theory. In redshift-space, our treatment of IR resummation must be modified slightly, since the observed displacement depends on peculiar velocities. Here, we will describe the modifications using the wiggly-smooth decomposition [114]; the kernel-based redshift-space alterations can be found in [104].

We start from the general expansion given in (6.4), working with unbiased matter for simplicity. In redshift-space at leading-order:

$$(2\pi)^3 \delta_{\text{D}}(\mathbf{k}) + P_s(\mathbf{k}, \tau) = \int d\mathbf{q}\, e^{i\mathbf{k} \cdot \mathbf{q}} \exp\left(-\frac{1}{2} k_i k_j A_s^{ij}(\mathbf{q}, \tau) + \cdots\right), \quad (8.24)$$

where the variance of the redshift-space displacement field, $A_s^{ij}(\mathbf{q}, \tau) \equiv \langle \Delta\Psi_s^i(\mathbf{q}, \tau) \Delta\Psi_s^j(\mathbf{q}, \tau) \rangle$, is given by

$$A_s^{ij}(\mathbf{q}, \tau) = 2D^2(\tau) R_{ik}^{(1)} R_{jl}^{(1)} \int_{\mathbf{p}} \frac{p^k p^l}{p^4} P_{\text{L}}(p) \left(1 - e^{i\mathbf{p} \cdot \mathbf{q}}\right) + \cdots, \quad (8.25)$$

at leading order. This is just the term appearing in the redshift-space Zel'dovich theory. As in §6, we proceed by expanding A_s into a wiggly and smooth component, and Taylor expanding the latter (as well as any higher-order terms. The methodology matches the former precisely, and leads to the smooth term being unaffected (by mass and momentum conservation), but a damping of the wiggly component in the form:

$$P_s^{\text{IR}-\text{res}}(\mathbf{k}, \tau) - P_{\text{nw},s}(\mathbf{k}, \tau) = e^{-k^2 \Sigma_s^2(\mu, \tau)} \left(P_{\text{lin,w},s}(\mathbf{k}) + \text{higher-order wiggly}\right), \quad (8.26)$$

where $P_{\text{nw},s}$ is the power spectrum computed using the 'no-wiggle' linear power spectrum and $P_{\text{lin,w}}$ is the linear component of the residual. The new, direction-dependent damping scale is given by [e.g., 32]

$$\Sigma_s^2(\mu, \tau) = \left[1 + f(\tau) \mu^2 (2 + f(\tau))\right] \Sigma^2(\tau) + f^2(\tau) \mu^2 (\mu^2 - 1) \delta\Sigma^2(\tau), \quad (8.27)$$

where Σ^2 is the real-space damping and we introduce

$$\delta\Sigma^2(\tau) \approx D^2(\tau) \int_0^{0.2h\,\text{Mpc}^{-1}} \frac{p^2 dp}{2\pi^2} \frac{P_{\text{nw}}(p)}{p^2} j_2(pq_{\text{BAO}}). \quad (8.28)$$

The one-loop IR-resummed power spectrum can be similarly derived and is identical to (6.11) except with $\Sigma^2(\tau) \to \Sigma_s^2(\mu, \tau)$.

*g.   *Selection Bias*   To define the tracer density field in redshift-space, we have first computed the bias expansion in real-space then transformed to real-space, and added the requisite new counterterms and stochasticities. But is this sufficient? Are there terms in the bias expansion arising only in redshift-space that we have missed? Below, we summarize this aspect (which is discussed extensively in [86, 99]), known often as selection bias.

The broken polar symmetry inherent in the redshift-space field allows for a number of new terms in the bias expansion, for example

$$\delta_{g,s}(\mathbf{s}, \tau) \supset \frac{b_{\partial_\parallel v_\parallel}(\tau)}{\mathcal{H}(\tau)} \partial_\parallel v_\parallel(\mathbf{s}, \tau) \equiv b_{\partial_\parallel v_\parallel}(\tau) \eta(\mathbf{s}, \tau) \quad (8.29)$$

where $\partial_\parallel = \hat{z}^i \partial_i$. This explicitly breaks isotropy, and leads to a term proportional to $\mu^2 \delta(\mathbf{k}, \tau)$ in Fourier-space. This occurs at linear order, modifying the Kaiser redshift-space power spectrum:

$$P_{g,s}^{\text{lin}}(\mathbf{k}, \tau) = D^2(\tau) \left[b_1(\tau) + f(\tau)(1 + b_{\partial_\parallel v_\parallel}(\tau)) \mu^2\right]^2 P_{\text{L}}(k). \quad (8.30)$$

Such an effect has important implications for cosmological measurements: one can no-longer use the μ-dependence to extract the clustering amplitude, since it is now degenerate with an unknown bias parameter.

At higher-order, we obtain a collection of new terms in the expansion of δ_g. These occur from powers of the line-of-sight velocity, η and its combination with real-space operators such as δ, projections of the shear onto the line of sight (such as $s_{ik}s^k_j\hat{z}^i\hat{z}^j$), derivatives of η (including $\nabla^2\eta$ and $\partial^2\eta$) and higher-order effects. Stochastic terms can also be formed; these have already been described above. Finally, we note that the galaxy velocity field should strictly be treated as a biased tracer: at leading order this gives the derivative expansion

$$\mathbf{v}_g(\mathbf{x},\tau) = \mathbf{v}(\mathbf{x},\tau) + b_{\nabla^2\mathbf{v}}(\tau)\nabla^2\mathbf{v}(\mathbf{x},\tau) + b_{\partial^2_\parallel\mathbf{v}}(\tau)\partial^2_\parallel\mathbf{v}(\mathbf{x},\tau) + \cdots, \tag{8.31}$$

dropping stochastic terms. Of course, all these operators are also subject to bias renormalization, as in §7. The full EFTofLSS model with the above terms included is described in detail in [99], and contains many more terms than the power spectrum without selection effects.

In a galaxy survey context, the inclusion of the above terms would seriously limit the experiment's utility, due to new degeneracies between, for example, the growth rate and the $b_{\partial_\parallel v_\parallel}$ bias [e.g., 86]. This occurs since the velocity, which is usually a protected quantity in the tracer expansion, now receives contributions from terms with unknown coefficients. However, one must ask whether such effects are actually physical. In the above, we have allowed the properties of the galaxy population to depend on the line-of-sight; whether this can occur depends on how the sample is selected. An ideal sample would not contain information on $\hat{\mathbf{z}}$; *i.e.* we should observe galaxies regardless of their orientations or positions with respect to the line-of-sight. If this is the case, then the new terms described above drop-out, since their accompanying bias coefficients are forced to zero. Due to the details of survey selection functions, this is usually an excellent approximation, thus the terms are ignored (though see [115, 116]). Some residual effects could be present; we may be more likely to observe edge-on galaxies, for example, (since their light profile is more concentrated). This would give a bias term depending on the projected tidal field, which would need to be included in the modeling.

Finally, let us consider these biases for other types of surveys. For the Lyman-α forest for example, we construct a bias expansion for the optical depth, $\tau(\mathbf{s})$, in redshift-space [117] Since the optical depth does not 'know' about the line-of-sight, it does not contain the above selection-bias contributions. However, our observable is not $\tau(\mathbf{s})$ but the Lyman-α flux, $F(\mathbf{s}) \propto e^{-\tau(\mathbf{s})}$. The presence of the exponential term mixes up contributions and, in the effective bias expansion for $F(\mathbf{s})$, yields velocity bias terms, giving a linear power spectrum akin to (8.30). This is difficult to avoid.

9. CORRELATORS AND OBSERVABLES

We are now ready to assemble all the EFTofLSS ingredients developed above and produce predictions for the physical observables that can be compared to data. In the below, we will present models for a variety of statistics that have been measured by recent experiments, focusing on the Eulerian power spectrum in all cases. Much of this is a summary of the above material, but we included it for reference and completeness. Further discussion of the models can be found in [e.g., 32, 87, 98, 118–121].

a. Cosmic Shear Weak lensing surveys (such as the Dark Energy Survey, the Kilo-Degree Survey, the Prime Focus Spectrograph, CFHTLens and many others), measure the shape distortions of galaxies, and through them the large-scale distribution of matter in the Universe [e.g., 102]. This effect depends on the following lensing potential [122–124]

$$\psi(\hat{\mathbf{n}}) = \frac{2}{c^2}\int\frac{d\chi}{\chi}q(\chi)\Phi(\chi\hat{\mathbf{n}},\chi), \tag{9.1}$$

projected onto the two-sphere at position $\hat{\mathbf{n}}$, where Φ is the physical Newtonian potential. We parametrize time by the comoving distance $\chi(\tau)$ and introduce the lensing efficiency $q(\chi)$, defined as

$$q(\chi) = \int_\chi^\infty d\chi'\frac{\chi-\chi'}{\chi'}\bar{n}(\chi), \tag{9.2}$$

where $\bar{n}$ is the background density of sources. Via the Poisson equation, the lensing potential can be written in terms of the real-space matter field, expressed in Fourier-space:

$$\psi_{\ell m} = -\frac{3H_0^2\Omega_{m,0}}{c^2}\int\frac{d\chi}{\chi}\frac{q(\chi)}{a(\chi)}\int_{\mathbf{k}}4\pi i^\ell j_\ell(k\chi)Y^*_{\ell m}(\hat{\mathbf{k}})\frac{\delta(\mathbf{k},\chi)}{k^2}, \tag{9.3}$$

expanding $\psi(\hat{\mathbf{n}}) \equiv \sum_{\ell m} \psi_{\ell m} Y_{\ell m}(\hat{\mathbf{n}})$. In practice, our observable is the spin-2 shear, $_{\pm 2}\gamma_{\ell m}$, related to the lensing potential by $_{\pm 2}\gamma_{\ell m} = \sqrt{\ell(\ell+1)}\psi_{\ell m}/2$. The corresponding power spectrum (in the E-mode) is given by

$$C_\ell^\gamma = \frac{1}{4}\frac{(\ell+2)!}{(\ell-2)!} \times \frac{2}{\pi}\left(\frac{3H_0^2\Omega_{m,0}}{c^2}\right)^2 \int \frac{dk}{k^2}\left[\int \frac{d\chi}{\chi}\frac{q(\chi)}{a(\chi)}j_\ell(k\chi)\right]\left[\int \frac{d\chi'}{\chi'}\frac{q(\chi')}{a(\chi')}j_\ell(k\chi')\right]P_\delta(k,\chi,\chi'), \tag{9.4}$$

depending on the (unequal-time) real-space matter power spectrum P_δ. Note that we have ignored intrinsic-alignment contributions, though these can also be treated perturbatively [e.g., 125, 126].

Within the EFTofLSS, the matter density is given by

$$\begin{aligned} P_\delta(k,\chi,\chi') &= D(\chi)D(\chi')P_\mathrm{L}(k) + D(\chi)D(\chi')\left[(D^2(\chi)+D^2(\chi'))P^{(13)}(k) + D(\chi)D(\chi')P^{(22)}(k)\right] \\ &\quad - D(\chi)D(\chi')\left(c_s^2(\chi)+c_s^2(\chi')\right)k^2 P_\mathrm{L}(k) \end{aligned} \tag{9.5}$$

with the one-loop components

$$P^{(22)}(k) = 2\int_\mathbf{p}|F_2(\mathbf{p},\mathbf{k}-\mathbf{p})|^2 P_\mathrm{L}(\mathbf{p})P_\mathrm{L}(\mathbf{k}-\mathbf{p}), \qquad P^{(13)}(k) = 3P_\mathrm{L}(k)\int_\mathbf{p} F_3(\mathbf{p},-\mathbf{p},\mathbf{k})P_\mathrm{L}(\mathbf{p}), \tag{9.6}$$

as in (3.14) for F_n kernels as defined in Appendix A. In the above forms (and all results below) we have implicitly included UV cut-offs at some scale Λ and the effects of IR resummation (§6). The above formulae can be straightforwardly inserted into the shear power spectrum, and various methods (including the Limber approximation) exist for evaluating the associated integrals [e.g., 123, 124, 127–129]. The resulting model depends on one unknown parameter: the sound-speed c_s^2, integrated over the kernel of relevance.

Analogous methods apply also for CMB lensing [e.g., 130], just with a modified kernel q (and observing now the lensing convergence). Finally, we note that, as usual, the EFTofLSS predictions are valid only on perturbative scales, i.e. $k \ll k_\mathrm{NL}$ (though may be extended through the baryonic cut-off, cf. [102]). For projected statistics such as shear, this cut can be non-trivial due to the wide lensing kernel, and the ensuing leakage of non-perturbative contributions. In terms of ℓ, the theory is valid for $\ell \lesssim k_\mathrm{NL}\chi_*$, where χ_* is the characteristic distance to the lensing source, i.e. the peak of $q(\chi)$.

b. *Photometric Galaxy Surveys* Alongside galaxy shapes, most cosmic shear surveys measure galaxy positions. Photometric surveys such as these observe the galaxy density in some redshift-bin projected onto the two-sphere. Neglecting redshift-error, this can be written [e.g., 123]

$$\delta_g(\hat{\mathbf{n}}) = \int d\chi\, W(\chi)\delta_g(\chi\hat{\mathbf{n}},\chi), \tag{9.7}$$

for some kernel $W(\chi)$, which can include arbitrary weighting functions, and the source-density $\bar{n}(\chi)$. Analogous to the above, this can be rewritten in harmonic space as

$$\delta_{g,\ell m}(\hat{\mathbf{n}}) = \int d\chi\, W(\chi)\int_\mathbf{k} 4\pi i^\ell j_\ell(k\chi)Y_{\ell m}^*(\hat{\mathbf{k}})\delta_g(\mathbf{k},\chi). \tag{9.8}$$

We can compute the projected power spectrum (and higher-order statistics) from this directly:

$$C_\ell^g = \frac{2}{\pi}\int_\mathbf{k} k^2 dk\left[\int d\chi\, W(\chi)j_\ell(k\chi)\right]\left[\int d\chi'\, W(\chi')j_\ell(k\chi')\right]P_g(k,\chi,\chi'), \tag{9.9}$$

which depends on the real-space matter power spectrum, P_g. Cross-spectra proceed similarly and involve the galaxy-matter power spectrum, $\langle\delta\delta_g\rangle$ [e.g., 131, 132].

Within the EFTofLSS, this can be modelled via the perturbative power spectrum P_g. In this case, we have the one-loop result

$$P_g(k,\chi,\chi') = P_g^\mathrm{det}(k,\chi,\chi') + P_g^\mathrm{stoch}(k,\chi,\chi') + P_g^\mathrm{ct}(k,\chi,\chi'), \tag{9.10}$$

where the deterministic, stochastic and counterterm contributions are given by at one-loop order

$$\begin{aligned} P_g^\mathrm{det}(k,\chi,\chi') &= D(\chi)D(\chi')b_1(\chi)b_1(\chi')P_\mathrm{L}(k) \\ &\quad + D(\chi)D(\chi')\left[(D^2(\chi)+D^2(\chi'))P_g^{(13)}(k,\chi,\chi') + D(\chi)D(\chi')P_g^{(22)}(k,\chi,\chi')\right] \end{aligned} \tag{9.11}$$

$$P^\mathrm{stoch}(k,\chi,\chi') = \frac{\delta_\mathrm{D}(\chi-\chi')}{\bar{n}(\chi)}\left[P_\mathrm{shot}(\chi) + a_0(\chi)k^2\right]$$

$$P^\mathrm{ct}(k,\chi,\chi') = -D(\chi)D(\chi')\left(c_s^2(\chi)+c_s^2(\chi')\right)k^2 P_\mathrm{L}(k)$$

with the loop results

$$P_g^{(22)}(k,\tau,\tau') = 2\int_{\mathbf{p}} |K_2(\mathbf{p},\mathbf{k}-\mathbf{p},\tau,\tau')|^2 P_\mathrm{L}(\mathbf{p}) P_\mathrm{L}(\mathbf{k}-\mathbf{p}) \tag{9.12}$$

$$P_g^{(13)}(k,\tau,\tau') = 3P_\mathrm{L}(k)\int_{\mathbf{p}} K_3(\mathbf{p},-\mathbf{p},\mathbf{k},\tau,\tau') P_\mathrm{L}(\mathbf{p}),$$

depending on real-space bias kernels, K_n (cf. Appendix A). Here, the model depends on the following parameters:

$$\{b_1, b_2, b_{\mathcal{G}_2}, b_{\Gamma_3}, P_\mathrm{shot}, a_0, c_s^2\}; \tag{9.13}$$

whilst these are technically time-dependent, we can take them out of the integral and define effective scalar parameters in all cases. Here, the biases scale in terms of the halo scale R_halo, whilst the counterterm depends on k_NL (or R_halo, from the absorbed derivative bias), and P_shot is $\mathcal{O}(1)$, since we have removed the leading Poisson dependence. Inserting (9.10) into (9.9), we obtain the EFTofLSS prediction for the projected galaxy power spectrum, noting the former discussion of the ℓ-range.

    c.   *Spectroscopic Galaxy Surveys*   With the inclusion of a spectrometer, galaxy surveys are able to resolve the three-dimensional positions of galaxies, and thus measure the associated power spectrum (and beyond) directly. Surveys such as the Dark Energy Spectroscopic Instrument, Euclid, and SDSS, measure the galaxy power spectra through its Legendre multipoles, defined as

$$P_g(\mathbf{k},\tau) = \sum_{\ell=0}^{\infty} P_{g,\ell}(k,\tau) L_\ell(\mu) \qquad \Leftrightarrow \qquad P_{g,\ell}(k,\tau) = \frac{(2\ell+1)}{2}\int_{-1}^{1} d\mu\, P_g(\mathbf{k},\tau) L_\ell(\mu) \tag{9.14}$$

where L_ℓ is a Legendre polynomial and μ is the angle of $\mathbf{k}$ to the line-of-sight. In practice, the surveys observe the galaxy positions in terms of redshifts and angles which are converted to comoving coordinates via a fiducial cosmology. This transformation gives a modification to the observed coordinates [32, 121]

$$k \to k' \equiv k\left[\left(\frac{H_\mathrm{true}}{H_\mathrm{fid}}\right)^2 \mu^2 + \left(\frac{D_{A,\mathrm{fid}}}{D_{A,\mathrm{true}}}\right)^2 (1-\mu^2)\right]^{1/2} \tag{9.15}$$

$$\mu \to \mu' \equiv \mu\left(\frac{H_\mathrm{true}}{H_\mathrm{fid}}\right)\left[\left(\frac{H_\mathrm{true}}{H_\mathrm{fid}}\right)^2 \mu^2 + \left(\frac{D_{A,\mathrm{fid}}}{D_{A,\mathrm{true}}}\right)^2 (1-\mu^2)\right]^{-1/2},$$

suppressing dependence on time, where D_A and H are the angular diameter distance and Hubble parameter in the fiducial and true cosmology. This is often erroneously known as the 'Alcock-Paczynski' distortion (which strictly applies only to the BAO feature [133]). The observed power spectrum multipoles are then defined as

$$P_{g,\ell}(k,\tau) = \frac{D_{A,\mathrm{fid}}^2 H_\mathrm{true}}{D_{A,\mathrm{true}}^2 H_\mathrm{fid}} \cdot \frac{2\ell+1}{2}\int_{-1}^{1} d\mu\, P_g\left(k'(k,\mu),\mu'(\mu),\tau\right) L_\ell(\mu). \tag{9.16}$$

    The EFTofLSS model for the redshift-space galaxy power spectrum is defined by the following components (ignoring selection bias, cf. §8) [32, 121, 134] (see also [98] in redshift-space):

$$P_{g,\ell}(k,\tau) = P_{g,\ell}^\mathrm{det}(k,\tau) + P_{g,\ell}^\mathrm{stoch}(k,\tau) + P_{g,\ell}^\mathrm{ct}(k,\tau). \tag{9.17}$$

The deterministic piece is analogous to the above:

$$P_g^\mathrm{det}(\mathbf{k},\tau) = D^2(\tau) b_1^2(\tau) P_\mathrm{L}(k) + D^4(\tau)\left[2P_g^{(13)}(\mathbf{k},\tau) + P_g^{(22)}(\mathbf{k},\tau)\right], \tag{9.18}$$

with the loop integral definitions

$$P_g^{(22)}(\mathbf{k},\tau) = 2\int_{\mathbf{p}} |Z_2(\mathbf{p},\mathbf{k}-\mathbf{p},\tau)|^2 P_\mathrm{L}(\mathbf{p}) P_\mathrm{L}(\mathbf{k}-\mathbf{p}) \tag{9.19}$$

$$P_g^{(13)}(\mathbf{k},\tau) = 3P_\mathrm{L}(k)\int_{\mathbf{p}} Z_3(\mathbf{p},-\mathbf{p},\mathbf{k},\tau) P_\mathrm{L}(\mathbf{p}),$$
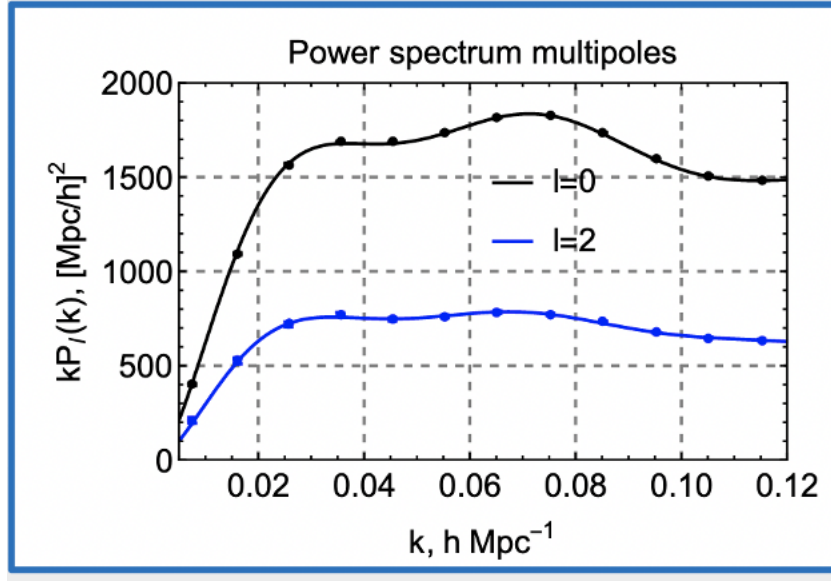
FIG. 3. Comparison of theoretical and simulated galaxy power spectra for the Perturbation Theory Challenge simulations of [135]. The solid lines show the one-loop EFTofLSS power spectrum monopole (black) and quadrupole (blue), whilst the points show the measurements (whose errors are too small to see). We find subpercent agreement on all the scales shown in the figure, after fitting for bias and cosmological parameters. The output cosmological parameters were also consistent with those of the (blinded) simulation inputs at high precision.

for redshift-space kernels defined in Appendix A. The stochastic piece can be written as

$$P_g^{\mathrm{stoch}}(\mathbf{k}, \tau) = \frac{1}{n(\tau)} \left[1 + P_{\mathrm{shot}}(\tau) + a_0(\tau)k^2 + a_2(\tau)k^2\mu^2 \right], \tag{9.20}$$

with the counterterm component (including the fingers-of-God pieces) taking the multipole form

$$
\begin{aligned}
P_g^{\mathrm{ct}}(\mathbf{k}, \tau) &= -2D^2(\tau) \left[c_0(\tau) + c_2(\tau)f(\tau)\mu^2 + c_4(\tau)f^2(\tau)\mu^4 \right] k^2 P_{\mathrm{L}}(k) \\
&\quad - D^2(\tau)\tilde{c}(\tau)f^4(\tau)\mu^4 k^4 \left[b_1(\tau) + f(\tau)\mu^2 \right]^2 P_{\mathrm{L}}(k).
\end{aligned}
\tag{9.21}
$$

The precise definition of counterterms (e.g., in 3D space or harmonic space, and with factor of $D(\tau)$, $f(\tau)$ *et cetera*) varies between works, but their k-scalings are universal. We note the appearance of a new term $(k\mu)^4 P_{\mathrm{L}}(k)$ term in the above; this is often included as a proxy for higher-order FoG effects, which are usually the first components of the model to become non-perturbative (see [109, 110] for approaches to null this feature). In essence, this term extends the FoG modelling to one higher loop in perturbation theory, which is useful if the characteristic scale is the smallest, *i.e.* $\sigma_{\mathrm{FoG}} < k_{\mathrm{NL}}, R_{\mathrm{halo}}$.

In full, the one-loop EFTofLSS galaxy model depends on the following parameters:

$$\{b_1, b_2, b_{\mathcal{G}_2}, b_{\Gamma_3}\} \times \{P_{\mathrm{shot}}, a_0, a_2\} \times \{c_0, c_2, c_4, \tilde{c}\}, \tag{9.22}$$

which can be measured from data and influence deterministic, stochastic, and counterterm contributions respectively. These also enter in the modeling of higher-order statistics such as bispectra, alongside new biases. An example of the EFTofLSS prediction is shown in Fig. 3. In this case, all bias and cosmological parameters were fit to the simulations (in a $\sim 600 h^{-3} \mathrm{Gpc}^3$ volume), and we find subpercent agreement, showing the precise nature of the theory [135].

d. Diffuse Emission Our final class of observations concern the measurement of diffuse emission such as neutral Hydrogen and metal lines. Various experiments to map these exist, including Lyman-α observations, 21-cm observatories (such as CHIME, HiRAX and PUMA), and line intensity mapping searches (including COMAP). Often, the physical quantity of interest is an optical depth, τ, encoding the fraction of matter. This is a biased tracer of the matter field, and can thus be expanded analogously to the above (cf. §8):

$$\tau(\mathbf{s}, \chi) = \tau_0(\chi) \left[1 + b_1(\chi)\delta(\mathbf{s}, \chi) + \cdots \right], \tag{9.23}$$

where we parametrize time by comoving distance χ to avoid confusion with optical depth and denote the background depth by $\tau_0 = \langle \tau \rangle$. Telescopes are sensitive to the flux of the specific line, defined by

$$F(\mathbf{s}, \chi) = e^{-\tau(\mathbf{s}, \chi)} \equiv F_0(\chi)\left[1 + \delta F(\mathbf{s}, \chi)\right]. \tag{9.24}$$

EFTofLSS modeling of diffuse emission then boils down to predicting the statistics of the fluctuation field $\delta F(\mathbf{s}, \tau)$. For neutral hydrogen, one often works directly with the 21-cm temperature, $T_{21}(\mathbf{x}, \tau)$ but a similar logic applies. In all cases, the field acts as a biased tracer of δ, and thus can be modelled with the same tools used for spectroscopic galaxy surveys above. We caution that a number of additional effects can complicate this however, including: (a) high-redshift fields can be strongly affected by long-wavelength fluctuations in the ionizing ultraviolet background that are difficult to treat perturbatively [e.g., 79, 136]; (b) due to the exponential mapping, the resulting theories often contain velocity bias, as described in §8. Detailed discussions of the corresponding EFTofLSS theories can be found in [e.g., 117, 137].

e. Practical Implementation   A variety of public codes exist implementing the above statistics in C and Python. The three most common are:

- Class-PT:[9] This is a C code based on Class [138, 139] that computes the one-loop power spectrum of matter and biased tracers in real- and redshift-space, optionally including primordial non-Gaussianity [32]. All above effects, including UV counterterms, IR resummation, and coordinate distortions are included by default. The code can be interfaced with the MontePython sampler [140] via Python likelihoods[10] which additionally include BAO parameters and the bispectrum.

- PyBird:[11] This is a Python code for computing the Eulerian one-loop power spectrum given an input linear power spectrum [141]. This includes the one-loop power spectrum of matter and biased tracers in real- and redshift-space, and additionally includes MontePython likelihoods.

- Velocileptors:[12] This is a Python code computing the one-loop power spectra of matter and biased tracers in real- and redshift-space, additionally including real-space velocity correlators [98]. Unlike the above codes, this is formulated using Lagrangian perturbation theory (with EFTofLSS corrections).

These codes rely heavily on the FFTLog procedure to compute loop integrals, as developed in [142]. Additionally, all three have been used in blind cosmological challenges and found to recover cosmological parameters to high-precision [135], and used in a wide variety of analyses of data, both using the power spectrum and beyond [e.g., 110, 121, 132, 134, 141, 143–184].

10.   CONCLUSION

The Effective Field Theory of Large Scale Structure allows for precision modeling of cosmological observables on large-scales. By treating the Universe as an imperfect fluid and solving the resulting equations perturbatively, we can model phenomena such as weak lensing, galaxy clustering, and the correlation properties of diffuse emission. The theory is mathematically rich, but the basic ideas are conceptually straightforward, arising from the requirement of perturbativity, and the associated restriction to smoothed fields. Concepts such as renormalization arise naturally from this and ensure that our theory is well behaved and physical.

Here, we have presented an overview of the key ideas of the EFTofLSS and derived models for the power spectra of various observables. There remains a number of topics that have not been discussed above, however, some of which we now briefly mention.

- **Baryonic Effects**: We have treated the Universe as a single imperfect fluid. In reality, the situation is more akin to a coupled fluid of cold dark matter (CDM) and baryons, interacting gravitationally and exchanging energy and momentum. Extensions of the EFTofLSS to this scenario exist [e.g., 130, 185]; however, on perturbative scales it is usually an excellent approximation to work with a single (CDM-plus-baryons) field noting that the leading-order corrections modify only the (unknown) values of the counterterms. This remains true in the presence of feedback (which the EFTofLSS naturally includes at lowest order), though difficulties can arise at high redshift due to radiation effects [e.g., 79, 136].

---

[9] GitHub.com/Michalychforever/CLASS-PT
[10] GitHub.com/oliverphilcox/full_shape_likelihoods
[11] GitHub.com/pierrexyz/pybird
[12] GitHub.com/sfschen/velocileptors

- **Massive Neutrinos**: Particle physics yields strong evidence that the Universe contains neutrinos with mass $M_\nu > 0.06\,\mathrm{eV}$. These may be included in the EFTofLSS in a similar manner to baryonic effects, as described in detail in [46, 186–190]. Once again, it is usually an excellent approximation to model the Universe as a single fluid inserting the relevant CDM+baryon linear power spectrum, which receives modifications from massive neutrinos, including the generation of a scale-dependent growth factor.

- **General Relativity**: Throughout this discussion we have assumed the Newtonian limit, *i.e.* that scales are small compared to the particle horizon, corresponding to $k\mathcal{H} \gg 1$. Perturbative approaches can be wrought on these large scales (and contain many contributions including from magnification and lensing) [e.g., 111, 191–193], but the EFTofLSS corrections are rarely of use, since they appear only on quasi-linear scales and below.

- **Primordial Non-Gaussianity**: Many models of inflation predict a non-Gaussian spectrum of primordial density fluctuations, which manifests in a non-Gaussian correlation structure for $\delta_{\rm L}$, for example the appearance of non-zero bispectra proportional to $\langle \delta_{\rm L}^3 \rangle$ [194]. These phenomena can be modeled in the EFTofLSS (and lead to additional loop contributions and biases) and have been used to place constraints on the underlying inflationary parameters [e.g., 77, 148, 149, 151, 157, 195].

- **Field-Level Inference**: Whilst most cosmological surveys have focused on measuring summary statistics such as power spectra and bispectra, one may also perform field-level inference, predicting the late-time observables directly. This technique, though still in its infancy, can be done using the EFTofLSS and essentially uses the above formulae to predict $\delta_g(\mathbf{x}, \tau)$ as a functional of $\delta_{\rm L}$ which is then compared to data [e.g., 44, 62, 196–202].

- **BAO Reconstruction**: Modern spectroscopic analyses have employed a reconstruction procedure to sharpen the BAO peak and thus extract more information on the Hubble parameter. This can be modelled within the EFTofLSS, and included within the analysis framework [146, 161, 203–207].

There remains much more progress to be made within the EFTofLSS. Examples of this include computing higher-order corrections to the above statistics (allowing for a greater range of scales to be modeled), as well as measuring and modeling new statistics and data. Many of these developments will come in the near future.

Appendix A: Eulerian Perturbation Theory Kernels

In this appendix we state explicitly the perturbation theory kernels up to third order. These have been derived many times before [e.g., 5], but we include them here for completeness. The kernels are given by:

$$
\begin{aligned}
Z_1(\mathbf{p}_1, \tau) &= b_1(\tau) \qquad\qquad\qquad\qquad\qquad\qquad\qquad\qquad\qquad\qquad\qquad\qquad\qquad\qquad (A.1)\\
Z_2(\mathbf{p}_1, \mathbf{p}_2, \tau) &= \frac{b_2(\tau)}{2} + b_{\mathcal{G}_2}(\tau)\left(\frac{(\mathbf{p}_1 \cdot \mathbf{p}_2)^2}{p_1^2 p_2^2} - 1\right) + b_1(\tau) F_2(\mathbf{p}_1, \mathbf{p}_2) + f(\tau)\mu^2 G_2(\mathbf{p}_1, \mathbf{p}_2)\\
&\quad + \frac{f(\tau)\mu k}{2}\left(\frac{\mu_1}{p_1}(b_1(\tau) + f(\tau)\mu_2^2) + \frac{\mu_2}{p_2}(b_1(\tau) + f(\tau)\mu_1^2)\right)\\
Z_3(\mathbf{p}_1, \mathbf{p}_2, \mathbf{p}_3, \tau) &= 2b_{\Gamma_3}(\tau)\left[\frac{(\mathbf{p}_1 \cdot \mathbf{p}_{23})^2}{p_1^2 p_{23}^2} - 1\right](F_2(\mathbf{p}_2, \mathbf{p}_3) - G_2(\mathbf{p}_2, \mathbf{p}_3)) + b_1(\tau) F_3(\mathbf{p}_1, \mathbf{p}_2, \mathbf{p}_3) + f(\tau)\mu^2 G_3(\mathbf{p}_1, \mathbf{p}_2, \mathbf{p}_3)\\
&\quad + \frac{(f(\tau)\mu k)^2}{2}(b_1(\tau) + f(\tau)\mu_1^2)\frac{\mu_2}{p_2}\frac{\mu_3}{p_3} + f(\tau)\mu k \frac{\mu_3}{p_3}\left[b_1(\tau) F_2(\mathbf{p}_1, \mathbf{p}_2) + f(\tau)\mu_{12}^2 G_2(\mathbf{p}_1, \mathbf{p}_2)\right]\\
&\quad + f(\tau)\mu k\left(b_1(\tau) + f(\tau)\mu_1^2\right)\frac{\mu_{23}}{p_{23}} G_2(\mathbf{p}_2, \mathbf{p}_3) + b_2(\tau) F_2(\mathbf{p}_1, \mathbf{p}_2)\\
&\quad + 2b_{\mathcal{G}_2}(\tau)\left[\frac{(\mathbf{p}_1 \cdot \mathbf{p}_{23})^2}{p_1^2 p_{23}^2} - 1\right] F_2(\mathbf{p}_2, \mathbf{p}_3) + \frac{b_2(\tau) f(\tau)\mu k}{2}\frac{\mu_1}{p_1} + b_{\mathcal{G}_2}(\tau) f(\tau)\mu k \frac{\mu_1}{p_1}\left[\frac{(\mathbf{p}_2 \cdot \mathbf{p}_3)^2}{p_2^2 p_3^2} - 1\right],
\end{aligned}
$$

where $\mathbf{p}_{ij} \equiv \mathbf{p}_i + \mathbf{p}_j$, $\mathbf{k} \equiv \mathbf{p}_1 + \cdots \mathbf{p}_n$, and the Z_3 kernel has not been symmetrized over its arguments. We keep only bias terms in Z_3 relevant for computation of the one-loop power spectrum. These functions involve the density and velocity kernels F_n and G_n, themselves given by (before symmetrization)

$$F_2(\mathbf{p}_1, \mathbf{p}_2) = \frac{5}{7}\alpha(\mathbf{p}_1, \mathbf{p}_2) + \frac{2}{7}\beta(\mathbf{p}_1, \mathbf{p}_2) \tag{A.2}$$

$$G_2(\mathbf{p}_1, \mathbf{p}_2) = \frac{3}{7}\alpha(\mathbf{p}_1, \mathbf{p}_2) + \frac{4}{7}\beta(\mathbf{p}_1, \mathbf{p}_2)$$

$$F_3(\mathbf{p}_1, \mathbf{p}_2, \mathbf{p}_3) = \frac{1}{18}\left[7\alpha(\mathbf{p}_1, \mathbf{p}_{23})F_2(\mathbf{p}_2, \mathbf{p}_3) + 2\beta(\mathbf{p}_1, \mathbf{p}_{23})G_2(\mathbf{p}_2, \mathbf{p}_3)\right] + \frac{G_2(\mathbf{p}_1, \mathbf{p}_2)}{18}\left[7\alpha(\mathbf{p}_{12}, \mathbf{p}_3) + 2\beta(\mathbf{p}_{12}, \mathbf{p}_3)\right]$$

$$G_3(\mathbf{p}_1, \mathbf{p}_2, \mathbf{p}_3) = \frac{1}{18}\left[3\alpha(\mathbf{p}_1, \mathbf{p}_{23})F_2(\mathbf{p}_2, \mathbf{p}_3) + 6\beta(\mathbf{p}_1, \mathbf{p}_{23})G_2(\mathbf{p}_2, \mathbf{p}_3)\right] + \frac{G_2(\mathbf{p}_1, \mathbf{p}_2)}{18}\left[3\alpha(\mathbf{p}_{12}, \mathbf{p}_3) + 6\beta(\mathbf{p}_{12}, \mathbf{p}_3)\right]$$

in terms of

$$\alpha(\mathbf{p}_1, \mathbf{p}_2) = \frac{\mathbf{p}_1 \cdot \mathbf{p}_{12}}{p_1^2} \qquad \text{and} \qquad \beta(\mathbf{p}_1, \mathbf{p}_2) = \frac{p_{12}^2}{2}\frac{\mathbf{p}_1 \cdot \mathbf{p}_2}{p_1^2 p_2^2}. \tag{A.3}$$

Note that the F_n and G_n kernels should be symmetrized, e.g., $F_2(\mathbf{p}_1, \mathbf{p}_2) \to [F_2(\mathbf{p}_1, \mathbf{p}_2) + F_2(\mathbf{p}_2, \mathbf{p}_1)]/2$. The real-space kernels can be extracted from (A.1) by setting $f(\tau) = 0$; likewise the matter kernels are obtained by setting $b_1(\tau) = 1$ and all other biases to zero.

[1] K. S. Dawson *et al.* (BOSS), Astron. J. **145**, 10 (2013), arXiv:1208.0022 [astro-ph.CO].
[2] A. Aghamousa *et al.* (DESI), (2016), arXiv:1611.00036 [astro-ph.IM].
[3] R. Laureijs *et al.* (EUCLID), (2011), arXiv:1110.3193 [astro-ph.CO].
[4] P. J. E. Peebles, in *Large Scale Structures in the Universe*, Vol. 79, edited by M. S. Longair and J. Einasto (1978) p. 217.
[5] F. Bernardeau, S. Colombi, E. Gaztanaga, and R. Scoccimarro, Phys. Rept. **367**, 1 (2002), arXiv:astro-ph/0112551.
[6] D. Baumann, A. Nicolis, L. Senatore, and M. Zaldarriaga, JCAP **07**, 051 (2012), arXiv:1004.2488 [astro-ph.CO].
[7] J. J. M. Carrasco, M. P. Hertzberg, and L. Senatore, JHEP **09**, 082 (2012), arXiv:1206.2926 [astro-ph.CO].
[8] K. Heitmann, M. White, C. Wagner, S. Habib, and D. Higdon, Astrophys. J. **715**, 104 (2010), arXiv:0812.1052 [astro-ph].
[9] T. Nishimichi *et al.*, Astrophys. J. **884**, 29 (2019), arXiv:1811.09504 [astro-ph.CO].
[10] M. Knabenhans *et al.* (Euclid), Mon. Not. Roy. Astron. Soc. **484**, 5509 (2019), arXiv:1809.04695 [astro-ph.CO].
[11] E. Lawrence, K. Heitmann, J. Kwan, A. Upadhye, D. Bingham, S. Habib, D. Higdon, A. Pope, H. Finkel, and N. Frontiere, Astrophys. J. **847**, 50 (2017), arXiv:1705.03388 [astro-ph.CO].
[12] U. Seljak and Z. Vlah, Phys. Rev. D **91**, 123516 (2015), arXiv:1501.07512 [astro-ph.CO].
[13] T. Okumura, N. Hand, U. Seljak, Z. Vlah, and V. Desjacques, Phys. Rev. D **92**, 103516 (2015), arXiv:1506.05814 [astro-ph.CO].
[14] O. H. E. Philcox, D. N. Spergel, and F. Villaescusa-Navarro, Phys. Rev. D **101**, 123520 (2020), arXiv:2004.09515 [astro-ph.CO].
[15] A. Cooray and R. K. Sheth, Phys. Rept. **372**, 1 (2002), arXiv:astro-ph/0206508.
[16] P. Valageas and T. Nishimichi, Astron. Astrophys. **527**, A87 (2011), arXiv:1009.0597 [astro-ph.CO].
[17] A. Mead, J. Peacock, C. Heymans, S. Joudaki, and A. Heavens, Mon. Not. Roy. Astron. Soc. **454**, 1958 (2015), arXiv:1505.07833 [astro-ph.CO].
[18] I. Mohammed and U. Seljak, Mon. Not. Roy. Astron. Soc. **445**, 3382 (2014), arXiv:1407.0060 [astro-ph.CO].
[19] R. Voivodic, H. Rubira, and M. Lima, JCAP **10**, 033 (2020), arXiv:2003.06411 [astro-ph.CO].
[20] F. Schmidt, Phys. Rev. D **93**, 063512 (2016), arXiv:1511.02231 [astro-ph.CO].
[21] R. E. Smith, J. A. Peacock, A. Jenkins, S. D. M. White, C. S. Frenk, F. R. Pearce, P. A. Thomas, G. Efstathiou, and H. M. P. Couchmann (VIRGO Consortium), Mon. Not. Roy. Astron. Soc. **341**, 1311 (2003), arXiv:astro-ph/0207664.
[22] R. Takahashi, M. Sato, T. Nishimichi, A. Taruya, and M. Oguri, Astrophys. J. **761**, 152 (2012), arXiv:1208.2701 [astro-ph.CO].
[23] T. Matsubara, Phys. Rev. D **77**, 063530 (2008), arXiv:0711.2521 [astro-ph].
[24] S. Matarrese and M. Pietroni, JCAP **06**, 026 (2007), arXiv:astro-ph/0703563.
[25] M. Crocce and R. Scoccimarro, Phys. Rev. D **73**, 063519 (2006), arXiv:astro-ph/0509418.
[26] A. Taruya, F. Bernardeau, T. Nishimichi, and S. Codis, Phys. Rev. D **86**, 103528 (2012), arXiv:1208.1191 [astro-ph.CO].
[27] A. Taruya, T. Nishimichi, and S. Saito, Phys. Rev. D **82**, 063522 (2010), arXiv:1006.0699 [astro-ph.CO].
[28] M. Peloso and M. Pietroni, JCAP **01**, 056 (2017), arXiv:1609.06624 [astro-ph.CO].
[29] M. Baumgart *et al.*, in *2022 Snowmass Summer Study* (2022) arXiv:2210.03199 [hep-ph].
[30] G. Cabass, M. M. Ivanov, M. Lewandowski, M. Mirbabayi, and M. Simonović, in *2022 Snowmass Summer Study* (2022) arXiv:2203.08232 [astro-ph.CO].

[31] F. Villaescusa-Navarro *et al.*, Astrophys. J. Suppl. **250**, 2 (2020), arXiv:1909.05273 [astro-ph.CO].
[32] A. Chudaykin, M. M. Ivanov, O. H. E. Philcox, and M. Simonović, Phys. Rev. D **102**, 063533 (2020), arXiv:2004.10607 [astro-ph.CO].
[33] E. Pajer and M. Zaldarriaga, JCAP **08**, 037 (2013), arXiv:1301.7182 [astro-ph.CO].
[34] J. J. M. Carrasco, S. Foreman, D. Green, and L. Senatore, JCAP **07**, 056 (2014), arXiv:1304.4946 [astro-ph.CO].
[35] M. Cataneo, S. Foreman, and L. Senatore, JCAP **04**, 026 (2017), arXiv:1606.03633 [astro-ph.CO].
[36] M. Lewandowski and L. Senatore, JCAP **08**, 037 (2017), arXiv:1701.07012 [astro-ph.CO].
[37] T. Baldauf, L. Mercolli, and M. Zaldarriaga, Phys. Rev. D **92**, 123007 (2015), arXiv:1507.02256 [astro-ph.CO].
[38] T. Baldauf, E. Schaan, and M. Zaldarriaga, JCAP **03**, 007 (2016), arXiv:1507.02255 [astro-ph.CO].
[39] D. Blas, M. Garny, and T. Konstandin, JCAP **01**, 010 (2014), arXiv:1309.3308 [astro-ph.CO].
[40] T. Konstandin, R. A. Porto, and H. Rubira, JCAP **11**, 027 (2019), arXiv:1906.00997 [astro-ph.CO].
[41] M. McQuinn and M. White, JCAP **01**, 043 (2016), arXiv:1502.07389 [astro-ph.CO].
[42] M. Fasiello, T. Fujita, and Z. Vlah, Phys. Rev. D **106**, 123504 (2022), arXiv:2205.10026 [astro-ph.CO].
[43] M. M. Ivanov, (2022), arXiv:2212.08488 [astro-ph.CO].
[44] G. Cabass and F. Schmidt, JCAP **04**, 042 (2020), arXiv:1909.04022 [astro-ph.CO].
[45] A. Chudaykin, M. M. Ivanov, and S. Sibiryakov, (2022), arXiv:2212.09799 [astro-ph.CO].
[46] R. de Belsunce and L. Senatore, JCAP **02**, 038 (2019), arXiv:1804.06849 [astro-ph.CO].
[47] S. Saito, T. Baldauf, Z. Vlah, U. Seljak, T. Okumura, and P. McDonald, Phys. Rev. D **90**, 123522 (2014), arXiv:1405.1447 [astro-ph.CO].
[48] M. Mirbabayi, M. Simonović, and M. Zaldarriaga, (2014), arXiv:1412.3796 [astro-ph.CO].
[49] R. E. Angulo, S. Foreman, M. Schmittfull, and L. Senatore, JCAP **10**, 039 (2015), arXiv:1406.4143 [astro-ph.CO].
[50] D. Bertolini, K. Schutz, M. P. Solon, and K. M. Zurek, JCAP **06**, 052 (2016), arXiv:1604.01770 [astro-ph.CO].
[51] T. Steele and T. Baldauf, Phys. Rev. D **103**, 103518 (2021), arXiv:2101.10289 [astro-ph.CO].
[52] O. H. E. Philcox, E. Massara, and D. N. Spergel, Phys. Rev. D **102**, 043516 (2020), arXiv:2006.10055 [astro-ph.CO].
[53] O. H. E. Philcox, A. Aviles, and E. Massara, JCAP **03**, 038 (2021), arXiv:2010.05914 [astro-ph.CO].
[54] H. Rubira and R. Voivodic, JCAP **03**, 070 (2021), arXiv:2011.12280 [astro-ph.CO].
[55] S. Foreman, H. Perrier, and L. Senatore, JCAP **05**, 027 (2016), arXiv:1507.05326 [astro-ph.CO].
[56] Z. Vlah, U. Seljak, and T. Baldauf, Phys. Rev. D **91**, 023508 (2015), arXiv:1410.1617 [astro-ph.CO].
[57] Z. Vlah, M. White, and A. Aviles, JCAP **09**, 014 (2015), arXiv:1506.05264 [astro-ph.CO].
[58] Z. Vlah, E. Castorina, and M. White, JCAP **12**, 007 (2016), arXiv:1609.02908 [astro-ph.CO].
[59] M. Zaldarriaga and M. Mirbabayi, (2015), arXiv:1511.01889 [astro-ph.CO].
[60] R. A. Porto, L. Senatore, and M. Zaldarriaga, JCAP **05**, 022 (2014), arXiv:1311.2168 [astro-ph.CO].
[61] M. White, Mon. Not. Roy. Astron. Soc. **439**, 3630 (2014), arXiv:1401.5466 [astro-ph.CO].
[62] F. Schmidt, JCAP **04**, 033 (2021), arXiv:2012.09837 [astro-ph.CO].
[63] T. Matsubara, Phys. Rev. D **92**, 023534 (2015), arXiv:1505.01481 [astro-ph.CO].
[64] L. Senatore and M. Zaldarriaga, JCAP **02**, 013 (2015), arXiv:1404.5954 [astro-ph.CO].
[65] L. Senatore and G. Trevisan, JCAP **05**, 019 (2018), arXiv:1710.02178 [astro-ph.CO].
[66] M. Lewandowski and L. Senatore, JCAP **03**, 018 (2020), arXiv:1810.11855 [astro-ph.CO].
[67] D. Blas, M. Garny, M. M. Ivanov, and S. Sibiryakov, JCAP **07**, 052 (2016), arXiv:1512.05807 [astro-ph.CO].
[68] D. Blas, M. Garny, M. M. Ivanov, and S. Sibiryakov, JCAP **07**, 028 (2016), arXiv:1605.02149 [astro-ph.CO].
[69] Z. Vlah, U. Seljak, M. Y. Chu, and Y. Feng, JCAP **03**, 057 (2016), arXiv:1509.02120 [astro-ph.CO].
[70] T. Baldauf, M. Mirbabayi, M. Simonović, and M. Zaldarriaga, Phys. Rev. D **92**, 043514 (2015), arXiv:1504.04366 [astro-ph.CO].
[71] S.-F. Chen, Z. Vlah, and M. White, JCAP **11**, 035 (2020), arXiv:2007.00704 [astro-ph.CO].
[72] L. Senatore, JCAP **11**, 007 (2015), arXiv:1406.7843 [astro-ph.CO].
[73] R. Angulo, M. Fasiello, L. Senatore, and Z. Vlah, JCAP **09**, 029 (2015), arXiv:1503.08826 [astro-ph.CO].
[74] A. Perko, L. Senatore, E. Jennings, and R. H. Wechsler, (2016), arXiv:1610.09321 [astro-ph.CO].
[75] Y. Donath and L. Senatore, JCAP **10**, 039 (2020), arXiv:2005.04805 [astro-ph.CO].
[76] T. Fujita, V. Mauerhofer, L. Senatore, Z. Vlah, and R. Angulo, JCAP **01**, 009 (2020), arXiv:1609.00717 [astro-ph.CO].
[77] V. Assassi, D. Baumann, and F. Schmidt, JCAP **12**, 043 (2015), arXiv:1510.03723 [astro-ph.CO].
[78] V. Desjacques, D. Jeong, and F. Schmidt, Phys. Rept. **733**, 1 (2018), arXiv:1611.09787 [astro-ph.CO].
[79] G. Cabass and F. Schmidt, JCAP **05**, 031 (2019), arXiv:1812.02731 [astro-ph.CO].
[80] S.-F. Chen, E. Castorina, and M. White, JCAP **06**, 006 (2019), arXiv:1903.00437 [astro-ph.CO].
[81] T. Fujita and Z. Vlah, JCAP **10**, 059 (2020), arXiv:2003.10114 [astro-ph.CO].
[82] V. Assassi, D. Baumann, D. Green, and M. Zaldarriaga, JCAP **08**, 056 (2014), arXiv:1402.5916 [astro-ph.CO].
[83] M. Mirbabayi, F. Schmidt, and M. Zaldarriaga, JCAP **07**, 030 (2015), arXiv:1412.5169 [astro-ph.CO].
[84] F. Schmidt, D. Jeong, and V. Desjacques, Phys. Rev. D **88**, 023515 (2013), arXiv:1212.0868 [astro-ph.CO].
[85] T. Lazeyras and F. Schmidt, JCAP **09**, 008 (2018), arXiv:1712.07531 [astro-ph.CO].
[86] N. Agarwal, V. Desjacques, D. Jeong, and F. Schmidt, JCAP **03**, 021 (2021), arXiv:2007.04340 [astro-ph.CO].
[87] A. Eggemeier, R. Scoccimarro, and R. E. Smith, Phys. Rev. D **99**, 123514 (2019), arXiv:1812.03208 [astro-ph.CO].
[88] A. Eggemeier, R. Scoccimarro, R. E. Smith, M. Crocce, A. Pezzotta, and A. G. Sánchez, Phys. Rev. D **103**, 123550 (2021), arXiv:2102.06902 [astro-ph.CO].
[89] P. McDonald and A. Roy, JCAP **08**, 020 (2009), arXiv:0902.0991 [astro-ph.CO].
[90] P. McDonald, Phys. Rev. D **74**, 103512 (2006), [Erratum: Phys.Rev.D 74, 129901 (2006)], arXiv:astro-ph/0609413.

[91] K. C. Chan and R. Scoccimarro, Phys. Rev. D **86**, 103519 (2012), arXiv:1204.5770 [astro-ph.CO].
[92] K. C. Chan, R. Scoccimarro, and R. K. Sheth, Phys. Rev. D **85**, 083509 (2012), arXiv:1201.3614 [astro-ph.CO].
[93] N. Kokron, J. DeRose, S.-F. Chen, M. White, and R. H. Wechsler, Mon. Not. Roy. Astron. Soc. **505**, 1422 (2021), arXiv:2101.11014 [astro-ph.CO].
[94] N. Kokron, J. DeRose, S.-F. Chen, M. White, and R. H. Wechsler, Mon. Not. Roy. Astron. Soc. **514**, 2198 (2022), arXiv:2112.00012 [astro-ph.CO].
[95] A. Nicolis, R. Rattazzi, and E. Trincherini, Phys. Rev. D **79**, 064036 (2009), arXiv:0811.2197 [hep-th].
[96] J. Carlson, B. Reid, and M. White, Mon. Not. Roy. Astron. Soc. **429**, 1674 (2013), arXiv:1209.0780 [astro-ph.CO].
[97] T. Matsubara, Phys. Rev. D **78**, 083519 (2008), [Erratum: Phys.Rev.D 78, 109901 (2008)], arXiv:0807.1733 [astro-ph].
[98] S.-F. Chen, Z. Vlah, and M. White, JCAP **07**, 062 (2020), arXiv:2005.00523 [astro-ph.CO].
[99] V. Desjacques, D. Jeong, and F. Schmidt, JCAP **12**, 035 (2018), arXiv:1806.04015 [astro-ph.CO].
[100] E. O. Nadler, A. Perko, and L. Senatore, JCAP **02**, 058 (2018), arXiv:1710.10308 [astro-ph.CO].
[101] L. Senatore and M. Zaldarriaga, (2014), arXiv:1409.1225 [astro-ph.CO].
[102] S. Foreman and L. Senatore, JCAP **04**, 033 (2016), arXiv:1503.01775 [astro-ph.CO].
[103] Z. Vlah and M. White, JCAP **03**, 007 (2019), arXiv:1812.02775 [astro-ph.CO].
[104] M. Lewandowski, L. Senatore, F. Prada, C. Zhao, and C.-H. Chuang, Phys. Rev. D **97**, 063526 (2018), arXiv:1512.06831 [astro-ph.CO].
[105] A. Aviles, G. Valogiannis, M. A. Rodriguez-Meza, J. L. Cervantes-Cota, B. Li, and R. Bean, JCAP **04**, 039 (2021), arXiv:2012.05077 [astro-ph.CO].
[106] N. Kaiser, Mon. Not. Roy. Astron. Soc. **227**, 1 (1987).
[107] A. J. S. Hamilton, in *Ringberg Workshop on Large Scale Structure* (1997) arXiv:astro-ph/9708102.
[108] J. C. Jackson, Mon. Not. Roy. Astron. Soc. **156**, 1P (1972), arXiv:0810.3908 [astro-ph].
[109] M. M. Ivanov, O. H. E. Philcox, M. Simonović, M. Zaldarriaga, T. Nischimichi, and M. Takada, Phys. Rev. D **105**, 043531 (2022), arXiv:2110.00006 [astro-ph.CO].
[110] G. D'Amico, L. Senatore, P. Zhang, and T. Nishimichi, (2021), arXiv:2110.00016 [astro-ph.CO].
[111] E. Castorina and M. White, Mon. Not. Roy. Astron. Soc. **479**, 741 (2018), arXiv:1803.08185 [astro-ph.CO].
[112] Z. Vlah, U. Seljak, P. McDonald, T. Okumura, and T. Baldauf, JCAP **11**, 009 (2012), arXiv:1207.0839 [astro-ph.CO].
[113] Z. Vlah, U. Seljak, T. Okumura, and V. Desjacques, JCAP **10**, 053 (2013), arXiv:1308.6294 [astro-ph.CO].
[114] M. M. Ivanov and S. Sibiryakov, JCAP **07**, 053 (2018), arXiv:1804.05080 [astro-ph.CO].
[115] A. Obuljen, N. Dalal, and W. J. Percival, JCAP **10**, 020 (2019), arXiv:1906.11823 [astro-ph.CO].
[116] A. Obuljen, W. J. Percival, and N. Dalal, JCAP **10**, 058 (2020), arXiv:2004.07240 [astro-ph.CO].
[117] S.-F. Chen, Z. Vlah, and M. White, JCAP **05**, 053 (2021), arXiv:2103.13498 [astro-ph.CO].
[118] G. D'Amico, Y. Donath, M. Lewandowski, L. Senatore, and P. Zhang, (2022), arXiv:2211.17130 [astro-ph.CO].
[119] O. H. E. Philcox, M. M. Ivanov, G. Cabass, M. Simonović, M. Zaldarriaga, and T. Nishimichi, Phys. Rev. D **106**, 043530 (2022), arXiv:2206.02800 [astro-ph.CO].
[120] M. M. Ivanov, O. H. E. Philcox, T. Nishimichi, M. Simonović, M. Takada, and M. Zaldarriaga, Phys. Rev. D **105**, 063512 (2022), arXiv:2110.10161 [astro-ph.CO].
[121] M. M. Ivanov, M. Simonović, and M. Zaldarriaga, JCAP **05**, 042 (2020), arXiv:1909.05277 [astro-ph.CO].
[122] M. Kilbinger *et al.*, Mon. Not. Roy. Astron. Soc. **472**, 2126 (2017), arXiv:1702.05301 [astro-ph.CO].
[123] P. Lemos, A. Challinor, and G. Efstathiou, JCAP **05**, 014 (2017), arXiv:1704.01054 [astro-ph.CO].
[124] X. Fang, E. Krause, T. Eifler, and N. MacCrann, JCAP **05**, 010 (2020), arXiv:1911.11947 [astro-ph.CO].
[125] Z. Vlah, N. E. Chisari, and F. Schmidt, JCAP **01**, 025 (2020), arXiv:1910.08085 [astro-ph.CO].
[126] Z. Vlah, N. E. Chisari, and F. Schmidt, JCAP **05**, 061 (2021), arXiv:2012.04114 [astro-ph.CO].
[127] N. Schöneberg, M. Simonović, J. Lesgourgues, and M. Zaldarriaga, JCAP **10**, 047 (2018), arXiv:1807.09540 [astro-ph.CO].
[128] V. Assassi, M. Simonović, and M. Zaldarriaga, JCAP **11**, 054 (2017), arXiv:1705.05022 [astro-ph.CO].
[129] P. Chakraborty, S.-F. Chen, and C. Dvorkin, JCAP **07**, 038 (2022), arXiv:2202.11724 [astro-ph.CO].
[130] D. P. L. Bragança, M. Lewandowski, D. Sekera, L. Senatore, and R. Sgier, JCAP **10**, 074 (2021), arXiv:2010.02929 [astro-ph.CO].
[131] C. Modi, M. White, and Z. Vlah, JCAP **08**, 009 (2017), arXiv:1706.03173 [astro-ph.CO].
[132] S.-F. Chen, M. White, J. DeRose, and N. Kokron, JCAP **07**, 041 (2022), arXiv:2204.10392 [astro-ph.CO].
[133] C. Alcock and B. Paczynski, Nature **281**, 358 (1979).
[134] G. D'Amico, J. Gleyzes, N. Kokron, K. Markovic, L. Senatore, P. Zhang, F. Beutler, and H. Gil-Marín, JCAP **05**, 005 (2020), arXiv:1909.05271 [astro-ph.CO].
[135] T. Nishimichi, G. D'Amico, M. M. Ivanov, L. Senatore, M. Simonović, M. Takada, M. Zaldarriaga, and P. Zhang, Phys. Rev. D **102**, 123541 (2020), arXiv:2003.08277 [astro-ph.CO].
[136] F. Schmidt and F. Beutler, Phys. Rev. D **96**, 083533 (2017), arXiv:1705.07843 [astro-ph.CO].
[137] A. Pourtsidou, (2022), 10.1093/mnras/stad127, arXiv:2206.14727 [astro-ph.CO].
[138] J. Lesgourgues, (2011), arXiv:1104.2932 [astro-ph.IM].
[139] D. Blas, J. Lesgourgues, and T. Tram, JCAP **07**, 034 (2011), arXiv:1104.2933 [astro-ph.CO].
[140] T. Brinckmann and J. Lesgourgues, Phys. Dark Univ. **24**, 100260 (2019), arXiv:1804.07261 [astro-ph.CO].
[141] G. D'Amico, L. Senatore, and P. Zhang, JCAP **01**, 006 (2021), arXiv:2003.07956 [astro-ph.CO].
[142] M. Simonović, T. Baldauf, M. Zaldarriaga, J. J. Carrasco, and J. A. Kollmeier, JCAP **04**, 030 (2018), arXiv:1708.08130 [astro-ph.CO].
[143] M. M. Ivanov, M. Simonović, and M. Zaldarriaga, Phys. Rev. D **101**, 083504 (2020), arXiv:1912.08208 [astro-ph.CO].

[144] M. M. Ivanov, E. McDonough, J. C. Hill, M. Simonović, M. W. Toomey, S. Alexander, and M. Zaldarriaga, Phys. Rev. D **102**, 103502 (2020), arXiv:2006.11235 [astro-ph.CO].

[145] O. H. E. Philcox and M. M. Ivanov, Phys. Rev. D **105**, 043517 (2022), arXiv:2112.04515 [astro-ph.CO].

[146] O. H. E. Philcox, M. M. Ivanov, M. Simonović, and M. Zaldarriaga, JCAP **05**, 032 (2020), arXiv:2002.04035 [astro-ph.CO].

[147] O. H. E. Philcox, M. M. Ivanov, M. Zaldarriaga, M. Simonovic, and M. Schmittfull, Phys. Rev. D **103**, 043508 (2021), arXiv:2009.03311 [astro-ph.CO].

[148] G. Cabass, M. M. Ivanov, O. H. E. Philcox, M. Simonović, and M. Zaldarriaga, Phys. Rev. Lett. **129**, 021301 (2022), arXiv:2201.07238 [astro-ph.CO].

[149] G. Cabass, M. M. Ivanov, O. H. E. Philcox, M. Simonović, and M. Zaldarriaga, Phys. Rev. D **106**, 043506 (2022), arXiv:2204.01781 [astro-ph.CO].

[150] K. K. Rogers, R. Hložek, A. Laguë, M. M. Ivanov, O. H. E. Philcox, G. Cabass, K. Akitsu, and D. J. E. Marsh, (2023), arXiv:2301.08361 [astro-ph.CO].

[151] G. Cabass, M. M. Ivanov, O. H. E. Philcox, M. Simonovic, and M. Zaldarriaga, (2022), arXiv:2211.14899 [astro-ph.CO].

[152] O. H. E. Philcox, B. D. Sherwin, G. S. Farren, and E. J. Baxter, Phys. Rev. D **103**, 023538 (2021), arXiv:2008.08084 [astro-ph.CO].

[153] O. H. E. Philcox, G. S. Farren, B. D. Sherwin, E. J. Baxter, and D. J. Brout, Phys. Rev. D **106**, 063530 (2022), arXiv:2204.02984 [astro-ph.CO].

[154] G. S. Farren, O. H. E. Philcox, and B. D. Sherwin, Phys. Rev. D **105**, 063503 (2022), arXiv:2112.10749 [astro-ph.CO].

[155] G. D'Amico, L. Senatore, P. Zhang, and H. Zheng, JCAP **05**, 072 (2021), arXiv:2006.12420 [astro-ph.CO].

[156] G. D'Amico, Y. Donath, L. Senatore, and P. Zhang, (2020), arXiv:2012.07554 [astro-ph.CO].

[157] G. D'Amico, M. Lewandowski, L. Senatore, and P. Zhang, (2022), arXiv:2201.11518 [astro-ph.CO].

[158] G. D'Amico, Y. Donath, M. Lewandowski, L. Senatore, and P. Zhang, (2022), arXiv:2206.08327 [astro-ph.CO].

[159] T. Colas, G. D'amico, L. Senatore, P. Zhang, and F. Beutler, JCAP **06**, 001 (2020), arXiv:1909.07951 [astro-ph.CO].

[160] P. Zhang, G. D'Amico, L. Senatore, C. Zhao, and Y. Cai, JCAP **02**, 036 (2022), arXiv:2110.07539 [astro-ph.CO].

[161] S.-F. Chen, Z. Vlah, and M. White, JCAP **02**, 008 (2022), arXiv:2110.05530 [astro-ph.CO].

[162] A. Chudaykin and M. M. Ivanov, JCAP **11**, 034 (2019), arXiv:1907.06666 [astro-ph.CO].

[163] A. Chudaykin, K. Dolgikh, and M. M. Ivanov, Phys. Rev. D **103**, 023507 (2021), arXiv:2009.10106 [astro-ph.CO].

[164] A. Chudaykin, D. Gorbunov, and N. Nedelko, (2022), arXiv:2203.03666 [astro-ph.CO].

[165] A. Chudaykin and M. M. Ivanov, (2022), arXiv:2210.17044 [astro-ph.CO].

[166] W. L. Xu, J. B. Muñoz, and C. Dvorkin, Phys. Rev. D **105**, 095029 (2022), arXiv:2107.09664 [astro-ph.CO].

[167] A. He, M. M. Ivanov, R. An, and V. Gluscevic, (2023), arXiv:2301.08260 [astro-ph.CO].

[168] L. Piga, M. Marinucci, G. D'Amico, M. Pietroni, F. Vernizzi, and B. S. Wright, (2022), arXiv:2211.12523 [astro-ph.CO].

[169] L. Herold and E. G. M. Ferreira, (2022), arXiv:2210.16296 [astro-ph.CO].

[170] H. Rubira, A. Mazoun, and M. Garny, JCAP **01**, 034 (2023), arXiv:2209.03974 [astro-ph.CO].

[171] T. L. Smith, V. Poulin, and T. Simon, (2022), arXiv:2208.12992 [astro-ph.CO].

[172] T. Simon, P. Zhang, V. Poulin, and T. L. Smith, (2022), arXiv:2208.05930 [astro-ph.CO].

[173] T. Simon, P. Zhang, V. Poulin, and T. L. Smith, (2022), arXiv:2208.05929 [astro-ph.CO].

[174] P. Carrilho, C. Moretti, and A. Pourtsidou, JCAP **01**, 028 (2023), arXiv:2207.14784 [astro-ph.CO].

[175] A. Glanville, C. Howlett, and T. M. Davis, Mon. Not. Roy. Astron. Soc. **517**, 3087 (2022), arXiv:2205.05892 [astro-ph.CO].

[176] S. Kumar, R. C. Nunes, and P. Yadav, JCAP **09**, 060 (2022), arXiv:2205.04292 [astro-ph.CO].

[177] R. C. Nunes, S. Vagnozzi, S. Kumar, E. Di Valentino, and O. Mena, Phys. Rev. D **105**, 123506 (2022), arXiv:2203.08093 [astro-ph.CO].

[178] T. Simon, G. Franco Abellán, P. Du, V. Poulin, and Y. Tsai, Phys. Rev. D **106**, 023516 (2022), arXiv:2203.07440 [astro-ph.CO].

[179] L. Herold, E. G. M. Ferreira, and E. Komatsu, Astrophys. J. Lett. **929**, L16 (2022), arXiv:2112.12140 [astro-ph.CO].

[180] G. Franco Abellán, R. Murgia, and V. Poulin, Phys. Rev. D **104**, 123533 (2021), arXiv:2102.12498 [astro-ph.CO].

[181] M. Garny, T. Konstandin, L. Sagunski, and M. Viel, JCAP **03**, 049 (2021), arXiv:2011.03050 [astro-ph.CO].

[182] S. Vagnozzi, E. Di Valentino, S. Gariazzo, A. Melchiorri, O. Mena, and J. Silk, Phys. Dark Univ. **33**, 100851 (2021), arXiv:2010.02230 [astro-ph.CO].

[183] D. Wadekar, M. M. Ivanov, and R. Scoccimarro, Phys. Rev. D **102**, 123521 (2020), arXiv:2009.00622 [astro-ph.CO].

[184] M. M. Ivanov, Y. Ali-Haïmoud, and J. Lesgourgues, Phys. Rev. D **102**, 063515 (2020), arXiv:2005.10656 [astro-ph.CO].

[185] M. Lewandowski, A. Perko, and L. Senatore, JCAP **05**, 019 (2015), arXiv:1412.5049 [astro-ph.CO].

[186] L. Senatore and M. Zaldarriaga, (2017), arXiv:1707.04698 [astro-ph.CO].

[187] A. Aviles, A. Banerjee, G. Niz, and Z. Slepian, JCAP **11**, 028 (2021), arXiv:2106.13771 [astro-ph.CO].

[188] M. Garny and P. Taule, JCAP **09**, 054 (2022), arXiv:2205.11533 [astro-ph.CO].

[189] M. Levi and Z. Vlah, (2016), arXiv:1605.09417 [astro-ph.CO].

[190] A. Boyle and F. Schmidt, JCAP **04**, 022 (2021), arXiv:2011.10594 [astro-ph.CO].

[191] D. Jeong and F. Schmidt, Class. Quant. Grav. **32**, 044001 (2015), arXiv:1407.7979 [astro-ph.CO].

[192] D. Bertacca, A. Raccanelli, N. Bartolo, M. Liguori, S. Matarrese, and L. Verde, Phys. Rev. D **97**, 023531 (2018), arXiv:1705.09306 [astro-ph.CO].

[193] E. Di Dio, R. Durrer, R. Maartens, F. Montanari, and O. Umeh, JCAP **04**, 053 (2019), arXiv:1812.09297 [astro-ph.CO].

[194] P. D. Meerburg *et al.*, (2019), arXiv:1903.04409 [astro-ph.CO].

[195] G. Cabass, M. M. Ivanov, and O. H. E. Philcox, Phys. Rev. D **107**, 023523 (2023), arXiv:2210.16320 [astro-ph.CO].

[196] A. Kostić, N.-M. Nguyen, F. Schmidt, and M. Reinecke, (2022), arXiv:2212.07875 [astro-ph.CO].

[197] A. Obuljen, M. Simonović, A. Schneider, and R. Feldmann, (2022), arXiv:2207.12398 [astro-ph.CO].
[198] M. Schmittfull, M. Simonović, V. Assassi, and M. Zaldarriaga, Phys. Rev. D **100**, 043514 (2019), arXiv:1811.10640 [astro-ph.CO].
[199] M. Schmittfull, M. Simonović, M. M. Ivanov, O. H. E. Philcox, and M. Zaldarriaga, JCAP **05**, 059 (2021), arXiv:2012.03334 [astro-ph.CO].
[200] F. Schmidt, F. Elsner, J. Jasche, N. M. Nguyen, and G. Lavaux, JCAP **01**, 042 (2019), arXiv:1808.02002 [astro-ph.CO].
[201] F. Schmidt, G. Cabass, J. Jasche, and G. Lavaux, JCAP **11**, 008 (2020), arXiv:2004.06707 [astro-ph.CO].
[202] I. Babić, F. Schmidt, and B. Tucci, JCAP **08**, 007 (2022), arXiv:2203.06177 [astro-ph.CO].
[203] D. J. Eisenstein, H.-j. Seo, E. Sirko, and D. Spergel, Astrophys. J. **664**, 675 (2007), arXiv:astro-ph/0604362.
[204] S.-F. Chen, Z. Vlah, and M. White, JCAP **09**, 017 (2019), arXiv:1907.00043 [astro-ph.CO].
[205] M. White, Mon. Not. Roy. Astron. Soc. **450**, 3822 (2015), arXiv:1504.03677 [astro-ph.CO].
[206] C. Hikage, K. Koyama, and A. Heavens, Phys. Rev. D **96**, 043513 (2017), arXiv:1703.07878 [astro-ph.CO].
[207] C. Hikage, K. Koyama, and R. Takahashi, Phys. Rev. D **101**, 043510 (2020), arXiv:1911.06461 [astro-ph.CO].